

RECONSTRUCTING THE DEPOSITIONAL HISTORY OF THE EEL RIVER PALEO  
MELTWATER CHANNEL, NORTHEASTERN INDIANA USING SEDIMENT  
PROVENANCE TECHNIQUES

Charles B. Goodwin

Submitted to the faculty of the University Graduate School  
in partial fulfillment of the requirements  
for the degree  
Master of Science  
in the Department of Earth Sciences,  
Indiana University

March 2015

Accepted by the Graduate Faculty, Indiana University, in partial fulfillment of the requirements for the degree of Master of Science.

---

Kathy Licht, PhD, Chair

Master's Thesis  
Committee

---

Pierre-André Jacinthe, PhD

---

Broxton Bird, PhD

## ACKNOWLEDGEMENTS

I express deep gratitude to my advisor, Dr. Kathy Licht, without whom this project would not have been possible. Dr. Licht fascinated me with her glacial geology course and was willing to work with me on developing a glacial geology thesis. Thank you, Kathy, for your knowledge, patience, and encouragement that allowed me to complete this thesis.

I also am very appreciative to my committee for their suggestions and guidance for my thesis, Dr. Pierre-Andre Jacinthe and Dr. Broxton Bird. They both incorporated great input from their areas of expertise.

I want to thank Mike Prentice and Sally Letsinger of the Indiana Geological Survey for all the information and insight they provided me. I really enjoyed working with them and admire their passion for the science. I would like to thank Patrick Ducey whom recently completed his thesis on parallel topic. I also thank J. Jeremy Webber for his assistance with LiDAR imagery.

I am very grateful to have an understanding and encouraging supervisor at work, Andy, whom has been extremely supportive and providing some very useful advice. I also would like to thank a colleague of mine, Bruce, for his assistance and support.

Last, but definitely not least, I want to thank my family. My parents, Jim and Susan, and sister Kerri, have always been there for me with unlimited support and encouragement. My wife, Chris, has also been extremely supportive and patient. I can't wait for our upcoming trip to Alaska after I receive my Masters Degree.

Charles B. Goodwin

Reconstructing the depositional history of the Eel River paleo meltwater channel, northeastern Indiana using sediment provenance techniques

The outwash deposits of the Eel River paleo meltwater channel in DeKalb and Allen Counties, Indiana predominantly originated from the Erie Lobe of the Laurentide Ice Sheet, but do contain some sediment from the Saginaw Lobe. This determination helps clarify the ice dynamics and Last Glacial Maximum sediment depositional history in northeastern Indiana, which is complicated because of the interactions between the Erie and Saginaw Lobes. Outwash deposits were analyzed from IGS core SC0802 in the Eel River paleo meltwater channel, which intersects the previously identified Huntertown Formation. The core includes 29.2 m of deposits underlain by the hard glacial till of the Trafalgar formation. Mean grain size, sediment skewness, lithology, magnetic susceptibility, and quantitative X-ray diffraction were used to evaluate the provenance of the outwash deposits. Representative samples of Erie Lobe and Saginaw Lobe deposits were analyzed to develop end member provenance signatures.

A weight of evidence approach was developed and revealed that deposits from 8.0-13.8 m are of mixed origin from the Erie and Saginaw Lobes, whereas the 0-8.0 and 13.8-29.2 m deposits are Erie Lobe in origin. Cluster analysis and discriminant function analysis supported the findings of this approach. These findings suggests that the Eel River paleo meltwater channel was formed as an outwash channel, and that the adjacent Huntertown Formation does not appear to have been directly deposited by the Saginaw Lobe. The sediments of Saginaw origin from ~8-14 m in the Eel River paleo meltwater channel were likely transported from an upgradient source. The sediments from this zone have a larger mean grain size indicating deposition occurred during higher meltwater

discharge, such as the release of meltwater from the drainage of proglacial or subglacial lake(s) associated with the disintegration of the Saginaw Lobe, thus resulting in the mixing of Saginaw Lobe deposits with Erie Lobe deposits. However, the majority of the sediment in the Eel River paleo channel near SC0802 is Erie Lobe in origin. Based on the provenance and depositional sequence at SC0802, the Saginaw Lobe disintegrated prior to the Erie Lobe retreat from the Wabash moraine around 16-17 cal ka.

Kathy Licht, PhD, Chair

## TABLE OF CONTENTS

LIST OF TABLES .....	vii
LIST OF FIGURES .....	viii
LIST OF APPENDICES .....	x
INTRODUCTION .....	1
BACKGROUND .....	4
Glacial Sediment Deposits – Allen County .....	5
Huntertown Formation.....	6
Clast Provenance of Erie Lobe and Saginaw Lobe Deposits.....	8
Age of Glacial Deposits .....	9
IGS Core SC0802 .....	10
METHODS .....	12
Sample Acquisition.....	12
Grain Size.....	13
Sediment Lithologic Analysis.....	13
Magnetic Susceptibility .....	14
Quantitative X-Ray Diffraction Analysis .....	15
RESULTS .....	17
Grain Size Analysis.....	17
Sediment Lithology Analysis.....	18
Magnetic Susceptibility .....	20
X-Ray Diffraction .....	21
DISCUSSION .....	24
Provenance Interpretation of Core SC0802 .....	24
Sediment Parent Material.....	29
Ice Lobe Interaction in Northeast Indiana and the Deposition of the Eel River Paleo Meltwater Channel.....	30
CONCLUSION.....	36
TABLES .....	38
FIGURES.....	55
APPENDICES .....	76
REFERENCES CITED.....	104
CURRICULUM VITAE .....	

## LIST OF TABLES

Table 1: Summary of end member samples and core SC0802 samples.....	39
Table 2: Sediment classification scheme.....	41
Table 3: Summary of grain size analysis.....	42
Table 4: Mean grain and skewness of all SC0802 samples.....	43
Table 5: End member clast lithology analysis.....	44
Table 6: SC0802 clast lithology analysis.....	45
Table 7: Sediment lithology ratios.....	46
Table 8: Magnetic susceptibility of end member and SC0802 samples.....	47
Table 9: Quantitative X-ray diffraction results, coarse sand samples.....	49
Table 10: Quantitative X-Ray Diffraction results, fine sand/silt/clay samples .....	50
Table 11: Weight of evidence scoring approach for provenance determination of SC0802 samples.....	51
Table 12: Discriminant function analysis scores and classification of SC0802 samples.....	52
Table 13: Discriminant function per analysis .....	53
Table 14: Summary of sediment provenance sources for Eel River meltwater channel deposits.....	54

## LIST OF FIGURES

Figure 1. Glacial lobes of southern Laurentide Ice Sheet during the late Wisconsin glaciation (Mickelson and Colgan, 2003).....	56
Figure 2. Sampling locations and orientation of ice sheet lobes in Indiana. ....	57
Figure 3. Distribution of glacial lobes and timing of related deposits in Indiana (Fleming, 1994). ....	58
Figure 4. Surficial geology of Allen County, IN (Letsinger, 2012) and location of core SC0802.....	59
Figure 5. Conceptual time-transgressive model of the glacial deposits in the Eel River paleo meltwater channel (Fleming, 1994) .....	60
Figure 6. Map of Indiana showing peat bogs and Saginaw Lobe orientation.....	61
Figure 7. Boring log of SC0802 (Letsinger, 2012).....	62
Figure 8. Grain size distribution of core SC0802. ....	63
Figure 9. Gravel lithology distribution of Erie Lobe and Saginaw Lobe end members with samples from core SC0802.....	64
Figure 10. Gravel lithology relationships in SC0802.....	65
Figure 11. Comparison of gravel lithology and grain size.....	66
Figure 12. Magnetic susceptibility in CGS units of sand size fraction samples from core SC0802.....	67
Figure 13. Quantitative X-ray diffraction of coarse sand samples .....	68
Figure 14. Quantitative X-ray diffraction of fine sand/silt/clay samples.....	69
Figure 15. Weight of evidence (WOE) interpretation of SC0802 provenance.....	70
Figure 16. Hierarchical cluster analysis of SC0802 samples.....	71
Figure 17. Discriminant function analysis of SC0802 samples.....	72



Figure 18. Map showing dominant parent material of soil (ISEE, 2014). .....	73
Figure 19. Topography and LiDAR maps (ISEE, 2014 and ISDP, 2015).....	74
Figure 20. Conceptual cross section of Eel River paleo meltwater channel at SC0802.....	75

LIST OF APPENDICES

Appendix A. Photolog of SC0802.....77

Appendix B. Grain size distribution of SC0802 samples .....102

## INTRODUCTION

Pleistocene ice sheets have affected a considerable portion of the landscape in North America (Fig. 1). Since its initiation around 3.2 Ma, the Laurentide Ice Sheet has advanced and retreated across Canada and the northern United States multiple times (Benn and Evans, 2010). After final retreat following the Last Glacial Maximum (LGM), the Laurentide Ice Sheet laid down extensive deposits of glacial till, sand and gravel. Glacial deposits cover about 13 million square kilometers of North America and frequently constitute a major groundwater source for domestic, industrial, and agricultural purposes (Stephenson et al., 1988). Many of these deposits are near the ground surface and are vulnerable to the introduction of pollutants, which can contaminate water supplies. These glacial deposits also have economical significance as sand and gravel resources. In 2009, a total of 18,800,000 metric tons of sand and gravel was sold at a unit value of \$5.31 per ton in Indiana (USGS, 2013).

In northeastern Indiana, several ice lobes of the Laurentide Ice Sheet shaped the landscape during the LGM, including the Saginaw Lobe and Erie Lobe (Fig. 2). The Eel River paleo meltwater channel, situated between the Wabash Moraine to the southeast and the Salamonie Moraine to the northwest (Fig. 2, Fig. 19), formed during the retreat of the Laurentide Ice Sheet; however, the origin of the deposits in this area is unclear. Here the interaction of the Erie and Saginaw Lobes and the associated depositional history in northeastern Indiana is quite complex (Bleuer and Moore, 1974). Of particular interest is the area of the Eel River paleo meltwater channel and adjacent Hometown Formation in northern Allen County and southwestern DeKalb County (Figs. 1 and 2). The glacial deposits associated with the Eel River paleo meltwater channel serve as a significant reservoir for water supplies, as well as a sand and gravel resource. A better understanding

of the depositional history will benefit resource managers by helping them identify key areas of the resources.

Fleming (1994) interpreted the Saginaw Lobe to have advanced as far southeast as northern Allen County resulting in the direct deposit of the Huntertown Formation and a portion of the Eel River paleo meltwater channel (Fig. 2). More recent studies (Prentice et al., 2012; Letsinger, 2012) infer that the area around the Huntertown Formation was deposited by the Erie Lobe and that the Saginaw Lobe did not advance far enough southeast to directly deposit these sediments. Despite an abundance of past work done, the chronology of the events that lead to the sedimentary deposits in and around Allen County, and the origin of the deposits is somewhat poorly understood, mainly due to the high complexity and variability of the glacial deposits coupled with lack of age control. This study is designed to further evaluate the provenance of the outwash deposits in the Eel River paleo meltwater channel in northern Allen County in order to resolve the debate on the origin of the Huntertown Formation.

Numerous samples from a core drilled and curated by the Indiana Geological Survey (IGS; core SC0802) were made available for this research. Samples were analyzed for mean grain size, sediment skewness, lithology by visual inspection, magnetic susceptibility, and quantitative x-ray diffraction. The results were evaluated in context of end member samples representative of the Erie and Saginaw Lobe deposits. The purpose of these analyses was to determine the provenance of the deposits throughout the ~30 m core of outwash deposits and test the hypothesis that the sediments within the Eel River paleo meltwater channel entirely originated from the Erie Lobe of

the Laurentide Ice Sheet and not the Saginaw Lobe, which is in support of more recent interpretations of deposition.

## BACKGROUND

Glaciations of the northern United States and Canada have occurred periodically throughout the Pleistocene from 2 Ma to approximately 10 cal ka. During this time, the Laurentide Ice Sheet occasionally occupied the northern United States east of the Rocky Mountains until its final retreat between 15 and 7 cal ka, depending on location (Benn and Evans, 2010). In northern Indiana, there are depositional records of several advances and retreats of the ice sheet during Illinoian Age and Wisconsin Age glaciations, which occurred during marine isotope stages 6 and 2, respectively (Gibbard and Van Kolfshoten, 2005). However, the vast majority of unconsolidated deposits in Indiana are of late Wisconsin Age, and generally deposited between 22 and 13 cal ka (Fleming, 1994). The Late Wisconsin, or LGM, occurred about 21 cal ka in Ohio and Indiana (Ekberg et. al, 1993). In Indiana, very few Illionian-age deposits of gravel have been recognized in river valleys, indicating that most of the Illionian outwash was cleaned out prior to deposition of LGM outwash (Thornbury, 1950). Some existing Illionian outwash, where present, may have been overridden by Wisconsin outwash. The vast majority of the unconsolidated deposits in Allen County, Indiana are of late Wisconsin Age, and thicknesses range from 10 to > 90 m within the county (Bleuer and Moore, 1978). Unconsolidated material thicknesses are greatest in the northwestern portion of Allen County. The underlying bedrock in northern Allen County is Devonian Age Antrim Shale and the Traverse and Detroit River Formations, which consist mostly of limestone and dolomite (Bleuer and Moore, 1978).

## **Glacial Sediment Deposits – Allen County**

The unconsolidated deposits of the study area in northern Allen County are dominated by three primary depositional formations: the Trafalgar Formation, the Huntertown Formation, and the Lagro Till. The Trafalgar Formation is by far the most extensive, covering nearly half of Indiana during the LGM (~22 to 17 cal ka; Fig. 3). The Trafalgar Formation was formed by the Huron-Erie Lobe of the Laurentide Ice Sheet, which entered northeastern and central Indiana from the east and northeast. Fleming (1994) suggests the overlying Huntertown Formation to originate from the Saginaw Lobe, a more northern source of ice. Stratigraphically above the Trafalgar, the Huntertown Formation was deposited from ~17 to 15 cal ka (Fleming, 1994). After the supposed sediment deposition from the Saginaw Lobe, the Erie Lobe re-entered Indiana from the east and northeast and deposited the Lagro Formation between ~ 15 to 12 cal ka (Fleming, 1994). Regional terrain in northeastern Indiana suggests that the two lobes acted independently and that the periods of ice-margin advance of one lobe was not generally synchronous with the other (IDNR, 1996). Radiocarbon dates of lacustrine organic material from a few samples near Allen County indicate the post-glaciation regeneration of organic material occurred approximately 16 to 17 cal ka (Shane and Anderson, 1993; Glover et al., 2011), which suggests that the time scale used by Fleming (1994) (Fig. 3) is in uncalibrated radiocarbon years. However, the ice lobe responsible for the deposits in northwestern Allen County remains unclear.

The Trafalgar Formation is characterized by over-consolidated loamy till. The surface of this formation rarely is present on the current ground surface in Allen County, but has been mapped using water well logs and gamma ray logs (Letsinger, 2012). Many water well drillers have identified the Trafalgar Formation as “hardpan”, and more than

300 blows have been required to penetrate less than 12 inches (IDNR, 1996). The surface of the Trafalgar Formation exerted considerable influence over the style of deposition from later ice lobe advances due to the extreme hardness of the till (Fleming, 1994). In Allen County, the Huntertown Formation is exposed mainly in the northwestern portion of the county (Fig. 4) and pinches out eastward toward Fort Wayne (Letsinger, 2012), which may be influenced by a higher elevation of the underlying Trafalgar Formation in eastern Allen County (Fleming, 1994). Northwest of the Eel River paleo meltwater channel, the ground surface above the Huntertown Formation in northwestern Allen County is slightly higher in elevation than most of the remainder of the county, and the surface is typically characterized by hummocky terrain (Bleuer, 1974). The surficial glacial deposits across much of Allen County are the clay-rich Lagro Till of varying thickness, which is greatest on the recessional Fort Wayne and Wabash moraines (Fleming, 1994). Where the Huntertown Formation is present in northwestern Allen County, the Lagro Till thickness above it is variable and occasionally absent (Fleming, 1994). The high clay content of the Lagro Till originates from the proglacial Lake Maumee basin, located in eastern Allen County and across much of northwestern Ohio (Bleuer, 1974).

### **Huntertown Formation**

The Huntertown Formation contains a variety of deposits, including lacustrine sand, silt, clay; ice-contact sand, gravel, and mudflows; sandy loam till; and outwash sand (Fleming, 1994). Within the majority of the formation, apparent ice-contact sand deposits generally overlie outwash sand (Fleming, 1994). Due to the generally coarse grained deposits, the Huntertown Formation is a productive aquifer serving as a major



water supply to the city of Huntertown and surrounding areas (Letsinger, 2012). The outwash valley identified as the Eel River paleo meltwater channel likely cuts into the Huntertown Formation (Fig. 5). In northern Allen County, Fleming (1994) described the deposits in the Eel River channel to contain 6-12 m of Erie Lobe outwash originating from the Cedar Creek tunnel valley and from meltwater further northeast. This outwash is underlain by northwest-southeast oriented ice-contact fan deposits, which are laterally contiguous on both sides of the valley (Fig. 5) (Fleming, 1994). The sand and gravel thicknesses in the Eel River channel are commonly 20-25 m and can be as thick as 30 m (Fleming, 1994). Collectively, the general sand and gravel deposits in this area, including the Eel River paleo meltwater channel were identified by Fleming (1994) as the Huntertown Formation.

The identity of the ice lobe responsible for the Huntertown Formation is still debated (Letsinger, 2012). The sediments associated with the Saginaw Lobe may be at least a couple thousand years older than the Lagro Formation from the Erie Lobe, based on stratigraphic successions (Prentice et al., 2012). Moraines in northern Indiana that may be related to the Saginaw Lobe are located in St. Joseph, Marshall, Kosciusko, Elkhart, Noble, and Lagrange Counties (Leverett and Taylor, 1915). This is consistent with the recent observations by the IGS that morainal features from the Saginaw Lobe are not as far south as Allen or DeKalb Counties. The demise of the Saginaw Lobe was characterized by stagnation and downmelting, and not marginal retreat, based on the hummocky terrain common to the area influenced by the Saginaw Lobe (Bleuer, 1974). The stagnation of ice is conducive to development of peatlands. The area in northern

Indiana determined to be influenced by the Saginaw Lobe based on peatland distribution (Swinehart and Parker, 2002) is greater than 20 km northwest of the study area (Fig. 6).

### **Clast Provenance of Erie Lobe and Saginaw Lobe Deposits**

Boulders from the Precambrian Shield of Canada are common in LGM tills of Indiana and Ohio, indicating transport distances of greater than 1,000 km by the Laurentide Ice Sheet (Harrison, 1960). The provenance of deposits is somewhat different between the more northern source of the Saginaw Lobe and the northeastern source of the Erie Lobe, and can be differentiated. The Saginaw Lobe till and outwash includes brown, sandy, coal- and sandstone-bearing till and outwash, and the Erie Lobe deposits contain fragments of black shale and gypsiferous limestone (IDNR, 1996). The Saginaw Lobe is the only LGM ice lobe in the Great Lakes area that contains jasper conglomerate and a tillite containing a Precambrian conglomerate (Anderson, 1957). However, the abundance of these indicator clasts would be quite low in northern Indiana because of the low initial abundance, long transport distance, and dilution with other sediments acquired by the ice lobe across Michigan.

The most noticeable difference between the sand and pebble lithologies is the greater abundance of shale in Erie Lobe deposits (Harrison, 1960; Anderson, 1957). The provenance of the shale source for the Erie Lobe is likely the Devonian bedrock in northwestern Ohio and the Lake Erie basin (Ohio Division of Geologic Survey, 2006). In general, the igneous and metamorphic clast abundance is greater in count for the Saginaw Lobe deposits, but similar in general lithology between the Saginaw and Erie Lobes (Anderson, 1957). In four till samples from the Erie Lobe Powell-Union City moraine in eastern Indiana, granitic clasts range from 3.13 to 18.30 percent (Strobel and Faure,

1987). The Saginaw Lobe contains a higher proportion of dolomite to limestone than the Erie Lobe deposits (Anderson, 1957). The presence of sandstone clasts in Saginaw Lobe deposits should be a noticeable difference when comparing Saginaw Lobe to Erie Lobe deposits in northeastern Indiana. The provenance of Saginaw Lobe sandstone clasts is likely the Marshall Sandstone in south-central Michigan (Fisher et al., 2003).

### **Age of Glacial Deposits**

Limited radiocarbon dating of glacial deposits has been conducted in northeastern Indiana, and the data that does exist has spatial gaps. Many of the dates from prior work were based on uncalibrated radiocarbon ages, and most of these studies did not specify whether the reported timeframes were cal ka or  $^{14}\text{C}$  ka. Typically, the ideal samples for radiocarbon dating for glacial reconstruction history are of organic deposits immediately above glacial deposits or between distinct lithological boundaries. At Pretty Lake in LaGrange County, the organic material at the interface of the lake deposits and underlying till yielded an age of approximately 13,250  $^{14}\text{C}$  years (Wetzel, 1970), or 15,940 cal years (Glover et al., 2011), and it was concluded that glacial retreat from Indiana occurred approximately ~16.3 cal ka. The glacial deposits in LaGrange County are likely from the Saginaw Lobe. By dating several depths of marl deposits in northwestern Whitley County, it was determined that the marl layers were produced between 16.3 to 12.4 cal ka (Swinehart and Richards, 2001). Sediments at this location were also likely deposited by the Saginaw lobe, which disintegrated >16 cal ka according to Swinehart and Richards (2001). Radiocarbon samples collected by Shane and Anderson (1993) and Glover et al. (2011) indicated ages of organic materials from generally 14-18 cal ka in northeastern Indiana and northwestern Ohio. The retreat of the

Erie Lobe is expected to occur after the demise of the Saginaw Lobe (Fleming, 1994); however, there is currently little evidence of ice lobe age based on available radiocarbon dates alone.

### **IGS Core SC0802**

The SC0802 core that is currently archived at the IGS was drilled in 2008 and is about 31.6 m long. The core was drilled with roto-sonic drilling technology near the intersection of Chapman Road and Coldwater Road in northern Allen County (UTM 655897E, 4567889N m). This location is in the Eel River paleo meltwater channel and consists of mostly sand and gravel deposits, with the base of the core (29.2-31.6 m) encountering a glacial till, most likely the Trafalgar Formation (Figs. 5 and 7, Appendix A). Fleming (1994) described deposits in the Eel River paleo meltwater channel to be approximately 12 m of Erie Lobe outwash deposits underlain by sand and gravel from the Huntertown Formation. The upper 6 to 12 m in this area were determined to be from the Erie Lobe in origin derived from Cedar Creek, and to some extent from meltwater discharged from the front of the Wabash moraine (Fleming, 1994). If the Saginaw Lobe of the Laurentide Ice Sheet deposited the Huntertown Formation, it would be expected that the clast lithology of the lower sand and gravel in the core below ~12 m would be somewhat different from that of the upper outwash deposits.

Based on previous analysis of SC0802 by the IGS, silty soil layers, possibly containing organic material, are situated at approximately 3 m and at 5 m below ground surface (Fig. 7). A paleosol, described as an organic horizon overlying translocated clays, was identified near 8 m below ground surface, which may demarcate the Erie Lobe

outwash/Huntertown Formation boundary previously described by Fleming (1994). A thin clay layer was also identified at about 17 m.

## METHODS

### Sample Acquisition

In order to test whether there are changes in the sediment composition and characteristics with depth in the SC0802 core, 9 samples that complement 30 previously evaluated samples by the IGS, were collected from the core. The depths of the samples were selected for several reasons including intervals with relatively high gravel content for lithological analysis, available recovery, and to cover larger gaps of the core not previously sampled by the IGS (Table 1). Each of the samples collected from SC0802 integrated material over a 5-5.5 cm interval. The sediments for each sample were carefully extracted from near the center of the core and not along the outside of the core.

Sediments representative of the Erie Lobe were collected from the Wabash River near Bluffton, IN (UTM 657331E, 4510271N m), and the Saginaw Lobe end-member samples were collected from the Elkhart River near Ligonier, IN (UTM 622077E, 4591114N m) (Fig. 2). In each case, sampling sites were near the river's headwaters and entirely within surficial sediments deposited by a single lobe of the Laurentide ice sheet. The sediment in these end-member samples would have originated from till deposits and then sorted through alluvial processes, similar to the core samples whose provenance is unknown. Three samples were collected from each site along a transect following the surface of point bars in order to recover material with a similar size distribution to core materials analyzed in this study. The locations were just below the stream bank (ID #1), adjacent to the edge of the water (ID #3), and equidistance between the water edge and bank (ID #2). During collection of the end-member samples, the upper 1 cm of sediment, large gravel, and/or any organic debris on the surface was removed and material was taken from depths of 1-3 cm. The sediment in each of the samples was representative of

the naturally occurring point bar deposit. Samples were air-dried under direct sun with temperatures up to 38° C for two days. Drought conditions in 2012 during sampling allowed for more of the river bed to be exposed than normal.

### **Grain Size**

The SC0802 samples from the IGS were previously sieved by grain size down to very fine sand. Most of the SC0802 samples had a very small amount of silt and clay fines (Letsinger, 2012). Visually identifiable organics were manually removed from the end member samples prior to sieving. Organics were not observed in the SC0802 samples. The additional subsamples collected from SC0802 (CG-1 through CG-9) and the end-member samples (WR-1, WR-2, WR-3, ER-1, ER-2, and ER-3) were dry sieved down to very fine sand using standard sieve meshes. The sieved fractions of the CG and end member samples were weighed, and the sieves were thoroughly cleaned between samples. All samples were characterized by mean grain size of the sand and gravel fraction using fractional weight frequencies (Swan et al., 1978). Skewness of the SC0802 samples were calculated using the inclusive graphic method (Folk and Ward, 1957) for the sand and gravel fraction.

### **Sediment Lithologic Analysis**

After washing of the samples, the lithology of the fine gravel and larger size fraction was evaluated from all samples collected from SC0802 and the end-member samples. Clasts were visually identified with the aid of a StereoZoom<sup>®</sup> 7 microscope and characterized as limestone (LS), dolomite (Dol), shale (Sh), sandstone (SS), siltstone (SiS), chert (Ch), or a general category of igneous and metamorphic clasts (IM). The limestone and dolomite gravel were characterized based on their reaction with 10%

hydrochloric acid. The limestone gravel reacted vigorously when the acid was applied, and gravel composed of dolomite reacted more subtly and sometimes only reacted when scratched. Table 2 summarizes the sediment classification scheme used. The clasts in each sample were summarized by raw count and percentages (Evans and Benn, 2004).

### **Magnetic Susceptibility**

Magnetic susceptibility was determined on the very fine gravel, very coarse sand, coarse sand, medium sand, and fine sand for all samples described above, provided enough sample volume was available to visually fill at least 10% of the 0.75-inch plastic sample cube. Most samples with mass less than 1 gram were still analyzed for magnetic susceptibility, but their results were noted as being potentially unreliable due to the limited sample volume. Sediment sizes larger than very fine gravel were not analyzed due to potential bias from larger grains and the fewer grains available per sample. A Bartington MS2 sensor magnetic susceptibility system with a MS2B sensor was used to determine mass magnetic susceptibility of the sediments. Each sample was weighed and placed into the MS2B sensor for a direct read of magnetic susceptibility in CGS units ( $10^{-6}\text{m}^3\text{kg}^{-1}$ ). The magnetic susceptibility system was calibrated to a 300 CGS standard prior to each use and periodically during analysis. Additionally, the meter was zeroed out after approximately every 5 readings. For added precision, all samples were analyzed in duplicate and averaged. The CGS measurements were multiplied by the mass of the sample resulting in mass-corrected magnetic susceptibility readings (Andrews et al., 2002). A bulk magnetic susceptibility evaluation on the SC0802 core was previously attempted by the IGS using the Bartington MS2 core logging sensor; however, the large gravel throughout the core and zones of low recovery produced unreliable results.



The mean, and one and two standard deviations were calculated for each of the end member set of samples (WR and ER). The results from the core SC0802 were evaluated with respect to the range of two standard deviations of each end member to determine if the SC0802 samples fall within the populations of either of the end members.

### **Quantitative X-Ray Diffraction Analysis**

Two size fractions of six samples were selected for quantitative X-Ray Diffraction (QXRD) analysis to provide a preliminary assessment of the potential of this analytical method for determining provenance. The selected samples included end member samples (WR and ER), and SC0802 samples CG-2, CG-3, CG-6, and GSA-18. The size fractions analyzed for each sample were (1) coarse sand and (2) fine sand/silt/clay combined. The samples and size fractions were selected based on comparing the end members to key samples in the SC0802 core, as determined by magnetic susceptibility variation, and stratigraphic representation in SC0802.

The QXRD analysis of the fine sand/silt/clay size fraction was conducted prior to the magnetic susceptibility analysis of fine sand only. Magnetic susceptibility of the fine sand/silt/clay fraction was previously analyzed and those results were similar to the fine sand only magnetic susceptibility results, most likely due to the minimal silt and clay content in the samples. Therefore, the QXRD results for the fine sand/silt/clay size fraction are generally comparable to the fine sand magnetic susceptibility results for each sample analyzed.

Using the methodology described by Eberl (2003, 2004), the samples were mixed with a corundum internal standard, and then ground with methanol in a McCrone

micronizing mill. After five minutes, the samples were dried and sieved, then side-loaded into an XRD holder. Samples were X-rayed from 5 to 65 degrees two-theta with Cu K-alpha radiation using a Siemens D500 diffractometer with graphite monochromator. Analyses were completed in the Sediment Analysis Laboratory at the University of Colorado – Boulder.

The QXRD data were converted into weight percent minerals using the RockJock program, Version 11 (Eberl, 2003). RockJock compares integrated X-ray intensities for minerals present in the sample with that of the internal standard, and weight percents of the minerals are calculated (Eberl, 2004). The analysis was carried out for two regions of the XRD pattern to separate clay and non-clay minerals.

Mineral content ratios were calculated, since the mineral contents were reported in percentages, and the percentage for each sample did not equal 100%. Proportional relationships between quartz, feldspars, dolomite, and calcite were determined.

## RESULTS

### Grain Size Analysis

Grain size was determined from the end-member samples and additional samples collected from SC0802 (CG-1 through CG-9) for all sand and gravel size fractions (Table 3). For the end-members samples, the Saginaw Lobe samples (ER) ranged in average grain size between coarse sand and very fine gravel, and the Erie Lobe end member (WR) ranged in size from very coarse sand to fine gravel. The CG samples from SC0802 were generally very coarse sand to very fine gravel in average grain size (Table 4). The IGS samples (labeled GSA-) from SC0802 were previously determined to range from fine sand to fine gravel in mean grain size with only sand and gravel included in the calculation.

Mean grain size data was plotted with sediment description of core SC0802 (Fig. 8). Other than the near surface fine sand, the mean grain size fluctuates between medium sand and fine gravel. Sediments tend to be more gravelly between 5 and 17 m in depth, and more medium-coarse sand between 17-29 m. Appendix B contains grain size distributions of the individual samples from SC0802.

Sediment skewness measures the deviation from a symmetrical distribution, i.e. the predominance of coarse or fine sediments (Srivastava and Khare, 2009). Samples that have a tail of fine particles are positively skewed, or skewed toward positive phi values, whereas a tail of coarse particles are negatively, or coarse, skewed (Boggs, 2001). Skewness of the SC0802 samples tend to be generally positively skewed, or fine skewed, to near symmetrical, with a few intermittent negatively skewed, or coarse skewed samples (Table 4). Skewness of the SC0802 samples correlates with mean grain size with an  $r^2=0.47$ , indicating as the mean grain size increases, the samples tend to be more finely

skewed (Fig. 8). Together, the samples collected from between 8 and 14 m generally have a greater mean grain size and are more finely skewed.

### **Sediment Lithology Analysis**

Three samples from each of the end members were analyzed and summed to determine the average sediment lithology representative for each sediment source (Table 5). The primary differences between the end members are a higher percent limestone and lower percent igneous/metamorphic (IM) in the samples representative of the Erie lobes deposits compared to that representative of the Saginaw Lobe. Although much less abundant than carbonate and IM deposits, the Saginaw Lobe deposits also had a notably higher percentage of sandstone than the Erie Lobe deposits. End member results were compared to an extensive sediment provenance study conducted by Anderson (1957), and the end member results were generally consistent with those findings. Also, gravel lithology data was generated from IGS core SC0801 (Ducey, 2013), which was located approximately one mile east of core SC0802 in Erie Lobe Lagro Till (Prentice et al., 2012), and those sediment lithology results were generally consistent with the Erie Lobe end member deposits. Minimal shale and more abundant dolomite in the Anderson (1957) and Ducey (2013) samples are the primary differences compared to the end member samples.

Table 6 summarizes the gravel lithology analysis for all samples collected from core SC0802. Several samples had 15 or fewer gravel clasts, and those individual sample results were not be evaluated further due to the small sample size. Limestone was the dominant sediment clast, and had percentages much higher than the Saginaw Lobe end member, and generally slightly higher than the Erie Lobe end member (Table 5, Fig. 9).

The IM content of the SC0802 samples were typically 15-25%, which correspond with the Erie Lobe end member (24.2%). Sample CG-3, which was located just below the apparent paleosol at approximately 8 m in depth, had 34.4% IM content, which is more similar to the Saginaw Lobe end member (33.2%). The IM content in two underlying samples was lower, and more similar to the range of the Erie Lobe end-member. The low abundance of sandstone gravel in the SC0802 samples suggest provenance from the Erie Lobe; however, this could be a function of preservation potential of sandstone gravel.

For further evaluation of gravel lithology, several ratios were calculated for the end members and SC0802 samples with greater than 15 gravel clasts (Table 7, Fig. 10). Of the ratios evaluated, the LS:IM, LS+Dol:IM, and LS:IM+SS ratios had a notable difference between end members. The LS:Dol ratio was also evaluated due to its high variability in the SC0802 samples, despite the limited difference between end member results. The LS+Dol:IM+SS ratio was also evaluated, but its results are similar to that of the LS:IM+SS due to a limited amount of sandstone clasts.

For LS:IM, the SC0802 samples had ratios near or greater than the Erie Lobe end member and no ratios were near that of the Saginaw end member. A similar trend was encountered with the LS+Dol:IM ratio. Only the CG-3 sample, which is just below the potential paleosol had a LS+Dol:IM ratio somewhat close to that of the Saginaw lobe end member. The LS:IM+SS ratio in the SC0802 samples also exhibited a trend indicative of the Erie Lobe end member. The LS:Dol ratio are too close between end members for end member differentiation. Throughout SC0802, there tends to be more variability in the sediment lithologies and ratios in the ~7-15 m samples compared to deeper samples.

The relationship between sample grain size and gravel composition in the SC0802 samples was also evaluated (Fig. 11). With increasing sample mean grain size, there tends to be more limestone, whereas samples that have lower mean grain size tend to have higher quantities of dolomite and IM gravel clasts. Other lithologies lack a relationship with mean grain size.

### **Magnetic Susceptibility**

Magnetic susceptibility analysis was conducted on several discrete size fractions smaller than those analyzed for lithology (Table 8). The magnetic susceptibility of the Erie Lobe end member samples increases with a decreasing grain size indicating more magnetism in the smaller grained samples, whereas an opposite trend occurs with the Saginaw Lobe end member samples. Overall, the majority of SC0802 samples had higher magnetic susceptibility with decreasing grain size, which is similar to the trend in the Erie Lobe end member samples (Table 8, Fig. 12). The magnetic susceptibility results are similar between the end members for the very fine gravel (-1 phi) and very coarse sand (0 phi) size fractions; therefore, magnetic susceptibility analysis of the coarse sand (1 phi) and smaller fractions was used to assess downcore changes in provenance. The similarity of the results between end members diverges with grain sizes smaller than very coarse sand.

For the coarse sand size fraction (1 phi), the magnetic susceptibility for most of the SC0802 samples varied between the two end member  $2\sigma$ , and several samples were in the overlap of two end member ranges. Approximately 74% of the SC0802 samples fall within the Saginaw Lobe end member range, and 63% falling with the Erie Lobe range. 40% of the coarse sand samples fall within overlap between end members.

Magnetic susceptibilities of the coarse sand were generally higher in the upper 11 m of SC0802 than below. All but one of the medium sand (2 phi) samples in the upper 10.75 m of SC0802 have magnetic susceptibility values within the Erie Lobe end member range. A few medium sand samples between 10.75 m and 13 m have magnetic susceptibility in or near the Saginaw Lobe end member range. Below 13 m, the medium sand magnetic susceptibilities are either between the end member ranges or on the low end of the Erie Lobe range. For both coarse and medium sand samples, there is less variability in magnetic susceptibilities below 14 m in SC0802. For fine sand (3 phi) (Fig. 12), most of the SC0802 magnetic susceptibility values fall between the relatively large gap between the end member 2  $\sigma$  ranges.

A notable low in magnetic susceptibility occurs at approximately 8 m below ground surface (sample CG-3), which is the location of the potential paleosol (Fig. 12). Another notable low occurs between 10.9 and 12.9 m below ground surface; these values generally fall within the range of Saginaw Lobe deposits. The variability of magnetic susceptibility tends to decrease with depth below 14 m in the medium and coarse sand fractions, whereas an opposite trend occurs with the fine sand fraction.

### **X-Ray Diffraction**

The mineral suites selected from RockJock that best represents the samples analyzed are shown for the coarse sand size samples (Table 9) and the fine sand/silt/clay size samples (Table 10). Overall, the most abundant non-clay minerals are quartz, calcite and dolomite, followed by chert and intermediate microcline feldspar. As expected, the amount of clay minerals in these samples is minimal (<10.3% weight). For the coarse sand end member samples, only quartz and dolomite have notable differences, with

higher quartz content and lower dolomite in the representative Saginaw Lobe end member compared to the Erie Lobe end member. Of the four coarse sand samples analyzed from SC0802, GSA-18 (17.35 m) has similar quartz content to the Saginaw Lobe end member, and the CG-2 (7.81 m), CG-3 (8.17 m), and CG-6 (24.69 m) samples have similar quartz to the Erie Lobe member (Fig. 13). Dolomite is more prevalent in the Erie Lobe end member, CG-2, and CG-3 samples than it is in the Saginaw Lobe end member, CG-6 and GSA-18 samples. The calcite content was greater in the SC0802 coarse sand samples than in that of the end members, which could reflect the greater LS abundance in the SC0802 samples when compared to the end members.

The only notable difference in the fine sand/silt/clay samples is less dolomite in the Erie Lobe end member compared to the Saginaw Lobe end member and the SC0802 samples (Fig. 14). The quartz content between end members is similar at 47% versus 41.2%, which are both higher than the quartz content of the SC0802 samples. Dolomite and Fe dolomite were notably greater in both CG-3 samples than in the other samples, including the end members.

The following ratios were evaluated to compare end member and SC0802 mineral content relationships: quartz : feldspar (combined), quartz+feldspar : dolomite, quartz+feldspar : dolomite+calcite, and dolomite:calcite. For the coarse sand samples (Table 9), there was a notable difference between end members for each of the mineral content ratios. With the exception of the dolomite:calcite ratio, the ratios in the CG-2 and CG-3 samples were generally more similar to the Erie Lobe end member ratios. The ratios in the GSA18 sample were similar to the ranges of the Saginaw Lobe end member ratios. End member ratio analysis was inconclusive of the fine sand/silt/clay samples. The



quartz:feldspar and dolomite:calcite ratios were too similar (within 15 %) between end members for analysis. The other two ratios exhibited much higher values in the end members than in the SC0802 samples.

## DISCUSSION

### Provenance Interpretation of Core SC0802

Evaluation of the various analyses in relation to the end members, and within the SC0802 core shows certain parameters are clearer indicators of sediment provenance in this case, and possibly in other similar situations for evaluating provenance of similar glacial outwash settings. Evaluation of the results from SC0802 with respect to the end members indicates that IM, SS and dolomite gravel lithologies, and magnetic susceptibility of the sand size fractions are the most important indicators of potential sediment provenance. Mean grain size and sediment skewness are also telling in the evaluation of SC0802; however, these analyses cannot be compared to end members because of the differing depositional environment of the end members being collected from a modern fluvial setting versus the Eel River paleo meltwater channel deposits of SC0802, thus resulting in a differing sediment size distribution. Mean grain size and skewness is useful for evaluating variability within SC0802 and associated depositional processes, but not provenance. QXRD analysis could be more valuable if additional samples were analyzed from SC0802. Also, with the available XRD data, there was no correlation between the amount of maghemite, the primary magnetic mineral with a detectable abundance, and the magnetic susceptibility of the representative samples. Of the four QXRD samples collected from SC0802, the CG-3 sample has the highest abundance of maghemite and is amongst the samples with the lowest magnetic susceptibility. Maghemite and magnetite are iron oxides capable of acquiring magnetic remanence, and of these two, magnetite is the strongest naturally occurring magnetic mineral (Mahar et al., 2009). Magnetite was not detected in the samples analyzed by QXRD. Based on the QXRD results, there does not appear to be evidence of

environmental magnetic influence in the Erie Lobe end member samples with elevated magnetic susceptibility, such as the in situ post-depositional formation of bacterial magnetite (Mahar et al., 2009).

Some studies have utilized magnetic susceptibility and particle size to define different types of glacial sediment deposits (Dearing, 1998). However, Waythomas (1991) found that a lack of correlation between bulk sediment magnetic susceptibility and particle size indicates that magnetic minerals are probably evenly distributed throughout the particle size distribution. Nonetheless, a significant vertical change in susceptibility, such as that in medium to coarse sand at about 8.0 m in SC0802, is likely consistent with a change in the sediment transport path in the glacial system which can indicate a change in the sedimentation unit (Prentice et al., 2012).

Overall, the analysis of the SC0802 core exhibit predominantly Erie Lobe characteristics; however, a few samples exhibit some Saginaw Lobe-like characteristics (i.e. high IM and low magnetic susceptibility). Because there was not a definitive set of samples within the core that were distinctly Saginaw deposits, it appears some samples represent a mixture of Erie and Saginaw Lobe deposits. To further evaluate the potential provenance throughout SC0802, eight key analyses with differentiating end members were selected for further evaluation, and included Dol, IM, SS, and LS+Dol:IM lithologies, the 1 phi, 2 phi and 3 phi magnetic susceptibilities, and the 3 phi:1 phi magnetic susceptibility ratio. Using these analyses, a weight of evidence point count approach was developed. For each of the SC0802 samples, each analysis was scored as +1 for Erie Lobe characteristics and -1 for Saginaw Lobe characteristics (Table 11). The scores were summed for the samples that had all eight analyses available, with higher

scores indicative of Erie Lobe provenance and lower scores representing Saginaw Lobe characteristics.

The end member criteria for determining whether to designate a result as either +1 or -1 are shown on Table 11. For the lithologic analyses and the magnetic susceptibility ratio analysis, the midpoint between end member results demarcated the difference between a positive score and negative score. Because the relative difference in magnetic susceptibilities between end members is much greater, the 2  $\sigma$  ranges were used for differentiation. If the sample result for magnetic susceptibility fell outside of the 2  $\sigma$  ranges or within both 2  $\sigma$  ranges, a neutral zero score was assigned to the result.

Very few samples exhibited a negative score; therefore, the lower scores (i.e. +1) were considered potential mixtures of Erie and Saginaw Lobe deposits, because there are characteristics of both in the analyses. The clearest boundary of different depositional modes in SC0802 is the buried paleosol at about 8 m. This paleosol likely developed during a period when glacial outwash deposition was absent at the location of SC0802. The IGS described the paleosol as an organic horizon overlying translocated clays (Fig. 7). The sample directly above the paleosol (CG-2) has a weight of evidence count of +5, and the sample directly below it is -3, which is the most negative of all samples from SC0802 suggesting a strong Saginaw influence. This paleosol represents the upper boundary of more recent Erie Lobe deposits from 0-8 m to a mixture of Erie and Saginaw deposits below it.

Several factors were jointly evaluated with the weight of evidence approach to determine if there is a bottom depth of the Erie / Saginaw mixed deposits within the core and what that depth is. In terms of mean grain size, the sediments are more gravelly from

5-17 m, and then become generally medium-coarse sand and more uniform below 17 m. The sediment lithologies are more variable between approximately 7-15 m than from below 15 m (Fig. 10), which could be indicative of mixing. The lowest magnetic susceptibility values, which are characteristic of the Saginaw source, are generally between 8-18 m. Also, samples GSA-8, GSA-9, and GSA-10 are quite similar to each other and fairly similar to GSA-7 in terms of lithology and magnetic susceptibility, all of which were from within the same gravelly unit between approximately 10.8 and 13.0 m. With these factors in consideration, the weight of evidence approach suggests the bottom of the Erie/Saginaw mixed zone is between samples GSA-11 and GSA-12 when looking at all samples, and between GSA-11 and GSA-14 when looking at samples with all data available. The unit boundary identified by the IGS at 13.87 m may demarcate a change in sediment characteristics (Appendix A). Therefore, below approximately 13.8 m, the deposits are dominantly, or entirely, Erie Lobe in origin. The average weight of evidence point count is 4.7 from the samples from 0-8.0 m, 3.6 from 13.8-30 m, and only 0.9 in the mixed zone from 8.0-13.8 m (Fig. 15). The 8.0-13.8 m zone corresponds with a slightly coarser mean grain size, more positive skewness, more variability in sediment lithology, and lower magnetic susceptibility readings when compared to the 0-8.0 m and 13.8-30 m intervals.

In order to test the hypothesis derived from the weight of evidence approach, hierarchical cluster analysis and discriminant function analysis were conducted. The same eight variables were used for the statistical analysis, and because the statistical approach was designed to test variability within core SC0802 and not with respect to the end members, mean grain size and skewness were also included as variables in the cluster

and discriminant analysis. Together these two statistical tests can provide definitive statistical evidence when the discriminant analysis confirms the results of the cluster analysis (Gielar et al., 2012). Discriminant function analysis is one of the most widely used multivariate procedures used in earth sciences (Davis, 2002).

The hypothesis tested was that the samples collected from between 8.0 and 13.8 m are statistically different than the samples collected above and below this interval, which corresponds with the weight of evidence point count analysis. The results of the hierarchical cluster analysis using the paired group algorithm (Hammer et al., 2001) indicate the samples within the 8.0-13.8 m interval are generally grouped together, with the exception of the CG-9 sample (Fig. 16). Hierarchical clustering joins the most similar observations, then successively connects the next most similar observations to these (Davis, 2002). In support of the cluster analysis, the discriminant function analysis showed a separation of the two groups, samples from 8.0-13.8 m and the other samples in the core (Fig. 17). The p-value for the Hotelling's t-squared test is 0.029 demonstrating a statistical significance between the two groups. 87% of the samples were correctly classified by discriminant analysis. Greater than 80% correct classification represents relatively high efficiency of the discriminant model (Kovacic et al., 2009).

Additional discriminant tests were conducted using SC0802 samples from the 8.0-17.2 m zone as the mixing zone and from 8.0-29.2 m as the mixing zone. The Trafalgar till deposited by the older Huron-Erie Lobe was encountered at the depth of 29.2 m. The statistical separation was not as distinct between the groups with p-values of 0.062 and 0.273 for the 8.0-17.2 m and 8.0-29.2 m depths, respectively, and a lesser percent of the samples were correctly classified by the discriminant analysis (82% and 79%).

Because there were only two sample groups, a simple linear discriminant function transforms the original set of measurements into a single discriminant score (Davis, 2002). The discriminant scores (Table 12) allowed for evaluation of the variables most representative of the two groups. The discriminant functions (Table 13) associated with mean grain size and magnetic susceptibility were more indicative of the Erie Lobe deposits from 0-8.0 m and 13.8-29.2 m, and the influence of IM lithology and the carbonate : IM ratio was most indicative of the Erie/Saginaw mixed zone between 8.0-13.8 m.

Overall, these results indicate that it is possible to discriminate sediments derived from differing material on the basis of lithology, magnetic susceptibility, and mean grain size. Discriminant function analysis provides a good qualitative sedimentary provenance model by establishing spatial relationships between the sources of sediment samples (Monasterio, 2000).

### **Sediment Parent Material**

The sediments in the Eel River paleo meltwater channel as determined by the evaluation of core SC0802 appear to mostly from the Erie Lobe, and minimally from the Saginaw Lobe of the Laurentide ice sheet. Ice sheet flow has the capability of transporting sediments for long distances and depositing them far from the origin of the material. The transport path of sediments in the ice sheet determines the wear processes experienced by the sediments, thus influencing the particle morphology, and sediment lithology can be influenced by the durability or rock types under different types of transport (Benn and Evans, 2010). Englacial transport allows for sediment clasts to be transported over long distances (Strobel and Faure, 1987); however, only continental ice

sheets are capable of long distant transport of sediments provided the topography and basal ice velocity are conducive (Clark, 1987).

A summary of potential sources of the sediments transported by the Erie and Saginaw Lobes is provided in Table 14, which focuses on the sources of sedimentary clasts primarily in Michigan, Ohio and northeastern Indiana. The IM clasts originated from the Precambrian basement rock in Ontario. For the Saginaw Lobe, the IM clasts are likely from north and northeast of Lake Huron, whereas for the Erie Lobe, the IM clasts likely originated north of Lake Ontario (Fig. 1). Strobel and Faure (1987) found that the relative abundance of IM clasts decreases rapidly when an ice sheet flows over carbonate rocks which fracture more readily, thus the abundance of IM clasts is diminished by the dilution with the carbonate clasts. Because the distance from the IM source rock is slightly shorter to Allen County, Indiana via the Saginaw Lobe than the Erie Lobe, a greater abundance of IM clasts in Saginaw Lobe deposits can be expected. However, there are many processes in play during ice lobe advancement that affect the transport of the sediment. Additionally, multiple advances and retreats of the ice lobes likely reworked the sediment deposits between their origin and northern Indiana.

### **Ice Lobe Interaction in Northeast Indiana and the Deposition of the Eel River Paleo Meltwater Channel**

Glacifluvial processes during the retreat or disintegration of ice sheet lobes are capable of transporting significant volumes of water and sediment to the proglacial environment. These large discharge volumes commonly carve out meltwater channels, which are typically filled back in by glacifluvial deposits once depositional processes overtake erosional processes. The location of meltwater channels is generally driven by the existing topography, the bed material, and the volume of meltwater and sediment



released from the ice. Meltwater channels cut by proglacial streams can achieve impressive dimensions due to the erosive power of high sediment discharges and sediment loads during peak flow, much more so than fluvial processes alone (Benn and Evans, 2010). Glacifluvial deposits are characterized as either ice contact fan deposits which are deposited adjacent to the ice margin, or outwash deposits which are beyond the glacial margin (proglacial). Meltwater draining along the ice lobe margins or in sub-marginal zones can be responsible for considerable incision of existing sediment and bedrock, producing lateral channels commonly quasi-parallel to the ice margin (Benn and Evans, 2010).

The scouring and deposition of the Eel River paleo meltwater channel in DeKalb and Allen Counties was likely initiated during the melting of the Erie Lobe when it was at its position terminating along the Wabash moraine. The initial deposition of sediments from the approximate lower half of the Eel River paleo meltwater channel (from 13.8 to 29.2 m at SC0802) likely originated from the sediment deposition from the Erie Lobe around the periphery of the Wabash moraine. After this period of deposition, sediment contribution from the disintegration of the Saginaw Lobe appears to have mixed sediments from the melting Erie Lobe, forming the mixed interval of deposits from 8.0 to 13.8 m at SC0802. The source of the Saginaw Lobe deposits likely ceased and the remaining deposits from the existing ground surface to 8.0 m in depth at SC0802 originated from continued melting and eventual retreat of the Erie Lobe. Therefore, the disintegration of the Saginaw Lobe in northern Indiana and associated meltwaters on its southeastern margin predates the final retreat of the Erie Lobe from the Wabash moraine.

The majority of the Saginaw Lobe meltwater drained by way of the present day Kankakee drainage basin (Zumberge, 1960; Fenelon et al., 1994).

There exist several possibilities for determining how the Saginaw deposits mixed with the Erie Lobe deposits in the 8.0-13.8 m depth at SC0802. Fleming (1994) conceptually modeled the ice margin of the Saginaw Lobe as entering the northern portion of Allen County and depositing an ice-contact fan in the Eel River valley, followed by deposition of outwash from the Erie Lobe. This ice contact fan was laterally continuous through the Eel River channel and was deposited between the Lagro and Trafalgar Formations. Fleming (1994) identified the unit as the Huntertown Formation. The fan sloped to the southeast where it thinned and eventually pinched out a few miles beyond the Eel River valley (Bleuer and Moore, 1974). However, this would result in direct deposition of Saginaw Lobe deposits and not a mix of Saginaw and Erie sediments, barring significant reworking of the deposits. Prentice et al. (2012) discussed recent findings of a sedimentary deposition problem where Saginaw Lobe sediments in far northern Indiana were deposited below and therefore older than the equivalent unit to the Trafalgar formation. Based on this finding and after evaluation of cores from the Wabash and Salamonie moraines, Prentice et al. (2012) inferred that no Saginaw deposits were present in Allen County, and the "Huntertown Formation" was deposited by the Erie Lobe.

Based on the stratigraphic problem presented by Prentice et. al. (2012) and the lack of evidence of purely Saginaw deposits in SC0802, it is assumed the Huntertown Formation in northwestern Allen and southwestern DeKalb Counties was deposited by the Erie Lobe, and not from an ice-contact fan originating from the Saginaw Lobe. The

notable Saginaw influence from 8.0-13.8 m at SC0802 was likely derived from an upgradient source. Based on evaluation of the soil parent material mapping in northeastern Indiana, along with the current topography, it appears possible that Saginaw deposits may have been transported down the Eel River paleo meltwater channel from a northern source (Fig. 18). Two potential areas of Saginaw Lobe deposits which were transported by meltwater channels have been identified. The more likely source area is in far southern Steuben County where the Eel River paleo meltwater channel originates. The other potential source area corresponds with the location further northwest of an outwash channel that intersects and likely drained into the Eel River paleo meltwater channel in Dekalb County, near the town of Waterloo (Fig. 18b). Surface topography and LIDAR imagery in these areas further supports the presence and locations of the paleo meltwater channels (Fig. 19a, 19b). The Steuben County source area of Saginaw sediments is more likely than the Noble County source due to the more direct path of flow along the paleo meltwater channel.

The zone of mixed source deposits from 8.0-13.8 m at SC0802 is generally more gravelly than the deposits above and below. This suggests the deposition of the coarser grained zone likely occurred during a period of higher meltwater flow volumes, which may be attributed to a large release of water, possibly from the drainage of a proglacial or subglacial lake. Catastrophic drainage of glacial lakes can produce flows orders of magnitude greater than a normal meltwater flow and can affect the resulting landscape (Benn and Evans, 2010). These large releases of water are short duration events and can make their appearance abruptly in depositional sequences (Fraser and Bleuer, 1988). At SC0802, the deposit of the paleosol at 8.0 m may demarcate the end of the depositional

sequence of the coarser-grained, higher flow deposit, and a period of little or no deposition. The abundance of lacustrine sediments deposited in intra-ice lakes in Indiana suggests that the storage and potential large volume release of meltwater was common (Fraser and Bleuer, 1988). Lacustrine deposits occur in the areas of the potential origin of the Saginaw deposits in Steuben County, and in northwestern DeKalb and northeastern Noble Counties (Fig. 18b), which indicates meltwater stored in glacial lakes were available to transport Saginaw Lobe sediments to the Eel River paleo meltwater channel and to the location of SC0802. The release of meltwater from a subglacial lake, or a series of lakes, from the melting Saginaw Lobe would more likely provide the volume of meltwater necessary to deposit the sediments from 8.0-13.8 m at SC0802. The high discharge of meltwater typically associated with the release of subglacial lakes may have rapidly deposited “sheets” of sediment into the Eel River paleo meltwater channel. Large meltwater releases from glacial lakes may be relatively common events when ice sheets are melting, such as the believed release of a subglacial lake into the Wabash Valley near Delphi, Indiana (Fraser and Bleuer, 1988).

It appears the maximum southeastern extent of the Saginaw Lobe coincides with the topographical high along the Mississinewa moraine in Noble and Steuben counties (Fig 19a), and the Packerton moraine further to the southwest (Fig. 2). This position of the Saginaw coincides with the peatland distribution in northern Indiana (Fig. 6). The formation of peatlands is indicative of the ice sheet disintegration instead of retreat (Swinehart and Parker, 2002). Overall, the glacial sediments comprising the Eel River paleo meltwater channel in Allen County were not directly deposited by the Saginaw Lobe and are dominantly Erie Lobe in origin. The Saginaw Lobe deposits were

mixed with Erie lobe deposits in the Eel River meltwater channel during a period of high flow velocity, possibly caused by the release of meltwater from glacial lake(s). Based on the depositional sequence at SC0802, the Saginaw Lobe disintegrated prior to the final retreat of the Erie Lobe from the Wabash moraine. Based on these findings, Fleming's (1994) conceptual cross section across the Eel River paleo meltwater channel in northern Allen County has been revised (Fig. 20).

## CONCLUSION

The ice lobe dynamics and glacial sediment depositional history in northeastern Indiana is complicated because of the interactions between the Erie and Saginaw Lobes of the Laurentide Ice Sheet during the LGM. Of particular interest is the area of the Eel River paleo meltwater channel and adjacent Huntertown Formation in northern Allen County and southwestern DeKalb County. The glacial deposits in this area have created a prolific water supply resource. Understanding the characteristics of the deposits in this area and interpreting their origin is useful with respect to the water supply, which can be vulnerable to groundwater contamination.

Fleming (1994) interpreted the Saginaw Lobe to have advanced as far southeast as northern Allen County resulting in the direct deposit of the Huntertown Formation. More recent studies (Prentice et al., 2012; Letsinger, 2012) infer the deposits in the area around the Huntertown formation originated from the Erie Lobe. The results of this study suggest that the Eel River paleo meltwater channel was formed as an outwash channel, and that it and the Huntertown Formation were not deposited by the Saginaw Lobe. There are some sediments of Saginaw origin in the Eel River paleo meltwater channel that were likely transported from an upgradient source in a high-energy event deposit (or series of such deposits); however, the majority of the sediment in the Eel River channel is Erie Lobe in origin.

At SC0802, outwash deposits from 13.8 to 29.2 m in depth are Erie Lobe deposits. The zone of mixed Erie and Saginaw deposits from 8.0-13.8 m at SC0802 coincides with a generally larger mean grain size of the core, which indicates a higher flow velocity during deposition of that interval. The source of the higher discharge may

be from the upgradient release of meltwater from the drainage of glacial lake(s), most likely subglacial lakes associated with the disintegration of the Saginaw Lobe, thus resulting in the mixing of Saginaw Lobe deposits into the Eel River paleo meltwater channel, followed by a period of landscape stability to allow formation of a paleosol. Additional outwash deposits from the Erie Lobe occurred from after the formation of the paleosol, depositing the sediments from ground surface to 0.8 m at SC0802. The provenance and depositional sequence of SC0802 sediments indicates the Saginaw Lobe disintegrated prior to the final Erie Lobe retreat from this area, approximately 16 to 17 cal ka (Glover et al., 2011).

Continued research in this area is needed to better understand the chronology of glacial deposits and associated depositional mechanisms. The provenance of the sediments and their depositional characteristics are important in evaluation of the susceptibility of water supply to contamination, as well as determining the economical relevance of sand and gravel resources.

## TABLES



Table 1: Summary of end member samples and core SC0802 samples

<b>Sample Source</b>	<b>Sample ID</b>	<b>Sample Depth (m)</b>	<b>Mean grain size<sup>(4)</sup></b>
Wabash River <sup>(1)</sup>	WR-1	Surface	Very Coarse Sand
Wabash River	WR-2	Surface	Very Fine Gravel
Wabash River	WR-3	Surface	Fine Gravel
Elkhart River <sup>(2)</sup>	ER-1	Surface	Coarse Sand
Elkhart River	ER-2	Surface	Very Fine Gravel
Elkhart River	ER-3	Surface	Very Fine Gravel
SC0802 <sup>(3)</sup>	GSA-1	1.974	Fine Sand
SC0802	GSA-2	3.378	Coarse Sand
SC0802	CG-1	5.050	Very Fine Gravel
SC0802	GSA-3	6.296	Coarse Sand
SC0802	GSA-4	6.636	Very Coarse Sand
SC0802	GSA-5	6.998	Coarse Sand
SC0802	GSA-6	7.368	Very Coarse Sand
SC0802	CG-2	7.805	Very Fine Gravel
SC0802	CG-3	8.170	Very Coarse Sand
SC0802	CG-8	9.290	Very Coarse Sand
SC0802	CG-9	10.745	Very Coarse Sand
SC0802	GSA-7	10.928	Very Fine Gravel
SC0802	GSA-8	12.427	Very Fine Gravel
SC0802	GSA-9	12.637	Very Fine Gravel
SC0802	GSA-10	12.897	Very Coarse Sand
SC0802	GSA-11	13.756	Very Coarse Sand
SC0802	GSA-12	13.881	Coarse Sand
SC0802	GSA-13	13.961	Very Fine Gravel
SC0802	GSA-14	14.096	Fine Gravel
SC0802	GSA-15	14.281	Very Coarse Sand
SC0802	GSA-16	16.874	Very Fine Gravel
SC0802	GSA-17	17.109	Very Fine Gravel

Table 1 cont: Summary of end members samples and core SC0802 samples

<b>Sample Source</b>	<b>Sample ID</b>	<b>Sample Depth (m)</b>	<b>Mean grain size <sup>(4)</sup></b>
SC0802	GSA-18	17.349	Medium Sand
SC0802	GSA-19	18.503	Coarse Sand
SC0802	GSA-20	18.683	Coarse Sand
SC0802	GSA-21	18.863	Very Coarse Sand
SC0802	GSA-22	19.008	Medium Sand
SC0802	GSA-23	20.057	Medium Sand
SC0802	GSA-24	20.347	Very Coarse Sand
SC0802	CG-4	21.530	Very Coarse Sand
SC0802	GSA-25	21.550	Coarse Sand
SC0802	GSA-26	21.620	Very Coarse Sand
SC0802	GSA-27	21.715	Very Fine Gravel
SC0802	CG-5	22.970	Fine Gravel
SC0802	CG-6	24.685	Very Coarse Sand
SC0802	GSA-28	26.053	Coarse Sand
SC0802	GSA-29	26.273	Medium Sand
SC0802	GSA-30	26.563	Medium Sand
SC0802	CG-7	29.085	Very Fine Gravel

<sup>(1)</sup>UTM Coordinates: 657331E, 4510271N (meters), Zone 16T

<sup>(2)</sup>UTM Coordinates: 622077E, 4591114N (meters), Zone 16T

<sup>(3)</sup>UTM Coordinates: 655897E, 4567889N (meters), Zone 16T

<sup>(4)</sup>Sediment descriptions determined from mean grain size of sand and gravel fractions (Swan et al., 1978; Letsinger, 2012).

Table 2: Sediment classification scheme

<b>Sediment Type</b>	<b>Classification Criteria</b>
Limestone	Moderate to strong reaction to 10% HCl when powdered Fine-grained matrix Fossil fragments
Dolomite	Slight reaction to 10% HCl, or reaction when powdered Fine-grained matrix
Shale	Dark brown to black in color Typically flat and oval shaped Commonly layered when broken No reaction to 10% HCl
Sandstone	Distinctly granular, visible with or without microscope Includes both calcareous and non-calcareous cement
Siltstone	Gritty, but grains not visible or barely visible under microscope Commonly light gray in color
Chert	Non-granular, microcrystalline Smooth, glassy appearance under microscope Conchoidal fracturing common Commonly multi-colored and banded
Igneous/Metamorphic	Igneous and metamorphic textures Quartzite and granite of various color were most common

Table 3: Summary of grain size analysis

Sample ID	Total mass (g)	% Coarse Gravel	% Medium Gravel	% Fine Gravel	% Very Fine Gravel	% Very Coarse Sand:	% Coarse Sand	% Medium Sand	% Fine Sand:	% Very Fine Sand:	% Silt and Clay	Total percent	Mean Grain Size <sup>(1)</sup> (phi)	Mean Grain Size
		-4 phi	-3 phi	-2 phi	-1 phi	0 phi	1 phi	2 phi	3 phi	4 phi	>4 phi			
ER1	491.43	21.52%	5.03%	0.82%	0.77%	1.89%	3.63%	16.14%	29.48%	12.09%	7.41%	98.78%	0.75	Coarse Sand
ER2	466.82	41.66%	8.82%	4.13%	2.14%	2.08%	5.63%	17.48%	12.09%	2.53%	1.32%	99.55%	-1.21	Very Fine Gravel
ER3	276.68	51.61%	14.70%	3.48%	1.45%	1.24%	4.08%	11.54%	6.55%	1.18%	0.75%	99.88%	-2.18	Very Fine Gravel
WR1	194.60	19.75%	10.85%	10.76%	11.21%	11.81%	18.01%	13.90%	1.36%	0.12%	0.07%	99.59%	-0.96	Very Coarse Sand
WR2	206.14	14.11%	18.08%	12.57%	12.20%	15.05%	16.33%	8.28%	0.72%	0.09%	0.06%	99.70%	-1.15	Very Fine Gravel
WR3	398.14	46.53%	9.52%	7.99%	8.54%	10.49%	9.66%	5.20%	0.66%	0.07%	0.05%	99.85%	-2.20	Fine Gravel
CG1	350.13	3.74%	35.20%	16.61%	10.45%	7.56%	8.83%	9.06%	3.32%	2.13%	2.72%	99.63%	-1.22	Very Fine Gravel
CG2	312.24	17.09%	38.97%	9.40%	5.34%	3.26%	3.30%	8.61%	3.96%	2.25%	2.87%	99.70%	-1.83	Very Fine Gravel
CG3	238.68	4.60%	30.64%	19.09%	9.27%	8.14%	7.02%	5.93%	2.77%	1.55%	6.18%	99.49%	-1.40	Very Coarse Sand
CG4	146.70	0.00%	4.22%	13.86%	50.59%	26.20%	4.42%	0.45%	0.03%	0.03%	0.05%	99.86%	-0.85	Very Coarse Sand
CG5	139.86	0.00%	48.55%	40.15%	10.98%	0.36%	0.01%	0.01%	0.00%	0.00%	0.00%	100.06%	-2.37	Fine Gravel
CG6	163.32	0.00%	1.03%	17.08%	26.63%	25.34%	17.12%	8.82%	0.48%	0.48%	2.91%	99.90%	-0.27	Very Coarse Sand
CG7	176.03	3.06%	29.88%	16.92%	12.31%	13.38%	11.61%	5.58%	2.46%	1.13%	3.18%	99.51%	-1.17	Very Fine Gravel
CG8	163.96	10.25%	7.40%	16.83%	17.38%	12.26%	9.18%	8.73%	4.56%	2.64%	9.99%	99.23%	-0.70	Very Coarse Sand
CG9	201.25	18.05%	9.20%	11.97%	12.24%	12.52%	11.63%	10.04%	4.63%	2.39%	6.69%	99.34%	-0.87	Very Coarse Sand

<sup>(1)</sup>Mean grain size calculated using fractional weight frequencies (Swan et al., 1978) for sand and gravel fractions.

Table 4: Mean grain size and skewness of all SC0802 samples

Sample ID	Depth (m)	Mean Grain Size <sup>(1)</sup> (phi)	D_5 (phi)	D_16 (phi)	D_50 (phi)	D_84 (phi)	D_95 (phi)	Skewness <sup>(2)</sup>	Skewness Description
GSA #1	1.97	2.56	-0.80	1.10	2.30	3.13	3.75	-0.27	Coarse-skewed
GSA #2	3.38	0.34	-1.90	-1.26	-0.34	0.97	2.20	0.21	Fine-skewed
CG-1	5.05	-1.22	-3.95	-3.70	-2.50	0.86	2.20	0.50	V. fine-skewed
GSA #3	6.30	0.96	-2.70	-0.95	0.70	1.73	2.45	-0.28	Coarse-skewed
GSA #4	6.64	-0.32	-3.45	-2.48	-0.82	0.70	1.70	-0.03	Near symmetrical
GSA #5	7.00	0.46	-4.00	-3.40	0.67	1.70	2.25	-0.55	V. coarse-skewed
GSA #6	7.37	-0.79	-3.80	-3.33	-1.70	0.92	1.95	0.25	Fine-skewed
CG-2	7.81	-1.83	-4.00	-4.00	-3.32	1.03	2.40	0.76	V. fine-skewed
CG-3	8.17	-1.40	-4.00	-3.70	-2.57	0.40	2.05	0.49	V. fine-skewed
CG-8	9.29	-0.70	-4.00	-3.35	-1.45	1.15	2.60	0.19	Fine-skewed
CG-9	10.74	-0.87	-3.80	-3.33	-1.67	0.92	1.87	0.23	Fine-skewed
GSA #7	10.93	-1.75	-4.00	-4.00	-2.95	0.65	1.92	0.60	V. fine-skewed
GSA #8	12.43	-1.83	-3.85	-3.55	-2.60	-1.35	0.05	0.25	Fine-skewed
GSA #9	12.64	-1.20	-3.72	-3.07	-1.83	-0.65	1.40	0.12	Fine-skewed
GSA #10	12.90	-0.31	-2.93	-2.44	-1.10	1.10	2.00	0.25	Fine-skewed
GSA #11	13.76	-0.29	-2.70	-2.16	-1.08	0.70	1.73	0.26	Fine-skewed
GSA #12	13.88	0.08	-3.65	-1.35	-0.10	0.72	1.15	-0.34	V. coarse-skewed
GSA #13	13.96	-1.26	-2.87	-2.56	-2.30	-1.05	-0.28	0.61	V. fine-skewed
GSA #14	14.10	-2.67	-4.00	-4.00	-3.42	-2.15	-0.95	0.50	V. fine-skewed
GSA #15	14.28	-0.35	-3.70	-2.95	-1.35	1.63	3.05	0.30	V. fine-skewed
GSA #16	16.88	-1.46	-3.82	-3.41	-2.10	-0.60	0.45	0.13	Fine-skewed
GSA #17	17.11	-1.68	-4.00	-3.92	-2.44	-0.43	1.15	0.27	Fine-skewed
GSA #18	17.35	1.76	-1.80	0.40	1.40	2.37	3.40	-0.12	Coarse-skewed
GSA #19	18.51	0.64	-1.53	-0.92	0.50	1.28	1.95	-0.23	Coarse-skewed
GSA #20	18.69	0.03	-1.90	-1.52	-0.60	0.60	1.60	0.19	Fine-skewed
GSA #21	18.87	-0.68	-3.05	-2.48	-1.38	0.10	1.45	0.20	Fine-skewed
GSA #22	19.01	1.49	-1.13	0.27	1.63	2.10	3.25	-0.37	V. coarse-skewed
GSA #23	20.06	1.43	-0.80	0.08	0.52	1.77	2.20	0.30	Fine-skewed
GSA #24	20.35	-0.20	-3.55	-2.43	-0.64	0.97	1.80	-0.07	Near symmetrical
CG-4	21.54	-0.85	-2.92	-2.08	-1.37	-0.54	-0.01	0.01	Near symmetrical
GSA #25	21.56	0.31	-2.40	-1.63	-0.30	1.33	2.15	0.09	Near symmetrical
GSA #26	21.63	-0.25	-3.55	-2.09	-0.72	0.72	1.70	-0.03	Near symmetrical
GSA #27	21.72	-1.43	-4.00	-3.60	-2.10	-0.57	1.60	0.17	Fine-skewed
CG-5	22.98	0.00	-3.90	-3.67	-2.95	-2.15	-1.65	0.10	Fine-skewed
CG-6	24.69	-2.37	-2.72	-2.10	-0.88	0.62	1.50	0.12	Fine-skewed
GSA #28	26.06	0.85	-2.70	-0.95	0.57	1.62	2.20	-0.26	Coarse-skewed
GSA #29	26.28	1.36	-0.80	0.05	0.92	1.72	2.15	-0.10	Coarse-skewed
GSA #30	26.57	1.62	-0.05	0.38	1.15	1.82	2.20	-0.07	Near symmetrical
CG-7	29.09	-1.17	-3.95	-3.60	-2.12	0.42	1.80	0.31	V. fine-skewed

<sup>(1)</sup>Mean grain size from fractional weight frequencies (Swan et al., 1978) for sand and gravel fractions.

<sup>(2)</sup>Skewness calculated using graphical method (Folk and Ward, 1957) for sand and gravel fractions.

<sup>(3)</sup>"GSA" samples collected by Indiana Geological Survey.

Table 5: End member clast lithology analysis

Sample Source	Sample ID	Clast Count	LS	Dol	IM	Sh	SS	SiS	Ch	Other	% LS	% Dol	% IM	% Sh	% SS	% SiS	% Ch
Erie Lobe	WR-1	81	31	10	16	12	5	2	5		38.3%	12.3%	19.8%	14.8%	6.2%	2.5%	6.2%
Erie Lobe	WR-2	56	12	6	25	1	5	2	5		21.4%	10.7%	44.6%	1.8%	8.9%	3.6%	8.9%
Erie Lobe	WR-3	147	55	16	36	15	6	4	15		37.4%	10.9%	24.5%	10.2%	4.1%	2.7%	10.2%
Erie Lobe	Sum-WR	351	135	47	85	31	17	10	26		38.5%	13.4%	24.2%	8.8%	4.8%	2.8%	7.4%
Erie Lobe	STD-WR										9.5%	0.9%	13.2%	6.6%	2.4%	0.6%	2.1%
Anderson, 1957	12 samples	1200	507	264	289	11	9	86	34		42.3%	22.0%	24.1%	0.9%	0.8%	7.2%	2.8%
Ducey, 2013	56 samples	2224	922	749	381	0	165	0	7		41.5%	33.7%	17.1%	0.0%	7.4%	0.0%	0.3%
Saginaw Lobe	ER-1	12	1	0	7	0	3	0	1		8.3%	0.0%	58.3%	0.0%	25.0%	0.0%	8.3%
Saginaw Lobe	ER-2	115	37	16	24	19	8	3	8		32.2%	13.9%	20.9%	16.5%	7.0%	2.6%	7.0%
Saginaw Lobe	ER-3	23	1	1	11	3	4	1	2		4.3%	4.3%	47.8%	13.0%	17.4%	4.3%	8.7%
Saginaw Lobe	Sum-ER	208	64	20	69	22	17	4	12		30.8%	9.6%	33.2%	10.6%	8.2%	1.9%	5.8%
Saginaw Lobe	STD-ER										15.0%	7.1%	19.3%	8.7%	9.1%	2.2%	0.9%
Anderson, 1957	24 samples	2400	471	554	940	1	86	64	76	208	19.6%	23.1%	39.2%	0.0%	3.6%	2.7%	3.2%

Note: LS=Limestone, Dol=Dolomite, IM=Igneous/Metamorphic, Sh=Shale, SS=Sandstone, SiS=Siltstone, and Ch=Chert. STD=standard deviation.

Table 6: SC0802 clast lithology analysis

Sample ID	Depth (m) midpoint	Depth (ft)	Clast Count	LS	Dol	IM	Sh	SS	SiS	Ch	% LS	% Dol	% IM	% Sh	% SS	% SiS	% Ch
GSA-1	1.974	6.48	--	--	--	--	--	--	--	--	--	--	--	--	--	--	--
GSA-2	3.378	11.08	13	4	3	3	3	0	0	0	30.8%	23.1%	23.1%	23.1%	0.0%	0.0%	0.0%
CG-1	5.050	16.57	--	--	--	--	--	--	--	--	--	--	--	--	--	--	--
GSA-3	6.296	20.66	15	7	3	2	2	0	0	1	46.7%	20.0%	13.3%	13.3%	0.0%	0.0%	6.7%
GSA-4	6.636	21.77	46	24	6	13	2	1	0	0	52.2%	13.0%	28.3%	4.3%	2.2%	0.0%	0.0%
GSA-5	6.998	22.96	8	6	1	0	1	0	0	0	75.0%	12.5%	0.0%	12.5%	0.0%	0.0%	0.0%
GSA-6	7.368	24.17	90	56	9	14	1	6	0	4	62.2%	10.0%	15.6%	1.1%	6.7%	0.0%	4.4%
CG-2	7.805	25.61	149	85	20	32	4	3	2	3	57.0%	13.4%	21.5%	2.7%	2.0%	1.3%	2.0%
CG-3	8.170	26.80	186	91	13	64	1	5	2	10	48.9%	7.0%	34.4%	0.5%	2.7%	1.1%	5.4%
CG-8	9.290	30.48	116	48	15	31	3	15		3	41.4%	12.9%	26.7%	2.6%	12.9%	0.9%	2.6%
CG-9	10.740	35.24	106	58	27	12	2	5		1	54.7%	25.5%	11.3%	1.9%	4.7%	0.9%	0.9%
GSA-7	10.928	35.85	103	60	8	22	7	2		3	58.3%	7.8%	21.4%	6.8%	1.9%	1.0%	2.9%
GSA-8	12.427	40.77	122	70	16	25	1	7	0	3	57.4%	13.1%	20.5%	0.8%	5.7%	0.0%	2.5%
GSA-9	12.637	41.46	97	48	18	17	7	4	1	2	49.5%	18.6%	17.5%	7.2%	4.1%	1.0%	2.1%
GSA-10	12.897	42.31	57	30	12	11	4	0	0	0	52.6%	21.1%	19.3%	7.0%	0.0%	0.0%	0.0%
GSA-11	13.756	45.13	58	25	7	16	5	5	0	0	43.1%	12.1%	27.6%	8.6%	8.6%	0.0%	0.0%
GSA-12	13.881	45.54	5	2	2	1	0	0	0	0	40.0%	40.0%	20.0%	0.0%	0.0%	0.0%	0.0%
GSA-13	13.961	45.80	221	111	40	35	13	14	2	6	50.2%	18.1%	15.8%	5.9%	6.3%	0.9%	2.7%
GSA-14	14.096	46.25	141	80	25	18	6	9	2	1	56.7%	17.7%	12.8%	4.3%	6.4%	1.4%	0.7%
GSA-15	14.281	46.85	52	29	10	10	2	1	0	0	55.8%	19.2%	19.2%	3.8%	1.9%	0.0%	0.0%
GSA-16	16.874	55.36	141	73	25	25	5	9	1	3	51.8%	17.7%	17.7%	3.5%	6.4%	0.7%	2.1%
GSA-17	17.109	56.13	124	59	25	20	11	5	1	3	47.6%	20.2%	16.1%	8.9%	4.0%	0.8%	2.4%
GSA-18	17.349	56.92	4	1	1	2	0	0	0	0	25.0%	25.0%	50.0%	0.0%	0.0%	0.0%	0.0%
GSA-19	18.503	60.71	3	2	0	0	0	1	0	0	66.7%	0.0%	0.0%	0.0%	33.3%	0.0%	0.0%
GSA-20	18.683	61.30	10	5	2	1	0	1	0	1	50.0%	20.0%	10.0%	0.0%	10.0%	0.0%	10.0%
GSA-21	18.863	61.89	57	28	12	10	2	4	0	1	49.1%	21.1%	17.5%	3.5%	7.0%	0.0%	1.8%
GSA-22	19.008	62.36	1	1	0	0	0	0	0	0	100.0%	0.0%	0.0%	0.0%	0.0%	0.0%	0.0%
GSA-23	20.057	65.80	--	--	--	--	--	--	--	--	--	--	--	--	--	--	--
GSA-24	20.347	66.76	52	30	3	10	2	5	1	1	57.7%	5.8%	19.2%	3.8%	9.6%	1.9%	1.9%
CG-4	21.530	70.64	112	52	21	28	8	2	0	1	46.4%	18.8%	25.0%	7.1%	1.8%	0.0%	0.9%
GSA-25	21.550	70.70	32	15	6	4	3	2	2	0	46.9%	18.8%	12.5%	9.4%	6.3%	6.3%	0.0%
GSA-26	21.620	70.93	27	11	6	6	0	1	0	3	40.7%	22.2%	22.2%	0.0%	3.7%	0.0%	11.1%
GSA-27	21.715	71.24	162	71	22	39	5	17	1	7	43.8%	13.6%	24.1%	3.1%	10.5%	0.6%	4.3%
CG-5	22.970	75.36	236	133	28	41	24	5	0	5	56.4%	11.9%	17.4%	10.2%	2.1%	0.0%	2.1%
CG-6	24.685	80.99	117	68	19	23	4	1	1	1	58.1%	16.2%	19.7%	3.4%	0.9%	0.9%	0.9%
GSA-28	26.053	85.48	15	8	2	3	1	1	0	0	53.3%	13.3%	20.0%	6.7%	6.7%	0.0%	0.0%
GSA-29	26.273	86.20	1	0	1	0	0	0	0	0	0.0%	100.0%	0.0%	0.0%	0.0%	0.0%	0.0%
GSA-30	26.563	87.15	--	--	--	--	--	--	--	--	--	--	--	--	--	--	--
CG-7	29.085	95.42	124	67	12	26	8	7	1	3	54.0%	9.7%	21.0%	6.5%	5.6%	0.8%	2.4%

Note: LS=Limestone, Dol=Dolomite, IM=Igneous/Metamorphic, Sh=Shale, SS=Sandstone, SiS=Siltstone, and Ch=Chert. Shaded samples had 15 or less sediment clasts that were fine gravel or larger.

Table 7: Sediment lithology ratios

Sample	Depth (m)	LS:IM	LS+Dol:IM	LS:IM+SS	LS:Dol
Erie (WR)	n/a	1.59	2.14	1.32	2.87
Saginaw (ER)	n/a	0.93	1.22	0.74	3.20
GSA-4	6.64	1.85	2.31	1.71	4.00
GSA-6	7.37	4.00	4.64	2.80	6.22
CG-2	7.81	2.66	3.28	2.43	4.25
CG-3	8.17	1.42	1.63	1.32	7.00
CG-8	9.29	1.55	2.03	1.04	3.20
CG-9	10.74	4.83	7.08	3.41	2.15
GSA-7	10.93	2.73	3.09	2.50	7.50
GSA-8	12.43	2.80	3.44	2.19	4.38
GSA-9	12.64	2.82	3.88	2.29	2.67
GSA-10	12.90	2.73	3.82	2.73	2.50
GSA-11	13.76	1.56	2.00	1.19	3.57
GSA-13	13.96	3.17	4.31	2.27	2.78
GSA-14	14.10	4.44	5.83	2.96	3.20
GSA-15	14.28	2.90	3.90	2.64	2.90
GSA-16	16.87	2.92	3.92	2.15	2.92
GSA-17	17.11	2.95	4.20	2.36	2.36
GSA-21	18.86	2.80	4.00	2.00	2.33
GSA-24	20.35	3.00	3.30	2.00	10.00
CG-4	21.53	1.86	2.61	1.73	2.48
GSA-25	21.55	3.75	5.25	2.50	2.50
GSA-26	21.62	1.83	2.83	1.57	1.83
GSA-27	21.72	1.82	2.38	1.27	3.23
CG-5	22.97	3.24	3.93	2.89	4.75
CG-6	24.69	2.96	3.78	2.83	3.58
CG-7	29.09	2.58	3.04	2.03	5.58

Notes: SC0802 samples with less than 15 gravel clasts not included. LS=limestone, IM=igneous metamorphic, Dol=dolomite, SS=sandstone. n/a=not applicable.



Table 8: Magnetic susceptibility of end member and SC0802 samples

Sample Source	Sample ID	Depth (m)	V. Fn. Gravel (-1 phi)	V. Crs. Sand (0 phi)	Crs. Sand (1 phi)	Med. Sand (2 phi)	Fn. Sand (3 phi)	3 phi : 1 phi ratio
Wabash River (Erie Lobe)	WR-1	Surface	30.5	29.7	30.1	55.6	300.1	10.0
	WR-2	Surface	31.4	40.2	35.2	90.9	205.1	5.8
	WR-3	Surface	19.6	44.1	49.4	120.7	258.7	5.2
	Average		27.2	38.0	38.3	89.1	254.6	7.0
	Std. Dev.		6.6	7.4	10.0	32.6	47.6	2.6
	2 Std. Dev.		14.0-40.4	23.2-52.8	18.3-58.3	23.9-154.3	159.1-349.8	--
Elkhart River (Saginaw Lobe)	ER-1	Surface	25.5	51.7	23.2	4.9	3.9	0.2
	ER-2	Surface	57.1	25.4	11.8	5.2	11.1	0.9
	ER-3	Surface	8.9	29.5	11.1	8.4	9.9	0.9
	Average		30.5	35.5	15.4	6.2	8.3	0.7
	Std. Dev.		24.5	14.2	6.8	1.9	3.8	0.4
2 Std. Dev.		0-79.5	7.1-63.9	1.8-29.0	2.4-10.0	0.7-15.9	--	
SC0802	GSA-1	1.97	61.7	39.8	48.1	31.3	--	--
	GSA-2	3.38	15.6	12.3	--	26.3	43.6	--
	CG-1	5.05	109.5	115.4	46.2	43.3	154.9	3.4
	GSA-3	6.30	33.6	37.4	--	23.8	94.3	--
	GSA-4	6.64	16.6	20.7	20.9	49.2	219.9	10.5
	GSA-5	7.00	3.1	23.2	17.2	26.5	146.2	8.5
	GSA-6	7.37	8.4	20.0	20.2	27.8	111.5	5.5
	CG-2	7.81	87.9	145.7	98.2	49.8	52.5	0.5
	CG-3	8.17	18.1	14.5	13.5	28.3	31.5	2.3
	CG-8	9.29	n/a	40.8	37.3	38.4	44.4	1.2
	CG-9	10.74	n/a	41.6	47.8	61.4	81.5	1.7
	GSA-7	10.93	33.2	14.3	9.6	5.6	6.5	0.7
	GSA-8	12.43	40.9	20.5	9.0	0.0	21.3	2.4
	GSA-9	12.64	17.8	24.4	11.4	12.0	10.4	0.9
	GSA-10	12.90	32.9	32.1	15.0	9.1	34.3	2.3
	GSA-11	13.76	16.8	32.2	28.0	20.8	37.1	1.3
	GSA-12	13.88	18.9	18.8	16.9	57.1	319.5	18.9
	GSA-13	13.96	16.8	41.2	29.2	78.9	--	--
	GSA-14	14.10	14.0	19.2	19.5	40.0	49.5	2.5
GSA-15	14.28	23.5	25.8	29.5	22.7	45.7	1.6	
GSA-16	16.87	54.2	28.4	42.3	23.3	--	--	
GSA-17	17.11	24.9	29.2	20.9	20.7	44.3	2.1	
GSA-18	17.35	25.1	16.9	18.8	12.5	33.7	1.8	
GSA-19	18.50	17.3	14.0	24.7	31.1	141.7	5.7	

Table 8 cont: Magnetic susceptibility of end member and SC0802 samples

Sample Source	Sample ID	Depth (m)	V. Fn. Gravel (-1 phi)	V. Crs. Sand (0 phi)	Crs. Sand (1 phi)	Med. Sand (2 phi)	Fn. Sand (3 phi)	3 phi : 1 phi ratio
SC0802	GSA-20	18.68	9.0	21.0	27.2	37.6	<i>137.8</i>	5.1
	GSA-21	18.86	27.6	22.2	26.7	22.5	<i>70.1</i>	2.6
	GSA-22	19.01	0.0	31.7	14.7	13.9	43.1	2.9
	GSA-23	20.06	20.8	16.8	--	13.6	<i>77.7</i>	--
	GSA-24	20.35	33.4	30.6	20.1	29.5	140.7	7.0
	CG-4	21.53	23.3	13.7	14.7	<i>0.0</i>	--	--
	GSA-25	21.55	46.8	24.4	20.3	26.4	94.1	4.6
	GSA-26	21.62	24.4	34.5	31.8	29.0	153.1	4.8
	GSA-27	21.72	34.1	30.8	17.9	16.8	60.4	3.4
	CG-5	22.97	11.4	--	--	--	--	--
	CG-6	24.69	41.8	30.1	27.4	35.5	53.6	2.0
	GSA-28	26.05	34.8	21.7	19.7	29.9	193.9	9.8
	GSA-29	26.27	0.0	14.3	17.0	41.1	305.2	18.0
	GSA-30	26.56	<i>0.0</i>	11.7	15.2	--	130.3	8.6
	CG-7	29.09	15.3	24.4	18.9	20.8	56.8	3.0

Notes: Magnetic susceptibility is mass corrected and reported in CGS units ( $10^{-6} \text{ m}^3 \text{ kg}^{-1}$ ). Shaded results represents the average, and one and two standard deviations for each end member. n/a=not analyzed. Italicized results indicate less than 1 gram of sample volume and sample cube was less than 10% full.

Table 9: Quantitative X-ray diffraction results, coarse sand samples

Sample name:	Saginaw (1 phi)	Erie (1 phi)	CG2 (1 phi)	CG3 (1 phi)	CG6 (1 phi)	GSA18 (1 phi)
Laboratory ID:	24214	24216	24218	24220	24222	24224
Full pattern degree of fit:	0.1071	0.0997	0.1301	0.1447	0.1045	0.1036
<b>NON-CLAY MINERAL</b>	<u>Weight %</u>	<u>Weight %</u>	<u>Weight %</u>	<u>Weight %</u>	<u>Weight %</u>	<u>Weight %</u>
Quartz	41.7	29.4	27.0	17.1	30.1	41.4
ordered Microcline feldspar	1.1					
intermediate Microcline feldspar	5.5	7.2	5.6	3.4	4.7	5.1
Orthoclase feldspar	0.1					
Anorthoclase feldspar	4.4					
Albite feldspar (Cleavelandite)	6.1	6.6	5.2	4.8	5.5	5.4
Oligoclase feldspar (Norway)	3.2	7.3	12.3	1.9	3.7	2.8
Labradorite feldspar	1.2	1.3	7.5	0.5	1.1	1.2
Calcite	6.5	6.2	15.5	16.0	21.5	13.9
Dolomite	8.8	12.9	15.3	22.9	9.6	5.9
Fe-Dolomite	5.3	6.8	6.6	13.7	12.3	7.2
Siderite	0.5		1.1			0.3
Amphibole (ferrotschermakite)	1.1	2.4	3.5	0.4	2.1	1.0
Pyroxene (diopside)	0.6		0.7			0.8
Pyrite	0.0					
Goethite			0.6			0.3
Hematite	0.2					
Maghemite		0.1	1.9	3.4		
Magnetite	0.0					
Diatoms	1.7					
Chert (8.4 nm)	9.2	11.7	4.4	5.2	7.1	11.0
Total non-clays	97.3	91.8	107.1	89.2	97.6	96.3
<b>CLAY MINERALS</b>						
Kaolinite (Dry Branch)	0.0					
Saponite						
Ferruginous smectite	1.1	0.1		6.4	0.1	
1M Illite (R>2; 88%I)	1.5					
1M illite (R>1, 70-80%I)	2.1					
Biotite (1M)	2.2	0.4	2.7	0.7	0.3	0.4
Berthierine		3.6	1.2	2.0	2.0	0.2
Fe-Chlorite (Tusc)	1.9					
Muscovite (2M1)	0.0	2.9	2.9	1.2	2.2	0.1
Montmorillonite (Webster Pass)						
Illite (1M, PD3B)						
Total clays	8.7	7.0	6.8	10.2	4.5	0.7
TOTAL (wt. %)	106.1	98.8	113.8	99.4	102.2	97.1
<b>MINERAL RATIOS</b>						
Quartz:Feldspar	1.9	1.3	0.9	1.6	2.0	2.8
Quartz+Feldspar:Dolomite	4.5	2.6	2.6	0.8	2.1	4.3
Quartz+Feldspar:Dolomite+Calcite	3.1	2.0	1.5	0.5	1.0	2.1
Dolomite:Calcite	2.2	3.2	1.4	2.3	1.0	0.9

Note: Shaded columns represent end member samples, other samples from core SC0802.

Table 10: Quantitative X-ray diffraction results, fine sand/silt/clay samples

Sample name:	Saginaw (>2 phi)	Erie (>2 phi)	CG2 (>2 phi)	CG3 (>2 phi)	CG6 (>2 phi)	GSA18 (>2 phi)
Laboratory ID:	24215.0	24217	24219	24221	24223	24225
Full pattern degree of fit:	0.1072	0.0993	0.1007	0.1452	0.1721	0.1091
<b>NON-CLAY MINERAL</b>	<u>Weight %</u>	<u>Weight %</u>	<u>Weight %</u>	<u>Weight %</u>	<u>Weight %</u>	<u>Weight %</u>
Quartz	47.0	41.2	30.6	9.4	28.2	12.0
ordered Microcline feldspar	1.5					
intermediate Microcline feldspar	6.1	8.7	7.1	2.6	5.5	4.5
Orthoclase feldspar	1.1					
Anorthoclase feldspar	3.4				1.7	
Albite feldspar (Cleavelandite)	4.5	4.1	2.2	1.6	6.0	3.4
Oligoclase feldspar (Norway)	3.9	6.1	6.0	1.2	1.1	3.0
Labradorite feldspar	2.0	3.5	2.8	0.0	0.9	1.9
Calcite	5.7	3.1	7.5	8.0	18.9	25.1
Dolomite	7.1	1.9	8.3	21.6	21.7	11.3
Fe-Dolomite	4.5	5.0	11.2	29.6	6.3	17.8
Siderite	0.2		0.3	0.4		0.3
Amphibole (ferrotschermakite)	1.7	3.7	2.1		1.1	1.5
Pyroxene (diopside)	0.4		1.2	0.0	1.7	1.1
Pyrite	0.1			0.8	0.6	
Goethite			0.6			0.2
Hematite	0.2			1.5		
Maghemite		4.7		4.0		
Magnetite	0.0			0.0		
Diatoms	0.0			1.5		
Chert (8.4 nm)	8.4	11.4	7.4	5.4	3.7	5.3
Total non-clays	97.9	93.5	87.2		97.4	87.5
<b>CLAY MINERALS</b>						
Kaolinite (Dry Branch)						
Saponite	0.0			1.9		
Ferruginous smectite	0.1	3.4		3.6	0.0	
1M Illite (R>2; 88%I)					4.3	
1M illite (R>1, 70-80%I)	0.8					
Biotite (1M)	1.1	0.4	1.3	0.8		0.5
Berthierine		0.7	0.5			0.7
Fe-Chlorite (Tusc)	0.6			1.7	1.9	
Muscovite (2M1)	0.0	3.4	1.3	2.2	0.8	1.1
Montmorillonite (Webster Pass)						1.1
Illite (1M, PD3B)	0.0					
Total clays	2.6	7.9	3.1	10.2	6.9	3.4
TOTAL (wt. %)	100.5	101.4	90.2	97.8	104.4	90.9
<b>MINERAL RATIOS</b>						
Quartz:Feldspar	2.1	1.8	1.7	1.7	1.9	0.9
Quartz+Feldspar:Dolomite	6.0	9.2	2.5	0.3	1.5	0.9
Quartz+Feldspar:Dolomite+Calcite	4.0	6.3	1.8	0.3	0.9	0.5
Dolomite:Calcite	2.0	2.2	2.6	6.4	1.5	1.2

Note: Shaded columns represent end member samples, other samples from core SC0802.

Table 11: Weight of evidence scoring approach for provenance determination of SC0802 samples

Sample ID	Depth (m)	WOE Count	% Dol	% IM	% SS	LS+Dol : IM	1 phi	2 phi	3 phi	3:1 phi
GSA #1	-1.97	+2					+	+		
GSA #2	-3.38	+1						+	0	
CG-1	-5.05	+1					+	+	0	-
GSA #3	-6.30	0						0	0	
GSA #4	-6.64	+7	+	+	+	+	0	+	+	+
GSA #5	-7.00	+1					-	+	0	+
GSA #6	-7.37	+2	-	+	-	+	0	+	0	+
CG-2	-7.81	+5	+	+	+	+	+	+	0	-
CG-3	-8.17	-3	-	-	+	-	-	+	0	-
CG-8	-9.29	+3	+	+	-	+	+	+	0	-
CG-9	-10.74	+5	+	+	+	+	+	+	0	-
GSA #7	-10.93	-2	-	+	+	+	-	-	-	-
GSA #8	-12.43	+1	+	+	+	+	-	-	0	-
GSA #9	-12.64	+1	+	+	+	+	-	0	-	-
GSA #10	-12.90	+1	+	+	+	+	-	-	0	-
GSA #11	-13.76	+1	+	+	-	+	0	0	0	-
GSA #12	-13.88	+2					-	+	+	+
GSA #13	-13.96	+6	+	+	+	+	+	+		
GSA #14	-14.10	+4	+	+	+	+	0	+	0	-
GSA #15	-14.28	+4	+	+	+	+	+	0	0	-
GSA #16	-16.88	+5	+	+	+	+	+	0		
GSA #17	-17.11	+3	+	+	+	+	0	0	0	-
GSA #18	-17.35	-1					0	0	0	-
GSA #19	-18.51	+2					0	+	0	+
GSA #20	-18.69	+2					0	+	0	+
GSA #21	-18.87	+3	+	+	+	+	0	0	0	-
GSA #22	-19.01	-2					-	0	0	-
GSA #23	-20.06	0						0	0	
GSA #24	-20.35	+2	-	+	-	+	0	+	0	+
CG-4	-21.54	+2	+	+	+	+	-	-		
GSA #25	-21.56	+6	+	+	+	+	0	+	0	+
GSA #26	-21.63	+7	+	+	+	+	+	+	0	+
GSA #27	-21.72	0	+	+	-	+	-	0	0	-
CG-5	-22.98	+4	+	+	+	+				
CG-6	-24.69	+4	+	+	+	+	0	+	0	-
GSA #28	-26.06	+3					0	+	+	+
GSA #29	-26.28	+2					-	+	+	+
GSA #30	-26.57	0					-		0	+
CG-7	-29.09	+3	-	+	+	+	0	0	0	+
Erie Lobe criteria (+)			>11.5%	<28.7%	<6.5%	>1.68	18-53	24-154	>182	>3.6
Saginaw Lobe criteria (-)			<11.5%	>28.7%	>6.5%	<1.68	<18	<10	<24	<3.6

Note: Shading indicates samples with all data available. "+" is Erie Lobe, "-" is Saginaw Lobe, and "0" is neither or both.

Table 12: Discriminant function analysis scores and classification of SC0802 samples

Sample ID	Discriminant Score	Assigned Group	Classification
GSA #1	4.298	1	1
GSA #2	0.306	1	1
CG-1	3.903	1	1
GSA #3	2.270	1	1
GSA #4	1.264	1	1
GSA #5	2.568	1	1
GSA #6	2.836	1	1
CG-2	3.777	1	1
CG-3	-8.563	2	2
CG-8	-2.344	2	2
CG-9	-2.709	2	2
GSA #7	-3.049	2	2
GSA #8	-1.925	2	2
GSA #9	0.469	2	1
GSA #10	0.552	2	1
GSA #11	-2.519	2	2
GSA #12	6.227	1	1
GSA #13	3.843	1	1
GSA #14	-2.317	1	2
GSA #15	1.152	1	1
GSA #16	2.315	1	1
GSA #17	1.598	1	1
GSA #18	1.089	1	1
GSA #19	3.429	1	1
GSA #20	3.215	1	1
GSA #21	1.257	1	1
GSA #22	0.867	1	1
GSA #23	1.869	1	1
GSA #24	5.008	1	1
CG-4	-0.736	1	2
GSA #25	3.466	1	1
GSA #26	4.151	1	1
GSA #27	-1.425	1	2
CG-5	5.409	1	1
CG-6	0.677	1	1
GSA #28	4.200	1	1
GSA #29	6.549	1	1
GSA #30	2.856	1	1
CG-7	1.921	1	1

Correctly classified = 87.18%  
Hotelling t2: p(same)= 0.029

Table 13: Discriminant function per analysis

Analysis	Discriminant Function
Mean grain size	0.7098
Skewness	-0.0134
Dolomite lithology (%)	-0.1286
IM lithology (%)	-1.2992
Sandstone lithology (%)	-0.3173
LS+Do1 : IM lithology	-4.5892
Magnetic susceptibility (1 phi)	0.0311
Magnetic susceptibility (2 phi)	0.0208
Magnetic susceptibility (3 phi)	0.0310
Magnetic susceptibility (3:1 phi)	-0.1980

Table 14: Summary of sediment provenance sources for Eel River meltwater channel deposits

	Anderson 1957				Ducey 2013			Bedrock Maps/USGS Mr.Data <sup>(1)</sup>		
	Description	Origin	Age	Location	Origin	Age	Location	Origin	Age	Location
<b>Erie Lobe</b>										
Limestone	Brown, gray, black, dense, fossiliferous	Trenton and Black River Limestones	Ordovician	Lake Ontario	1-Wabash Fm. 2-Salina Gr. 3-Antrim Sh. 4-Muscatatuck Gr. 5-Waldron Shale 6-Monroe Fm. 7-Ohio Fm. 8-Delaware Fm. 9-Rochester Fm.	Devonian and Silurian	1-5: NE Indiana, 6-9: northern Ohio	Coldwater Sh, Traverse Gr., Detroit River Gr.	Mississippian and Devonian	Northern Ohio
	Brown to buff, porous	Uncertain	Devonian	NW Ohio and NE Indiana						
Dolomite	Buff to gray-black, cherty, porous		Silurian		1-Wabash Fm. 2-Salina Gr. 3-Cataract Fm. 4-Muscatatuck Gr. 5-Waldron Shale 6-Pleasant Mills Fm. 7-Detroit River Fm. 8-Monroe Fm. 9-Niagara Fm. 10-Delaware Fm. 11-Rochester Fm. 12-Sylvania SS	Devonian and Silurian	1-7: NE Indiana, 8-12: northern Ohio	Traverse Gr., Detroit River Gr., unnamed dolomite, Lockport Fm.	Mississippian, Devonian and Silurian	Northern Ohio
Igneous/Metamorphic			Precambrian							
Shale	gray to black, fissile	New Albany Shale	Upper Devonian	Northern Indiana and NW Ohio				Sunbury Sh, Bedford Sh, Traverse Gr.	Mississippian and Devonian	Northern Ohio
Sandstone	reddish brown, fine grained friable	Sylvania SS	Pennsylvanian	NW Ohio, SE Mich	1-Coldwater Sh 2-Antrim Sh 3-Traverse Fm. 4-Muscatatuck Group 5-Waverly Fm. 6-Ohio Fm. 7-Delaware Fm.	Devonian and Silurian	1-4: NE Indiana, 5-7: northern Ohio	Sunbury Sh, Bedford Sh, Detroit River Gr.	Mississippian and Devonian	Northern Ohio
Siltstone		Ohio Shale	Devonian	NW Ohio, NE Indiana				Coldwater Sh	Mississippian	NW Ohio
Chert			Silurian		Wabash Fm, Monroe Fm	Devonian and Silurian	1-NE Indiana, 2 northern Ohio			
<b>Saginaw Lobe</b>										
Limestone	Brown, gray, black, dense, fossiliferous	Trenton and Black River Limestones	Ordovician	Lake Ontario	1-Bass Islands Gr., Racine Fm. 2-Berea SS and Bedford Sh. 3-Traverse Group, Rogers City LS			Saginaw Fm, Marshall Fm, Coldwater Sh	Pennsylvanian and Mississippian	Central and Southern Michigan
	Buff, porous, sandy	Bayport Limestone	Mississippian				Michigan			
Dolomite	Buff to gray, porous to dense, cherty	Niagara Series	Silurian	Georgian Bay	1-Bass Islands Gr., Racine Fm. 2-Berea SS 3-Bedford Sh. 4-Clinton Group 5-Lucas Fm., Sylvania SS			Coldwater Sh	Mississippian	Southern Michigan
Igneous/Metamorphic			Precambrian							
Shale	gray to black, fissile	New Albany Shale	Upper Devonian	Northern Indiana (only 1 found)				Grand River Fm, Saginaw Fm, Marshall Fm, Coldwater Sh	Pennsylvanian and Mississippian	Central and Southern Michigan
Sandstone	buff white, fine, well cemented, qtz SS	Marshall, Parma	Mississippian, Pennsylvanian	Central Michigan	1-Marshall SS 2-Berea SS and Bedford Sh 3-Traverse Group, Rogers City LS			Grand River Fm, Saginaw Fm, Marshall Fm, Coldwater Sh	Pennsylvanian and Mississippian	Central and Southern Michigan
Siltstone	brown to red, poorly indurated	unknown	Devonian	Southern Michigan				Marshall Fm, Coldwater Sh	Pennsylvanian and Mississippian	Southern Michigan
Chert			Silurian	Georgian Bay	Racine Fm, Bass Islands Group		Michigan			

(1) Michigan DNR (1987), Ohio Division of Geological Survey (1990, 2006), <http://mrdata.usgs.gov>



## FIGURES

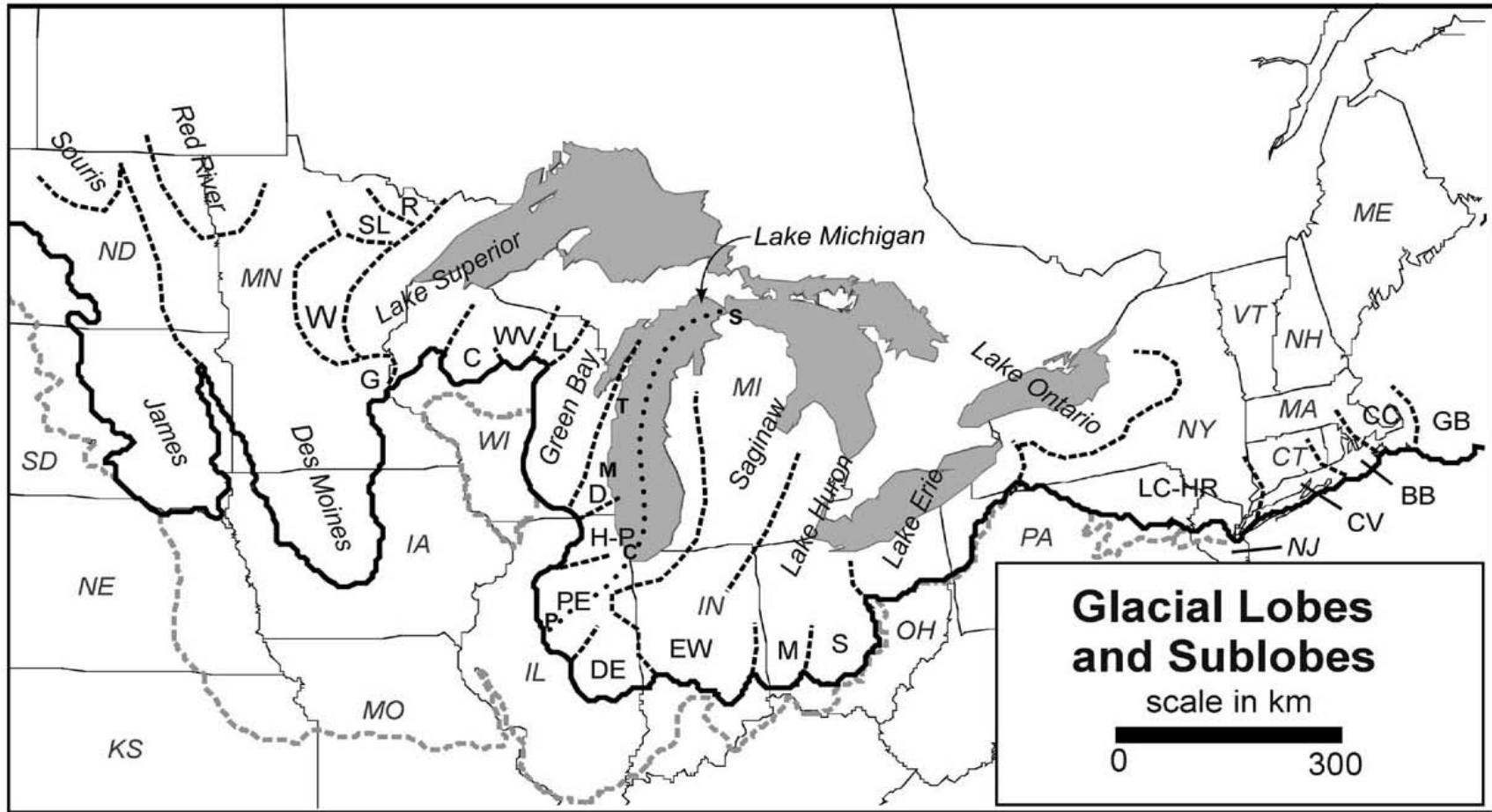


Figure 1. Glacial lobes of southern Laurentide Ice Sheet during the late Wisconsin glaciation (Mickelson and Colgan, 2003). Light dashed line shows maximum extent of ice sheet.

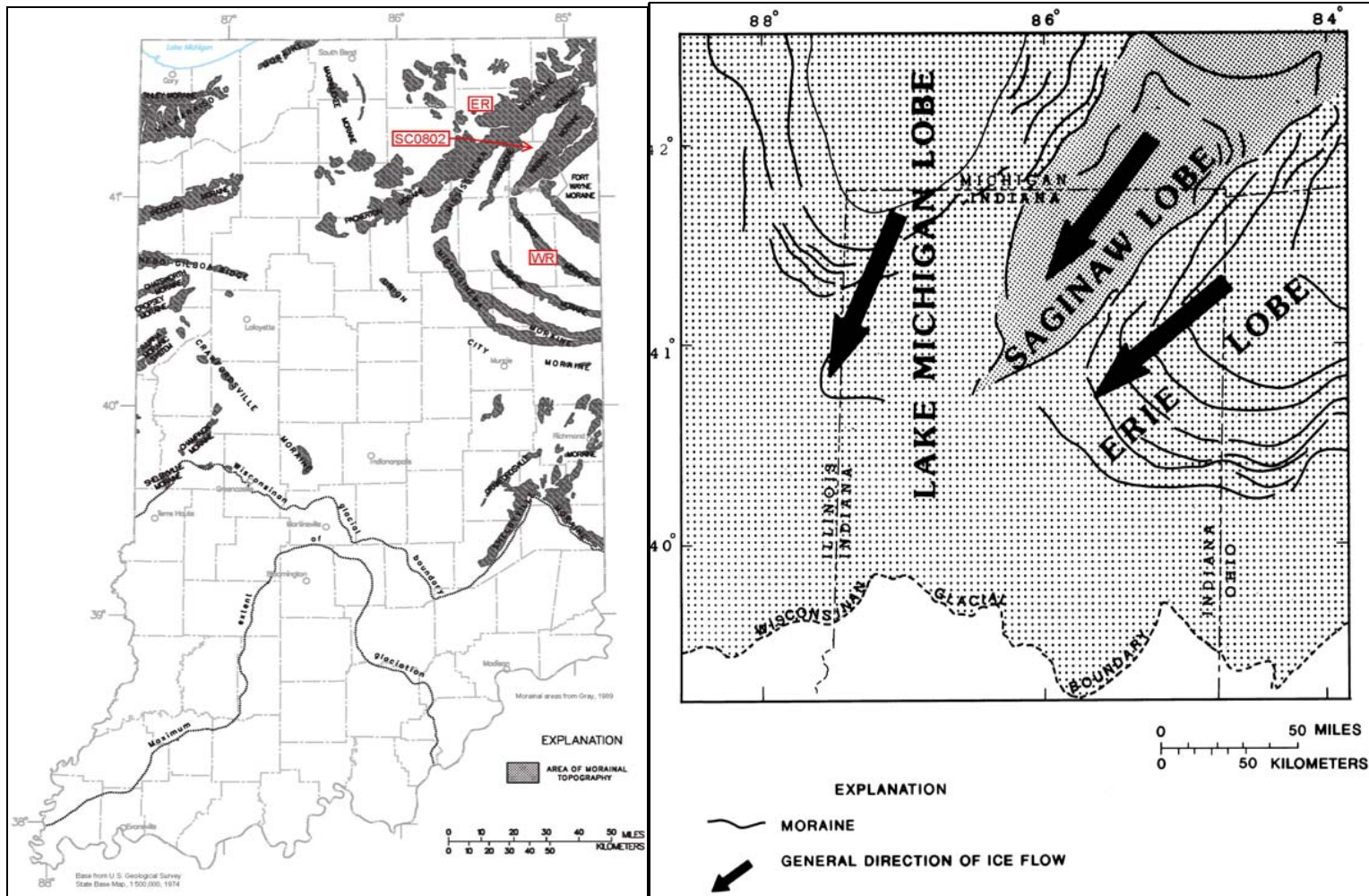


Figure 2. Sample locations and orientations of ice sheet lobes in Indiana. ER denotes Elkhart River end member sample representative of the Saginaw Lobe and WR denotes Wabash River end member sample from the Erie Lobe. Adapted from Fenelon et al. (1994).

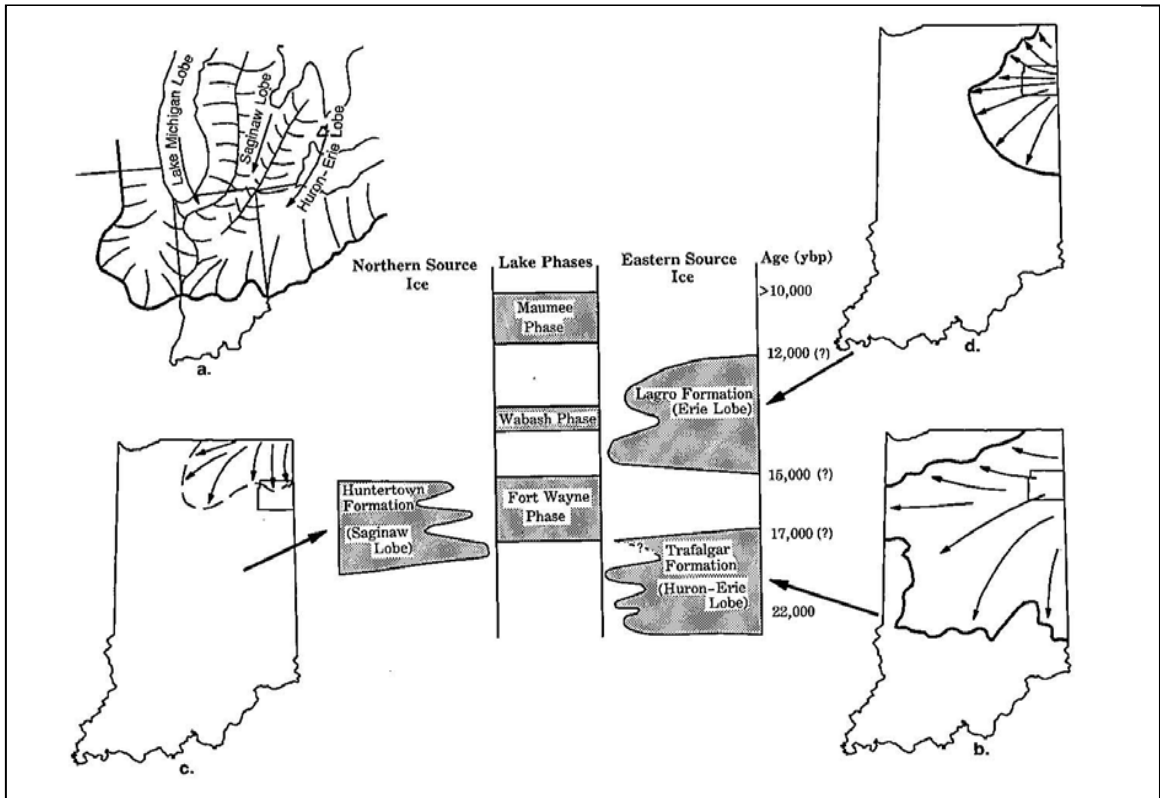


Figure 3. Distribution of glacial lobes and timing of related deposits in Indiana (Fleming, 1994). There is currently debate as to whether or not the Saginaw lobe deposited the Huntertown Formation.

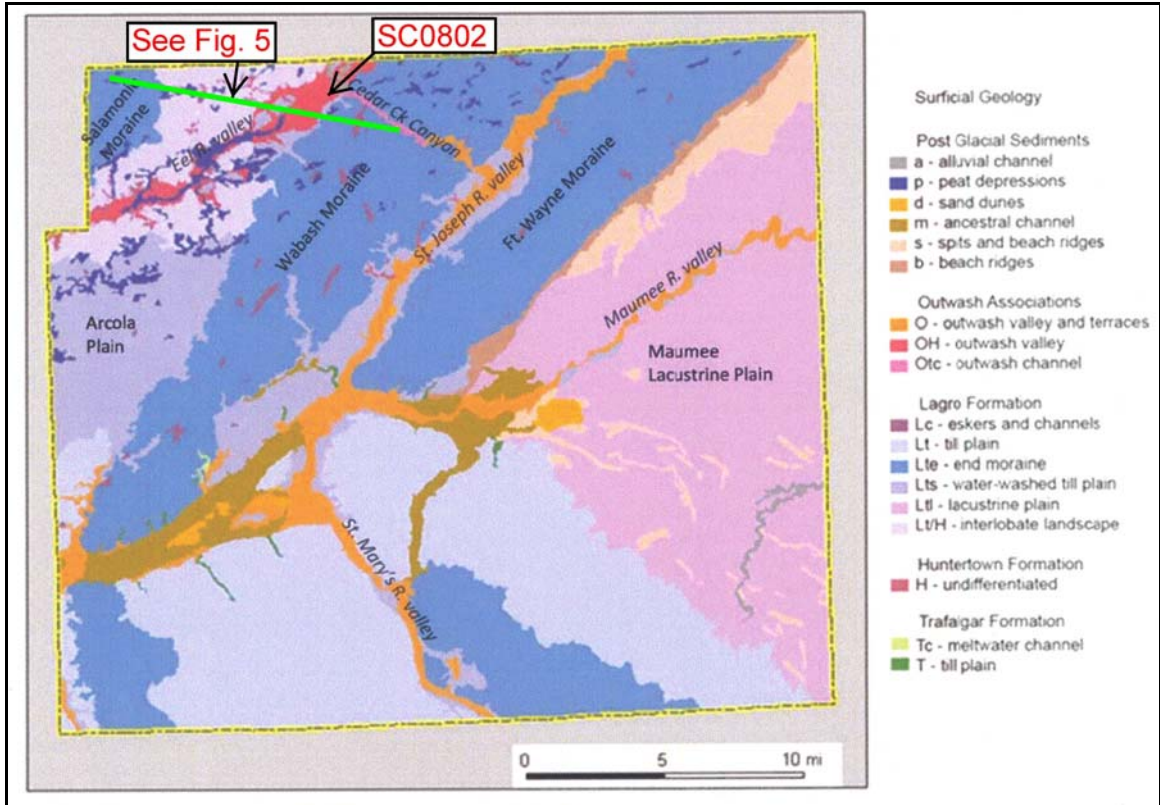


Figure 4. Surficial geology of Allen County, Indiana (Letsinger, 2012) and location of core SC0802. The study area is near the intersection of the Eel River outwash valley with the Cedar Creek Canyon in northern Allen County. Green line depicts orientation of conceptual model shown in Fig. 5.

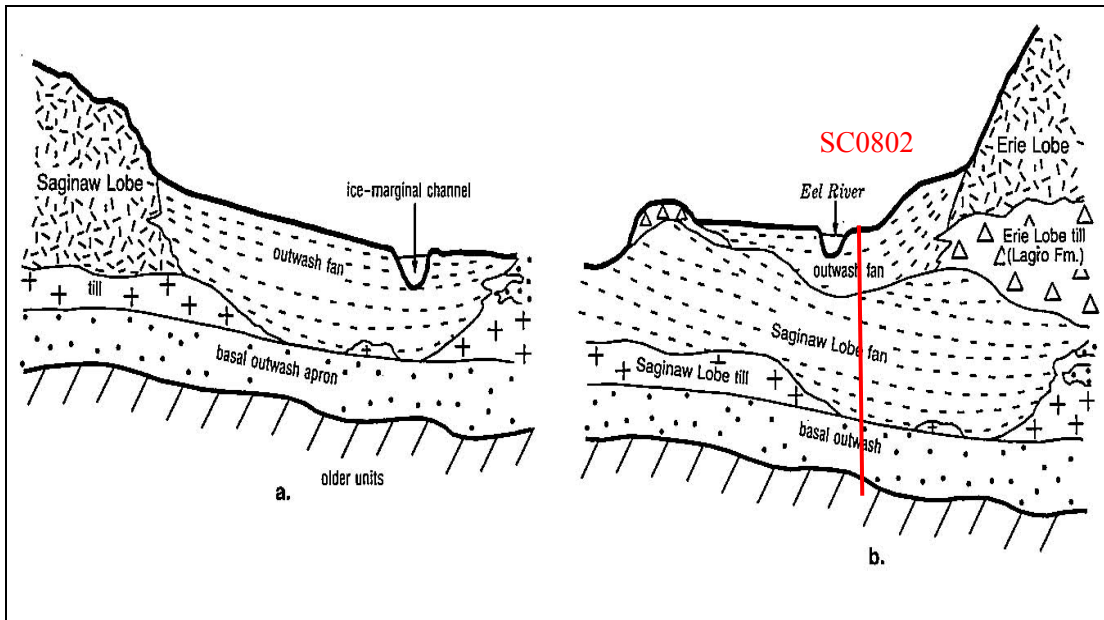


Figure 5. Conceptual time-transgressive model of the glacial deposits in the Eel River paleo meltwater channel developed by Fleming (1994). (a) Fleming determined that the Saginaw Lobe outwash fan deposits are ice-contact deposits that comprise the Hunteartown Formation. (b) Later, the Erie Lobe deposited an outwash fan when it was at its terminus along the Wabash Moraine (Fig. 4). The location of core SC0802 is depicted and would be adjacent to the Eel River, which is currently a paleo meltwater channel and not a surficial river at this location. The head of the modern Eel River is a few miles southwest of the study area.

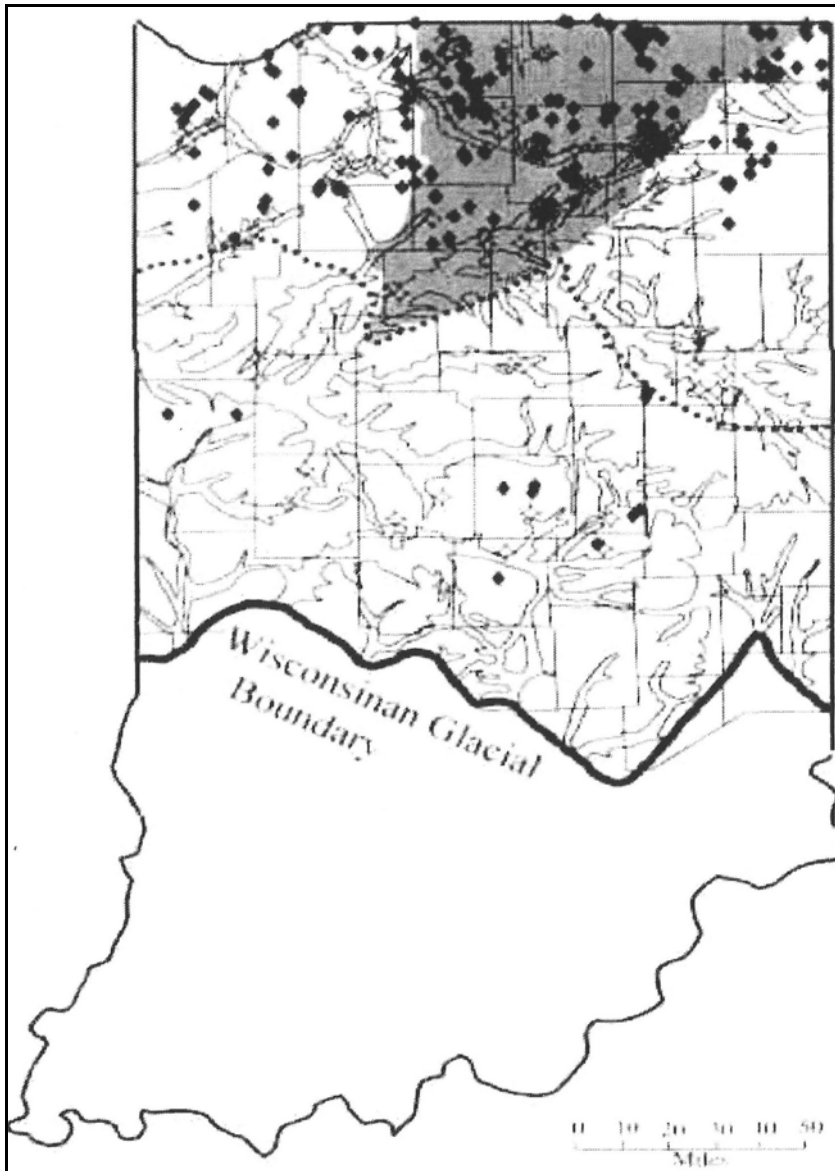


Figure 6. Map of Indiana showing peat bogs and Saginaw Lobe orientation (Swinehart and Parker, 2002). Black dots indicate commercial quality peat deposits, gray shading infers Saginaw Lobe position circa 15 ka.

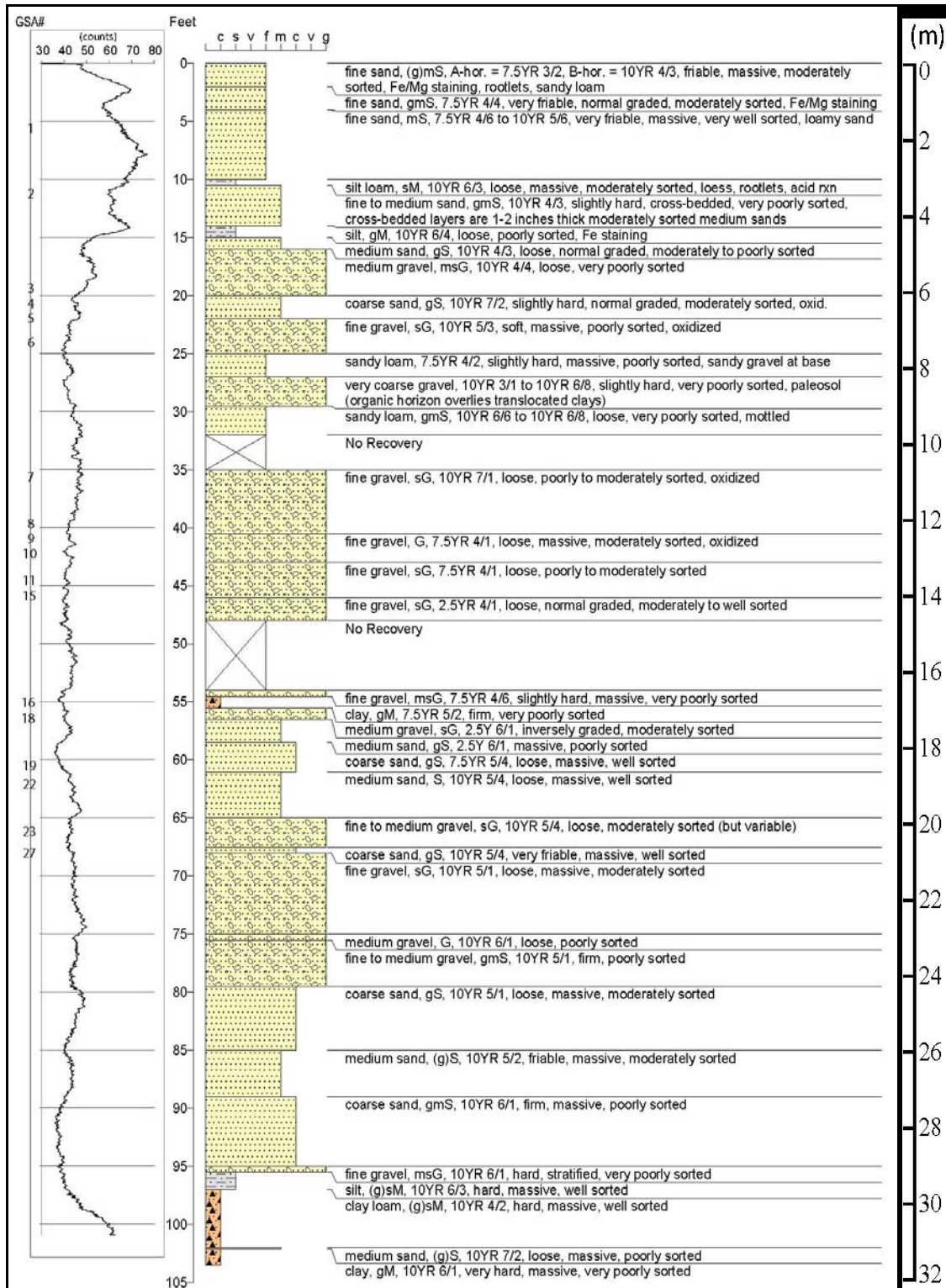


Figure 7. Boring log of SC0802 (Letsinger, 2012). The GSA numbers on the left side indicate samples collected by the IGS for grain size analyses. The graph is a gamma ray log collected by the IGS during installation of the core.



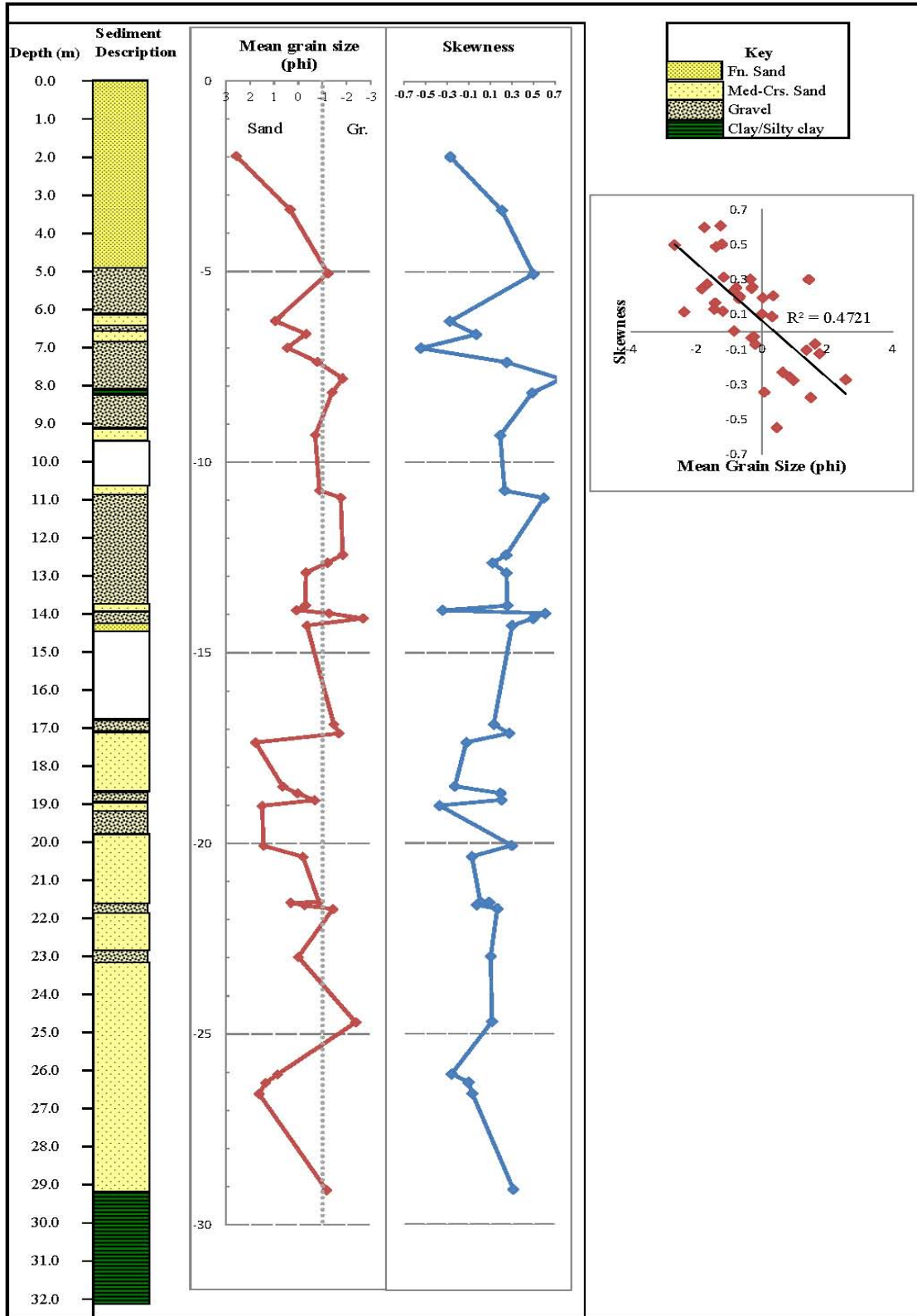


Figure 8. Grain size distribution of core SC0802. Sediment interpretation derived from IGS boring log descriptions (Letsinger, 2012) and the SC0802 photolog (Appendix A). Mean grain size and skewness relationships are shown.

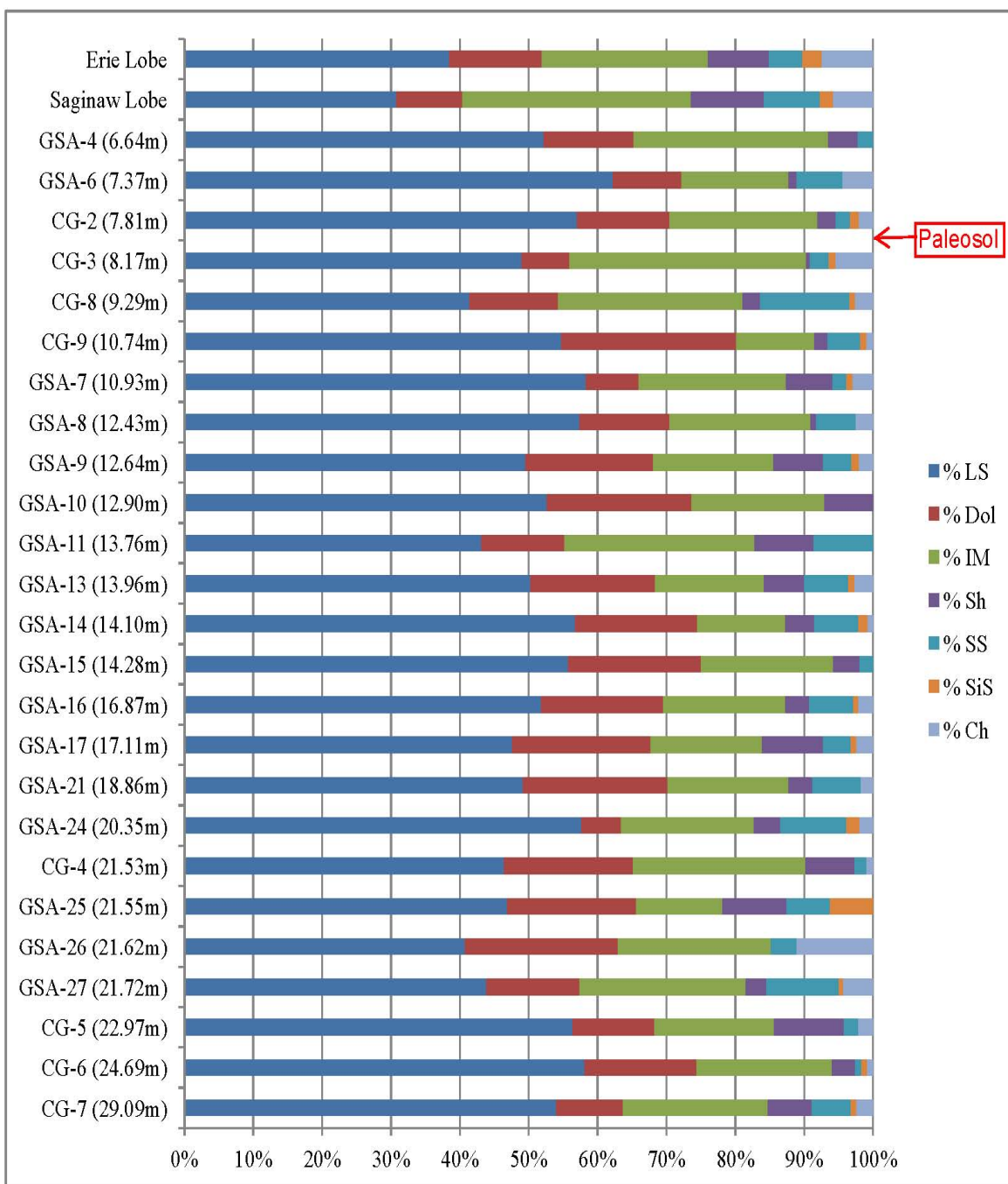


Figure 9. Gravel lithology distribution for Erie Lobe and Saginaw Lobe end members shown with samples from core SC0802. Depth below ground surface is shown next to the sample identifications. LS=Limestone, Dol=Dolomite, IM=Igneous/Metamorphic, Sh=Shale, SS=Sandstone, SiS=Siltstone, Ch=Chert.

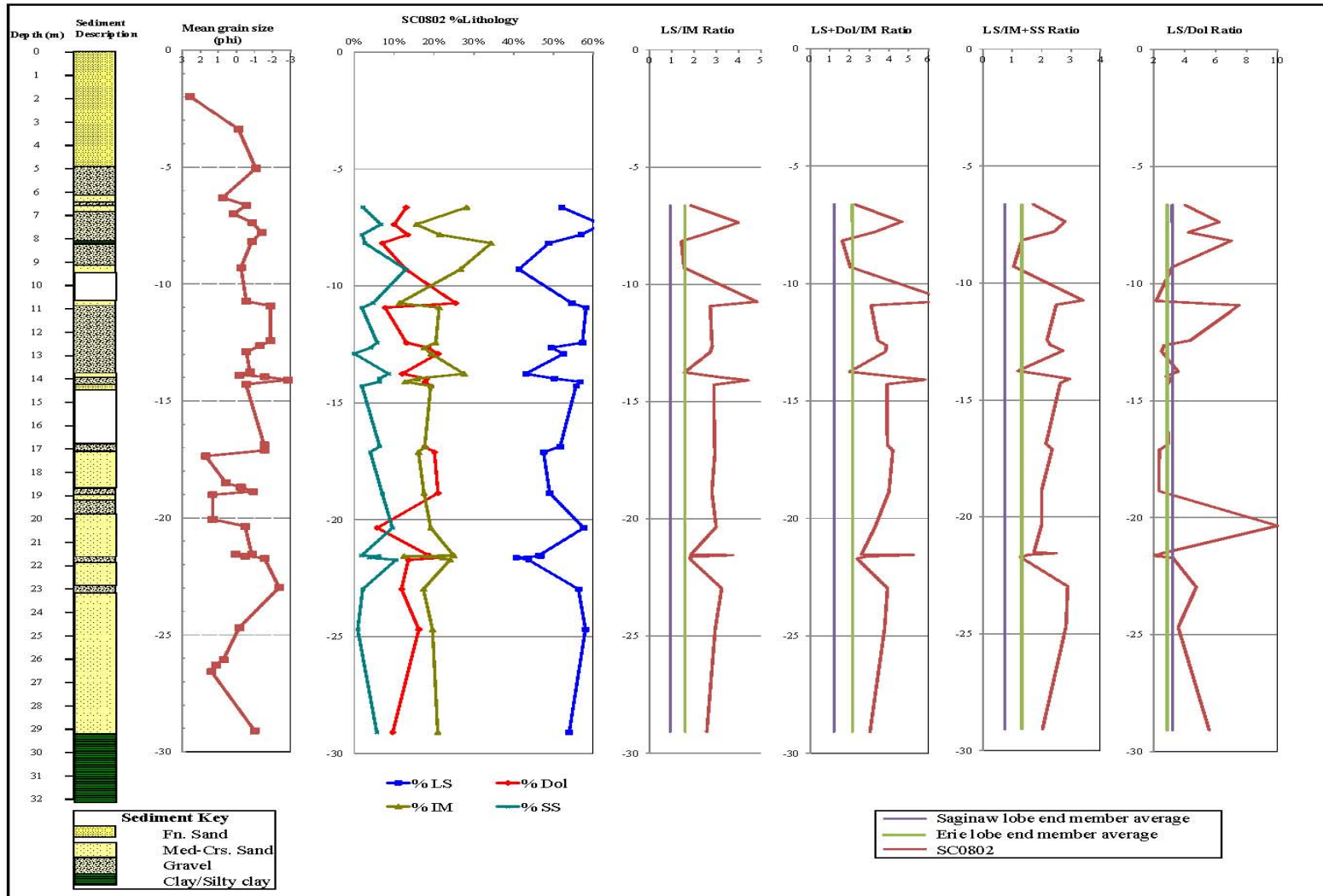


Figure 10. Gravel lithology relationships in SC0802. Sediment units derived from IGS boring log (Letsinger, 2012) and SC0802 photolog interpretation (Appendix A). LS=Limestone, Dol=Dolomite, IM=Igneous/Metamorphic, SS=Sandstone.

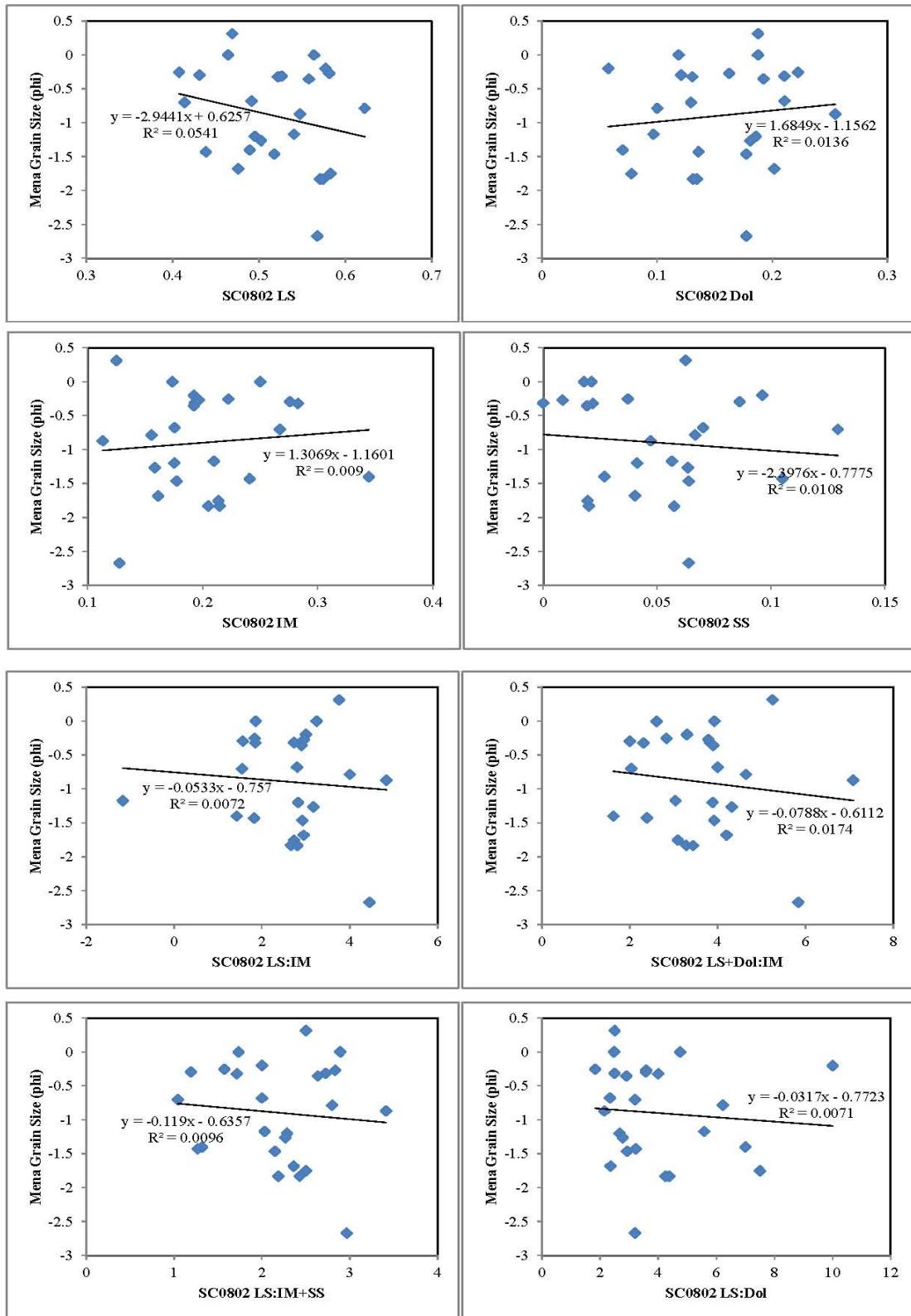


Figure 11. Comparison of gravel lithology and grain size. Only samples with 15 or more gravel clasts are plotted.

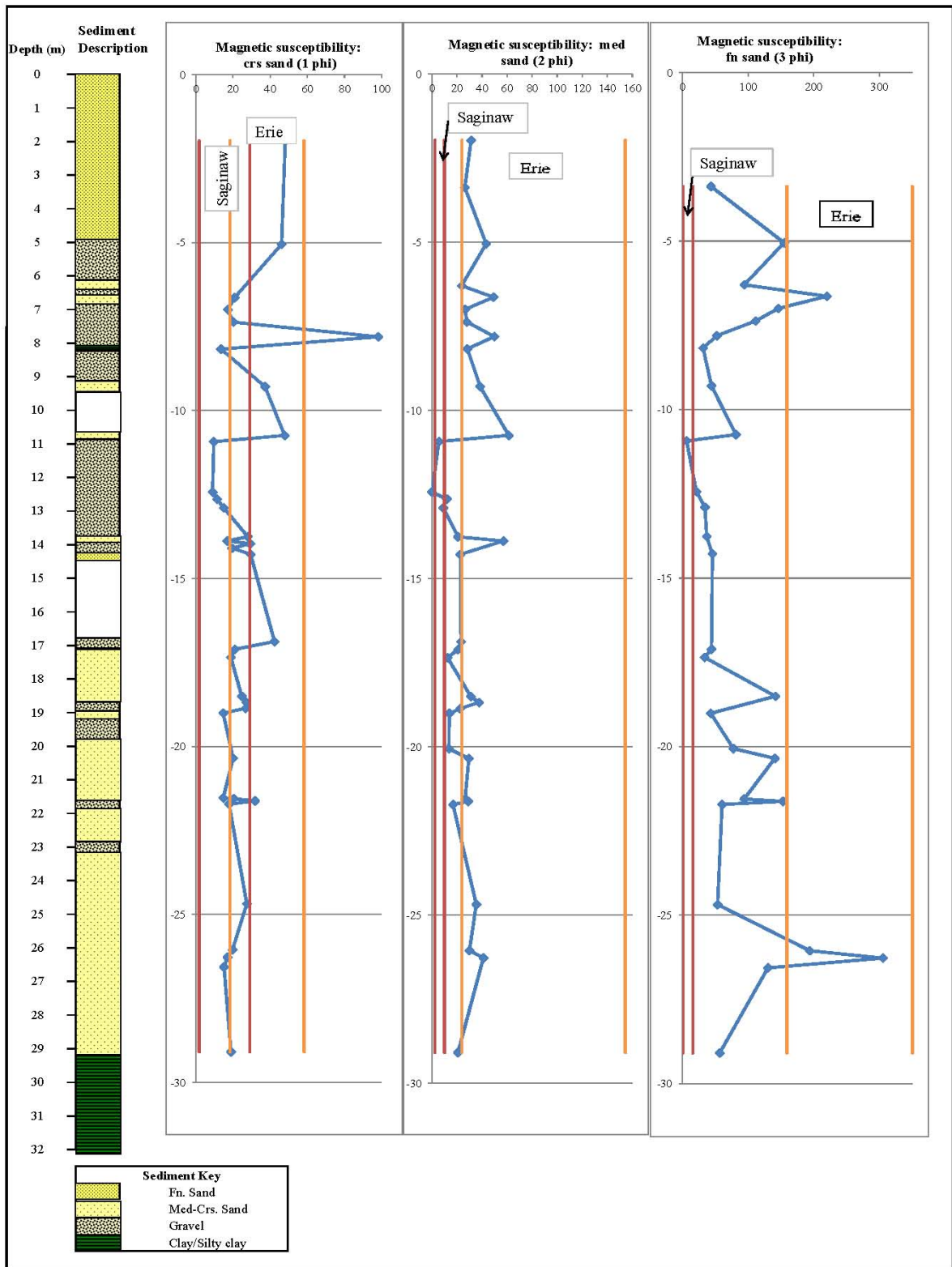


Figure 12. Magnetic susceptibility in CGS units of sand size fraction samples from core SC0802. End member magnetic susceptibility is shown with the lower and upper boundaries of two standard deviations.

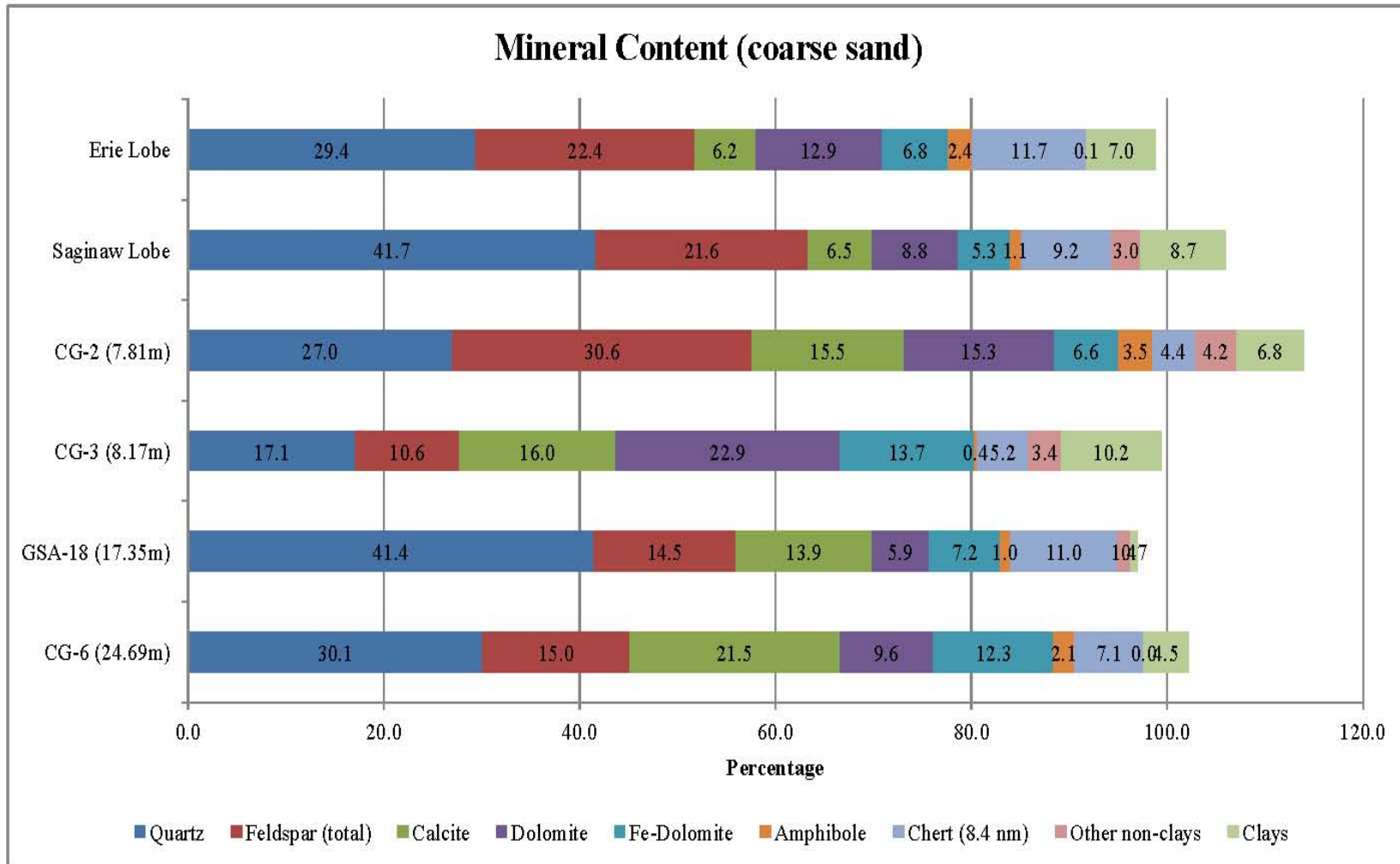


Figure 13. Quantitative X-ray diffraction of coarse sand sediments. Individual feldspars are consolidated into total feldspar.

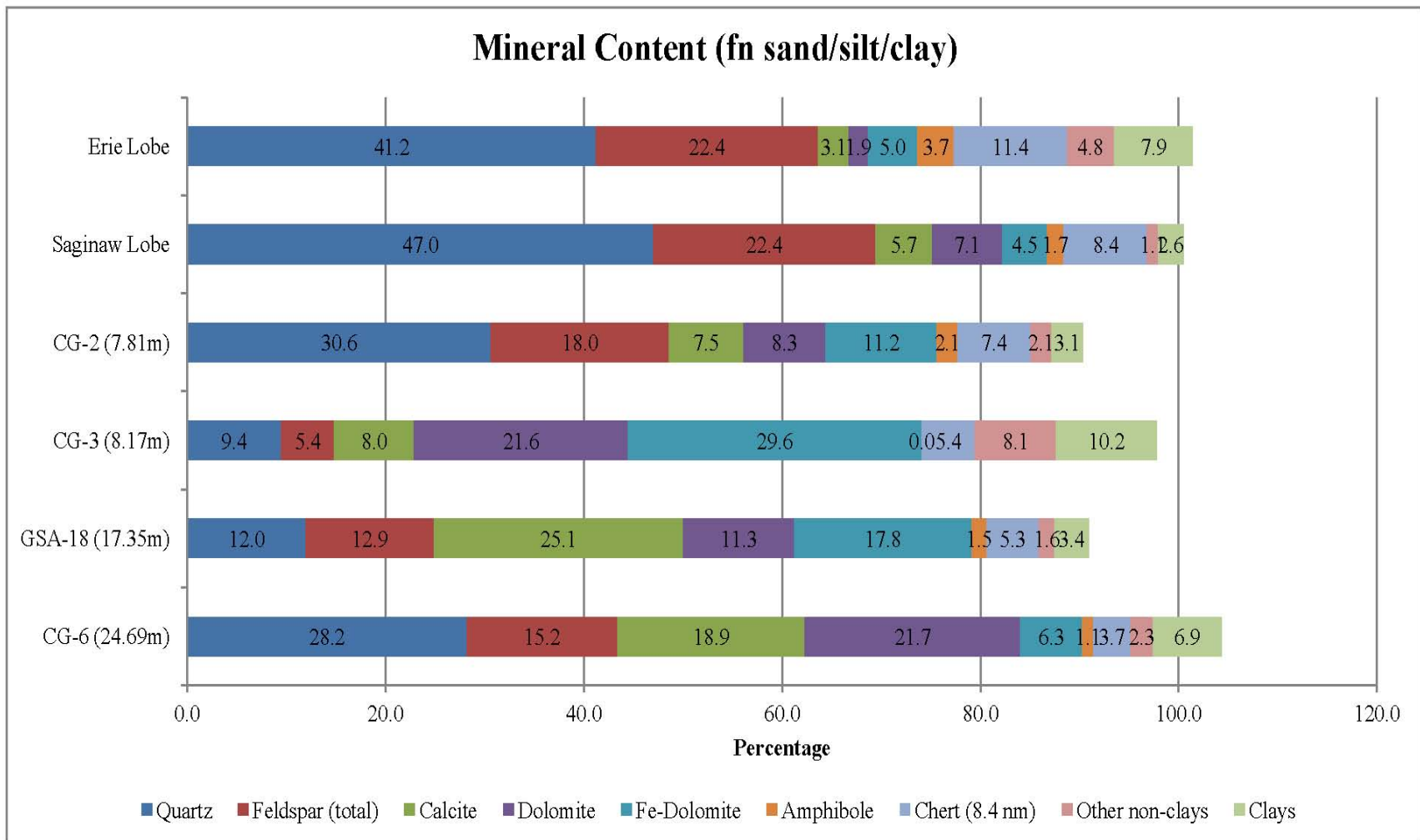


Figure 14. Quantitative X-ray diffraction of fine sand/silt/clay sediments. Individual feldspars are consolidated into total feldspar.

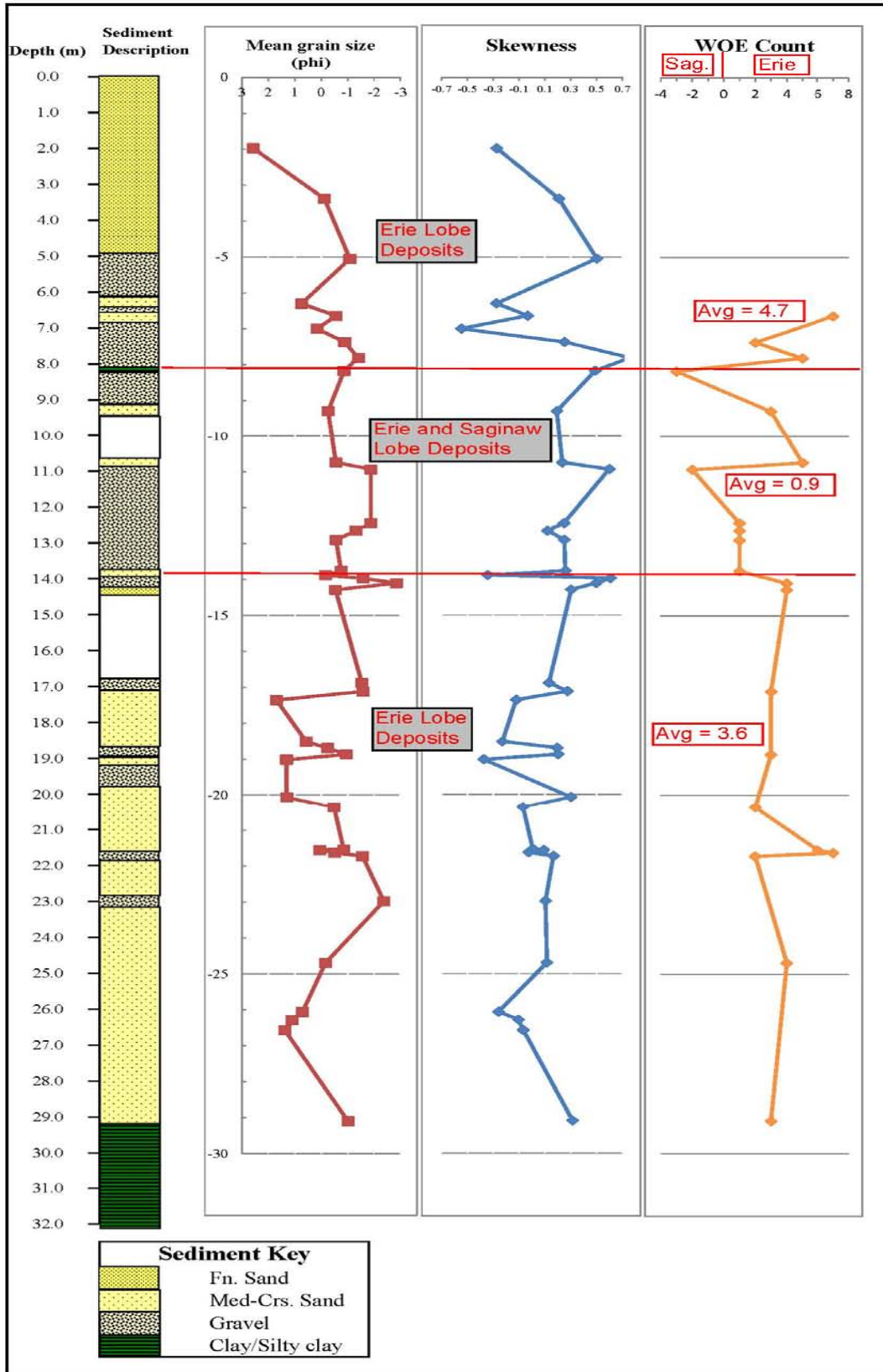


Figure 15. Weight of evidence (WOE) interpretation of SC0802 provenance. Mean grain size and skewness also shown.



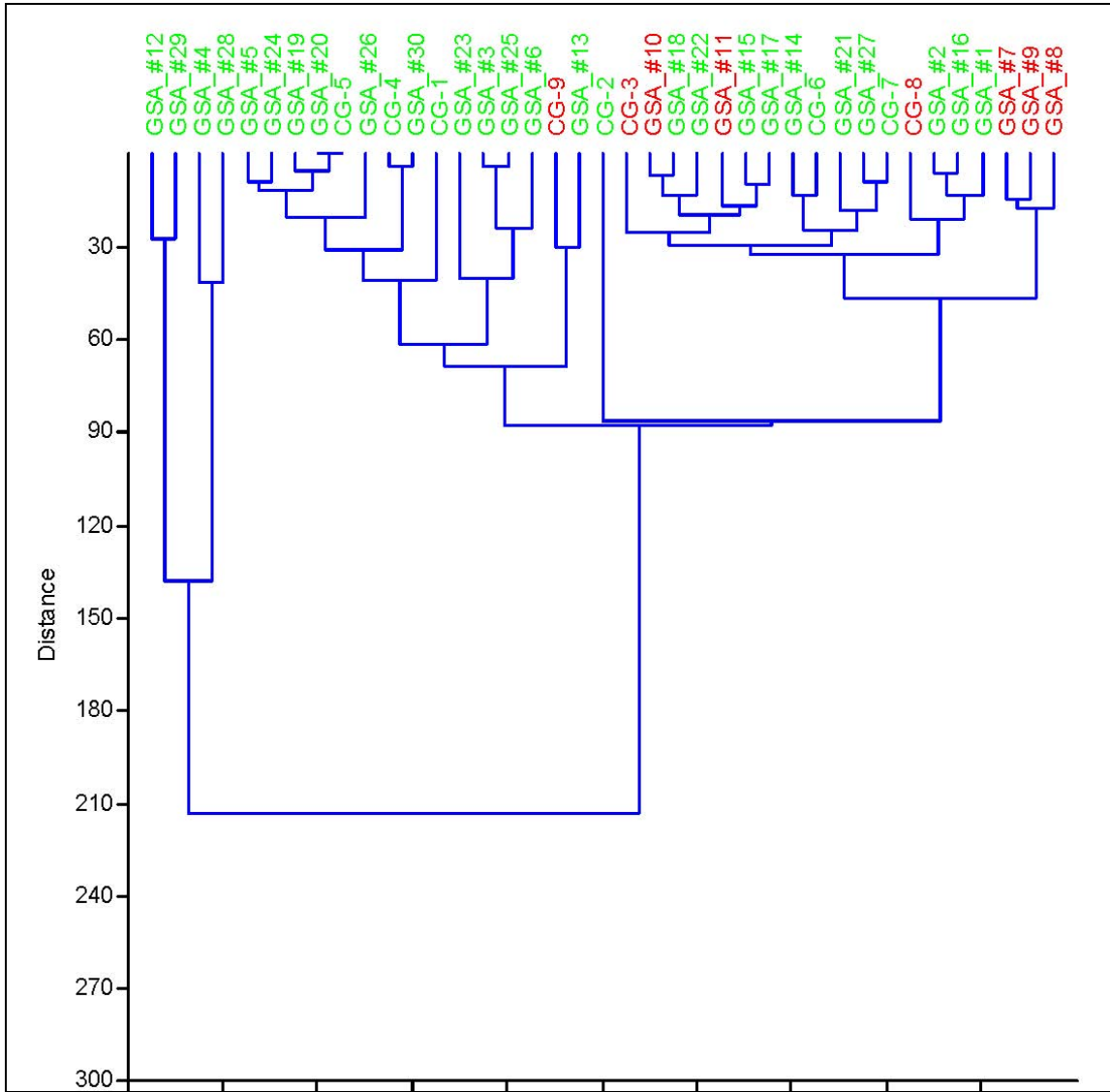


Figure 16. Hierarchical cluster analysis of SC0802 samples. Green samples are Erie Lobe deposits; red samples are mixed Erie and Saginaw Lobe deposits. This dendrogram uses the Euclidean similarity measure, and the cophenetic correlation coefficient is 0.73.

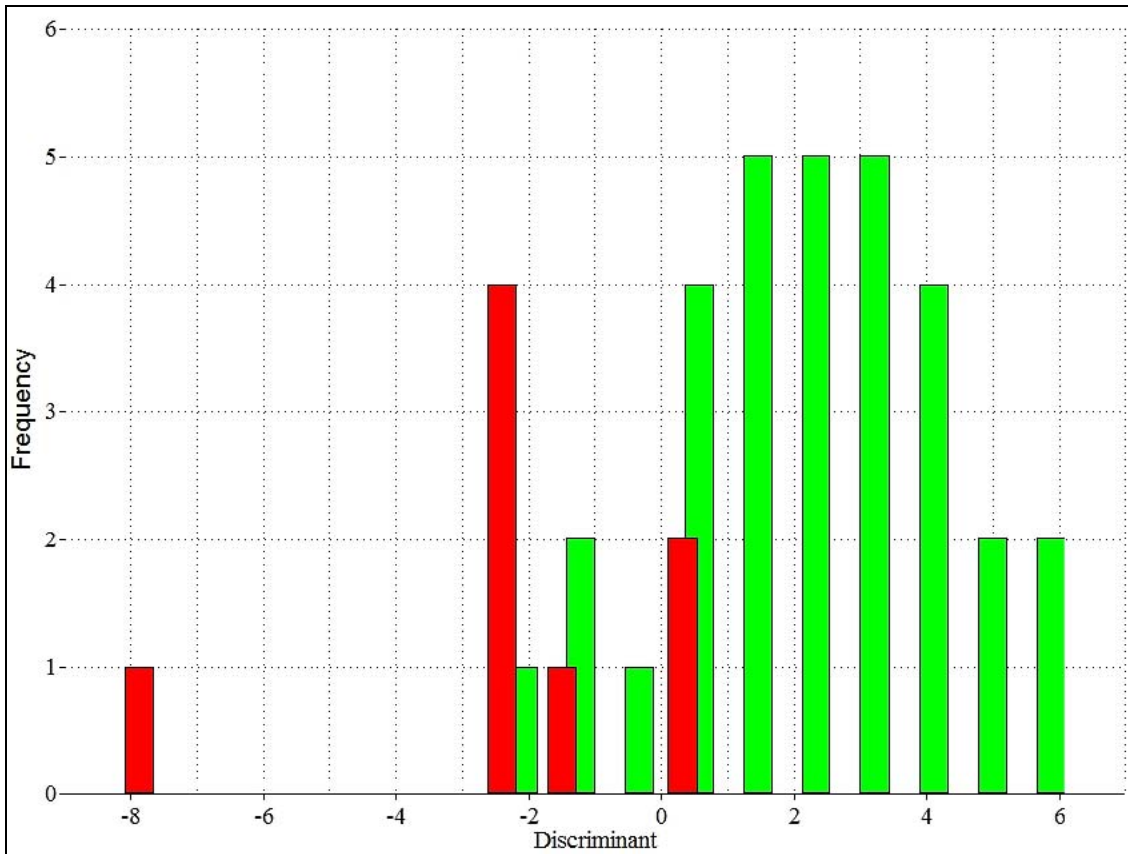


Figure 17. Discriminant function analysis of SC0802 samples. Green bars are representative of Erie Lobe deposits; red bars are representative of mixed Erie and Saginaw Lobe deposits. Refer to Table 14 for the individual sample discriminant scores.

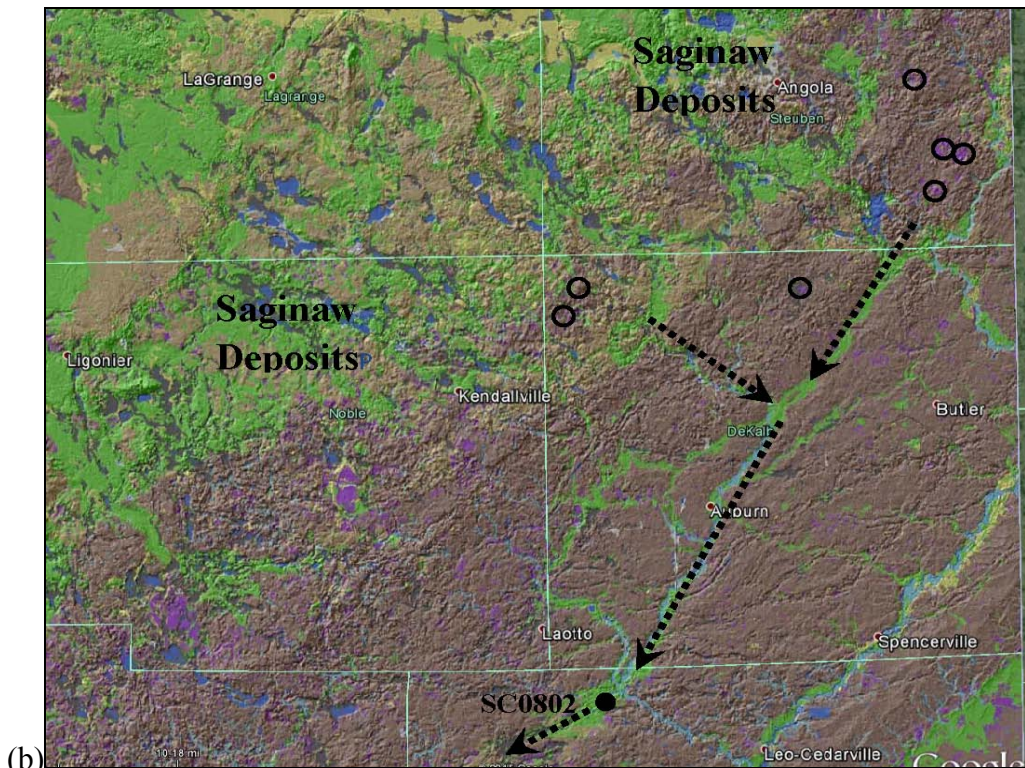
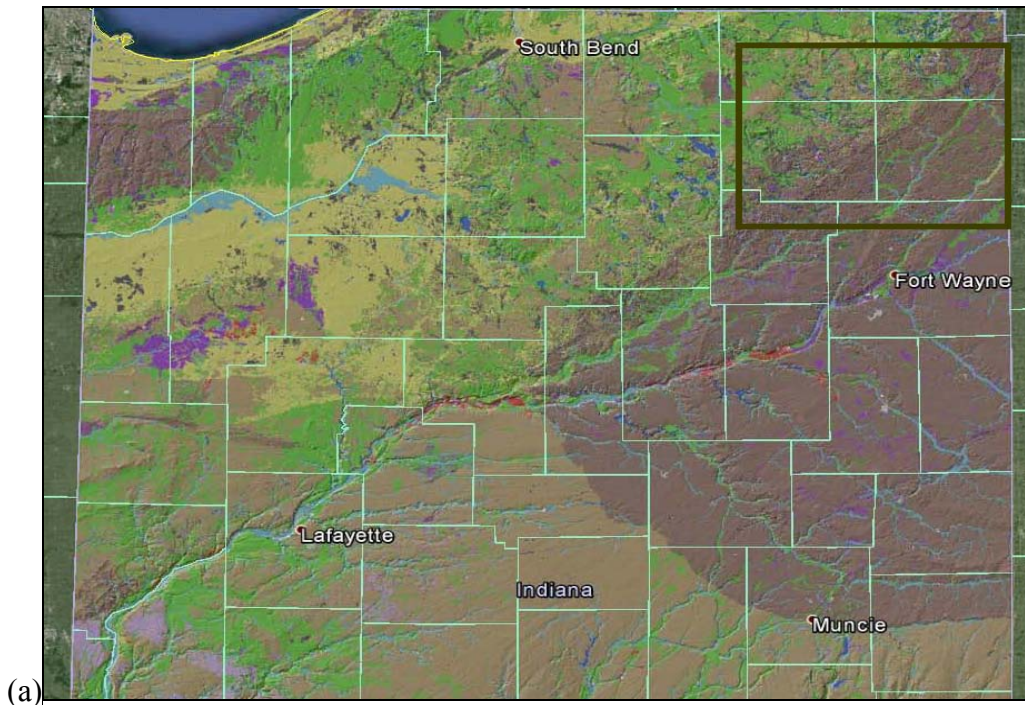


Figure 18. Map showing dominant parent material of soil (ISEE, 2014). Brownish purple is clayey Wisconsin till (Lagro), green is outwash, blue is old alluvium, light blue is recent alluvium, yellow is eolian sand, and purple is lacustrine deposits. (a) northern Indiana. (b) northeastern portion of Indiana. Arrows depict possible flow paths of Saginaw sediments in outwash deposits to SC0802. Circles highlight notable surficial lacustrine deposits.

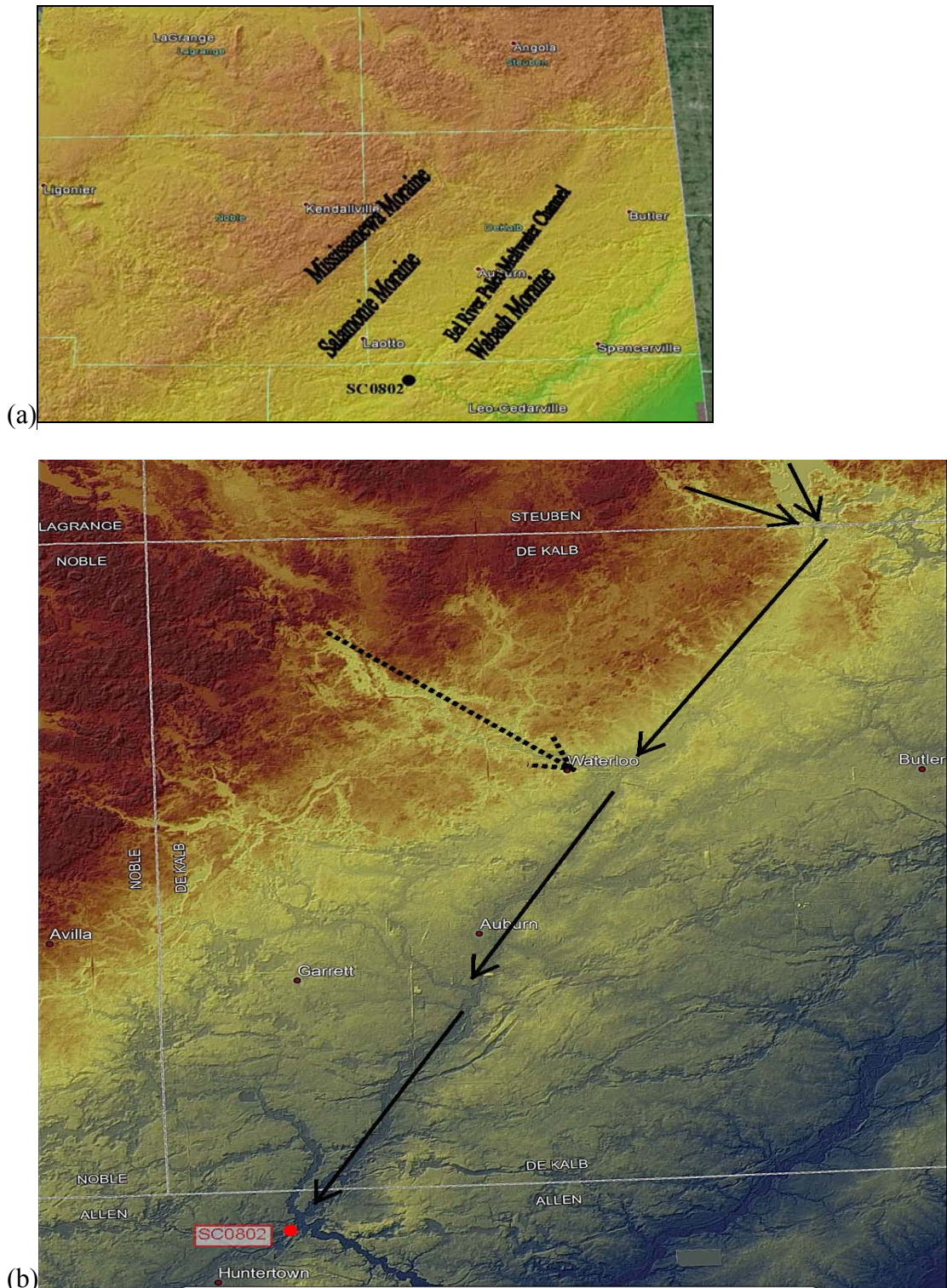


Figure 19. Topography and LiDAR maps. (a) Topography and notable features associated with the Eel River paleo meltwater channel (ISEE, 2014). (b) LiDAR DEM imagery of DeKalb County and surrounding areas (ISDP, 2015). Solid arrows depict Eel River paleo meltwater channel and suspected source of Saginaw deposits at SC0802. Dashed arrow is an outwash channel that likely drained into the Eel River paleo meltwater channel.

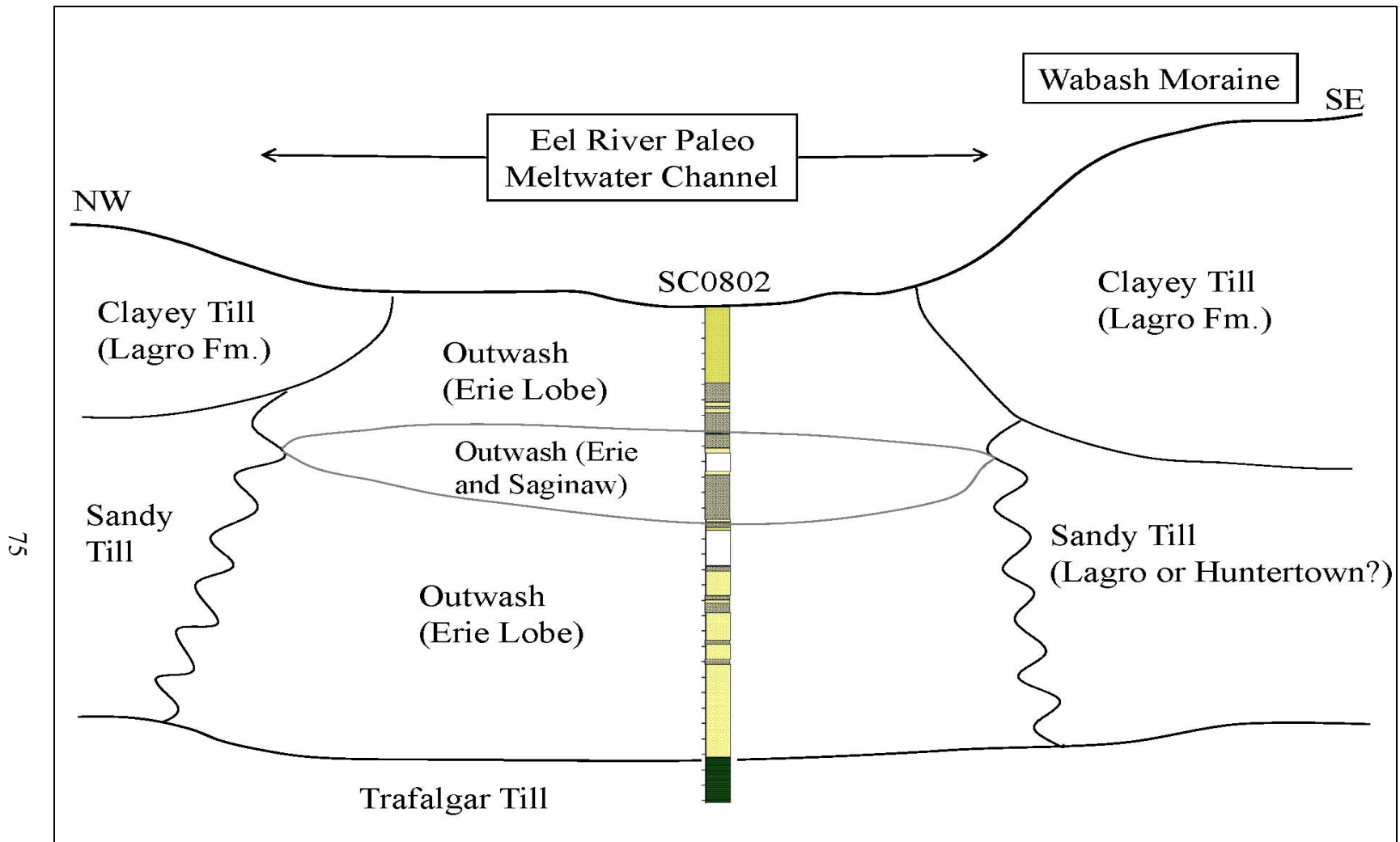
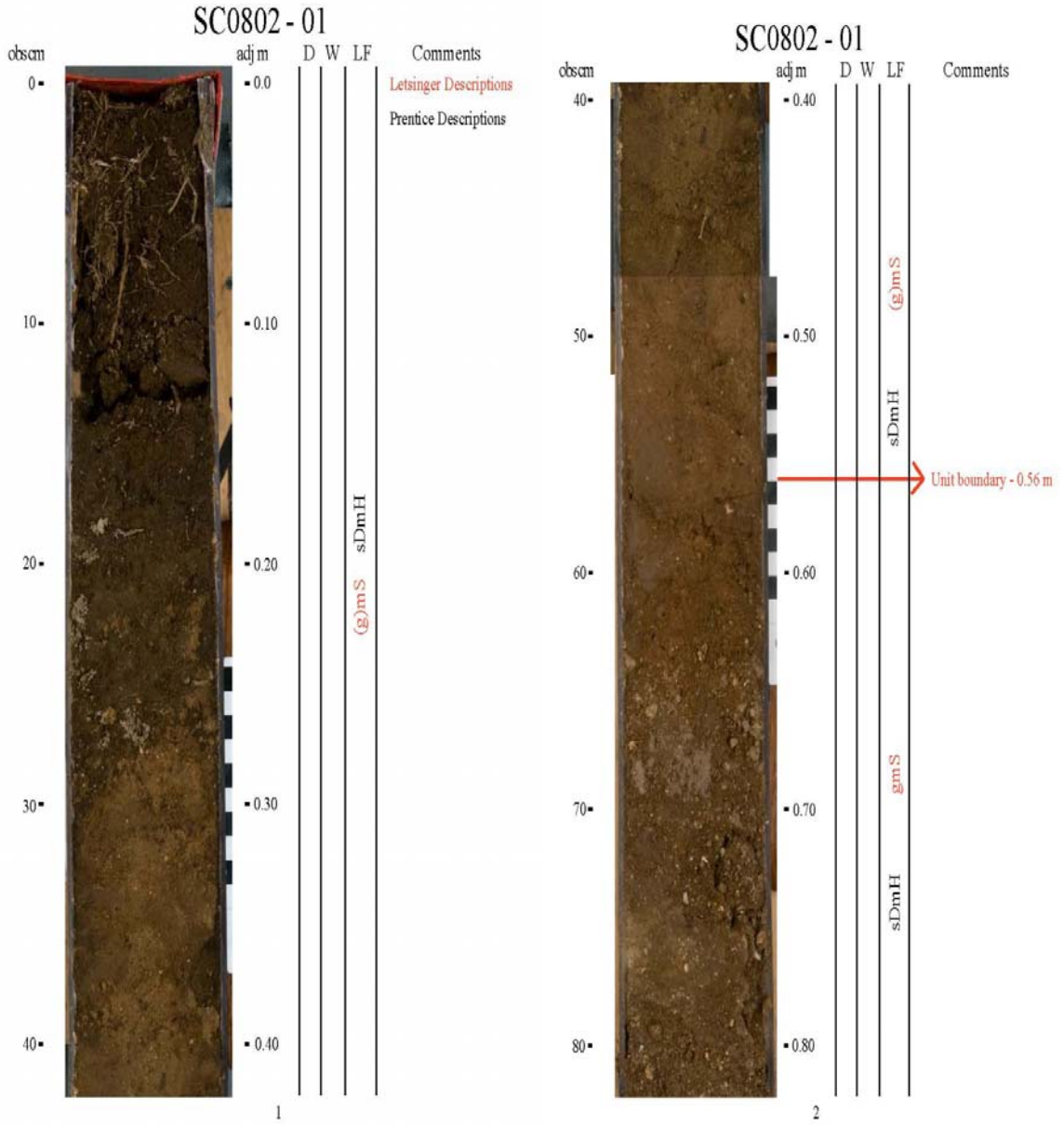


Figure 20. Conceptual cross section of Eel River paleo meltwater channel at SC0802. This is an alternative interpretation of Fig. 5, which was proposed by Fleming (1994). Till stratigraphy modified from Fleming (1994, Plate 6). Vertically exaggerated and not to scale.

## APPENDICES

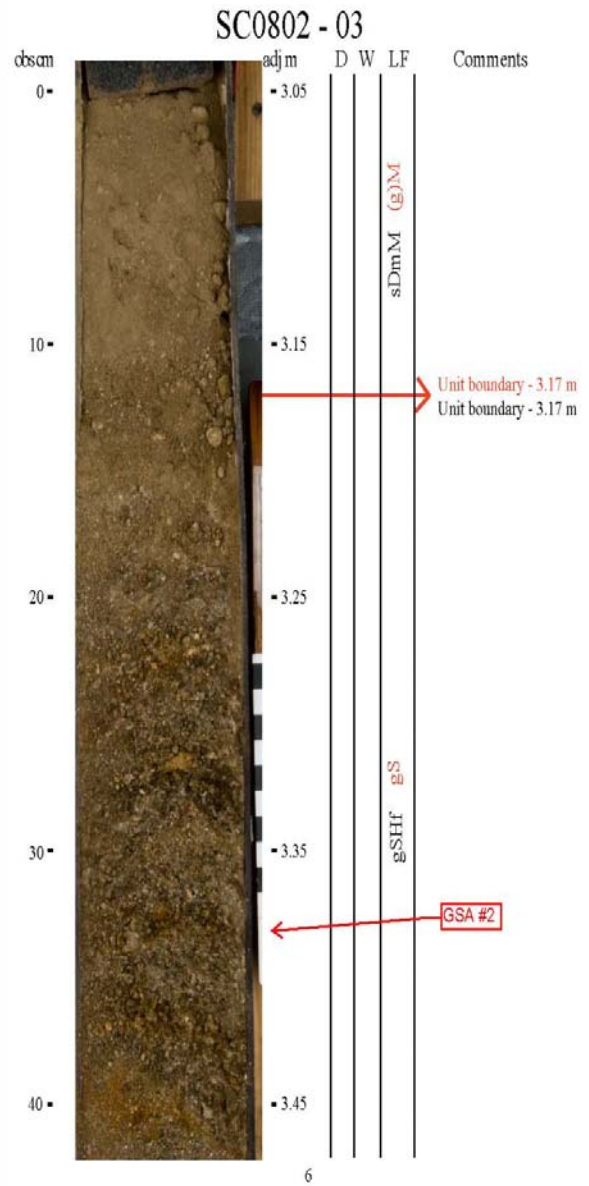
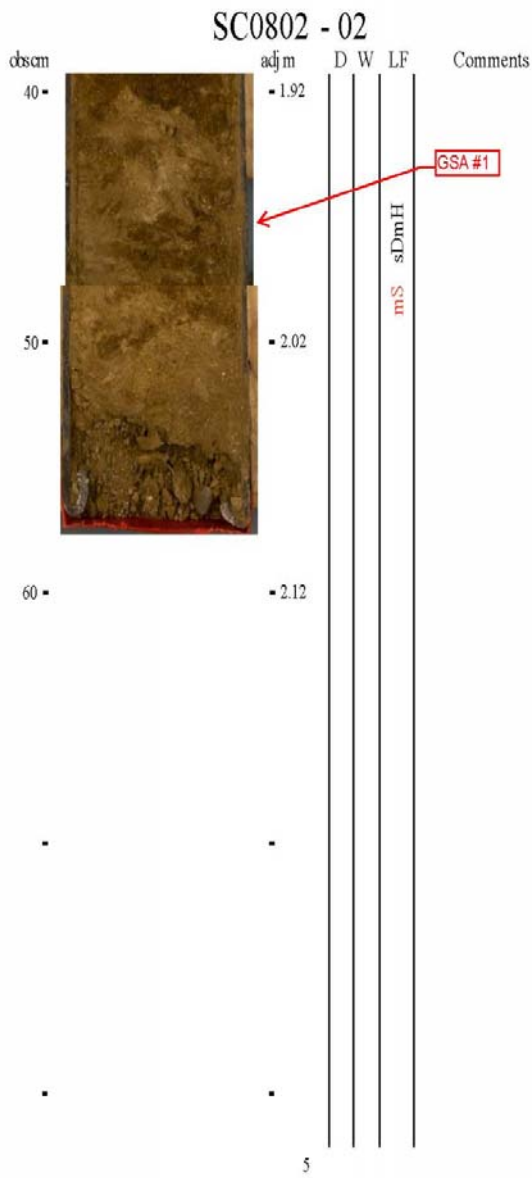
Appendix A: Photolog of SC0802 (modified from IGS)



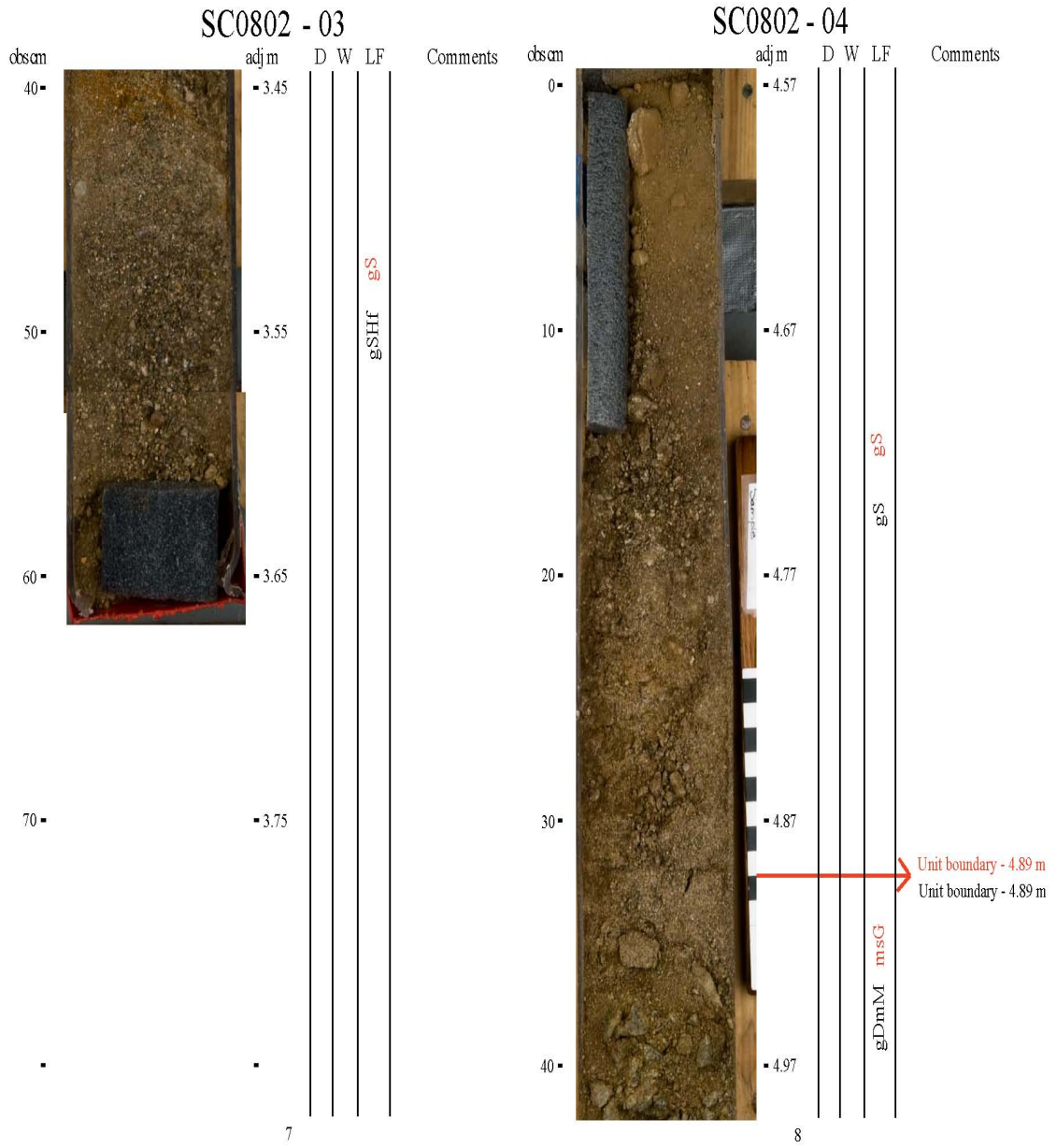




Appendix A cont: Photolog of SC0802

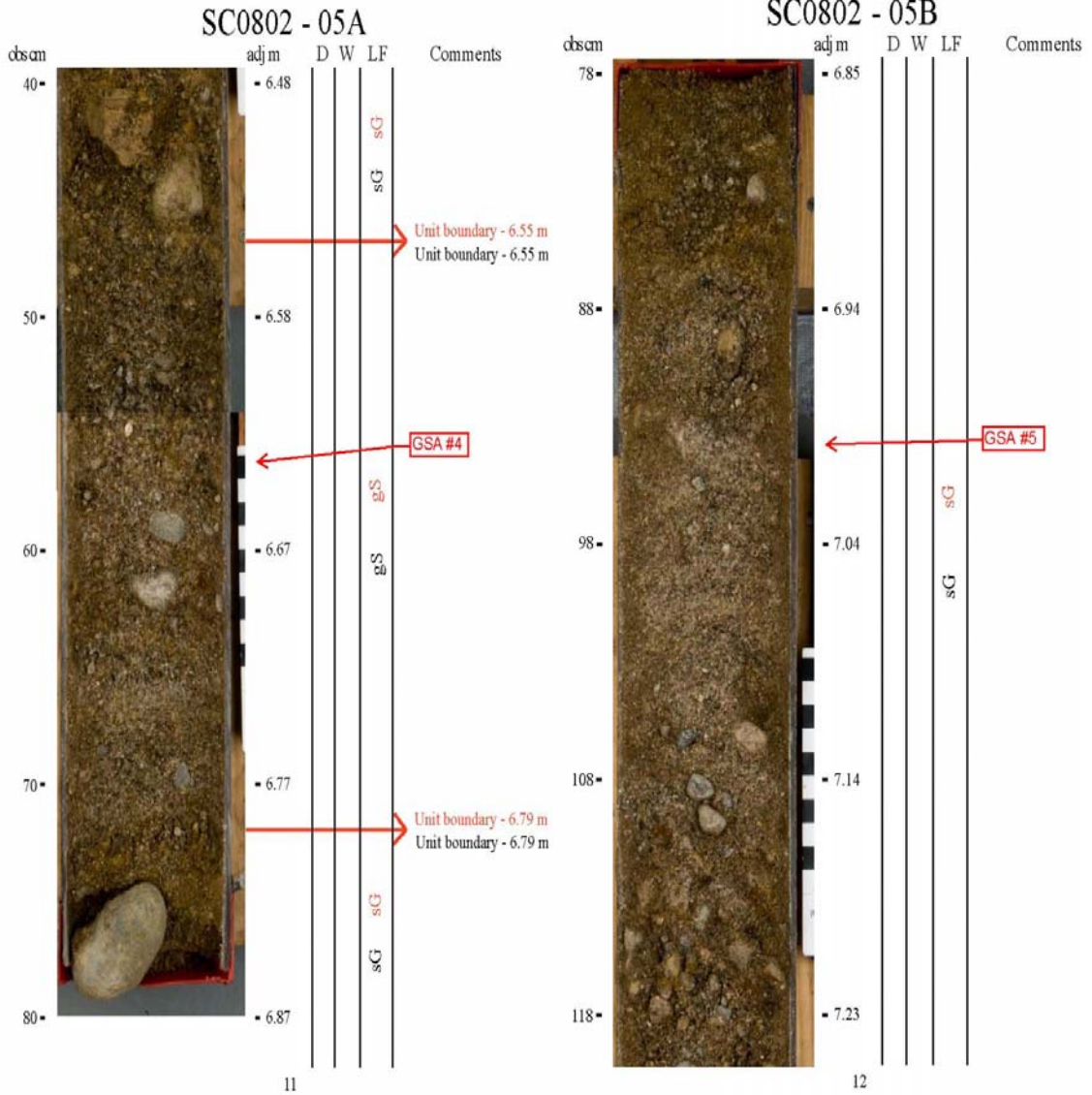


Appendix A cont: Photolog of SC0802

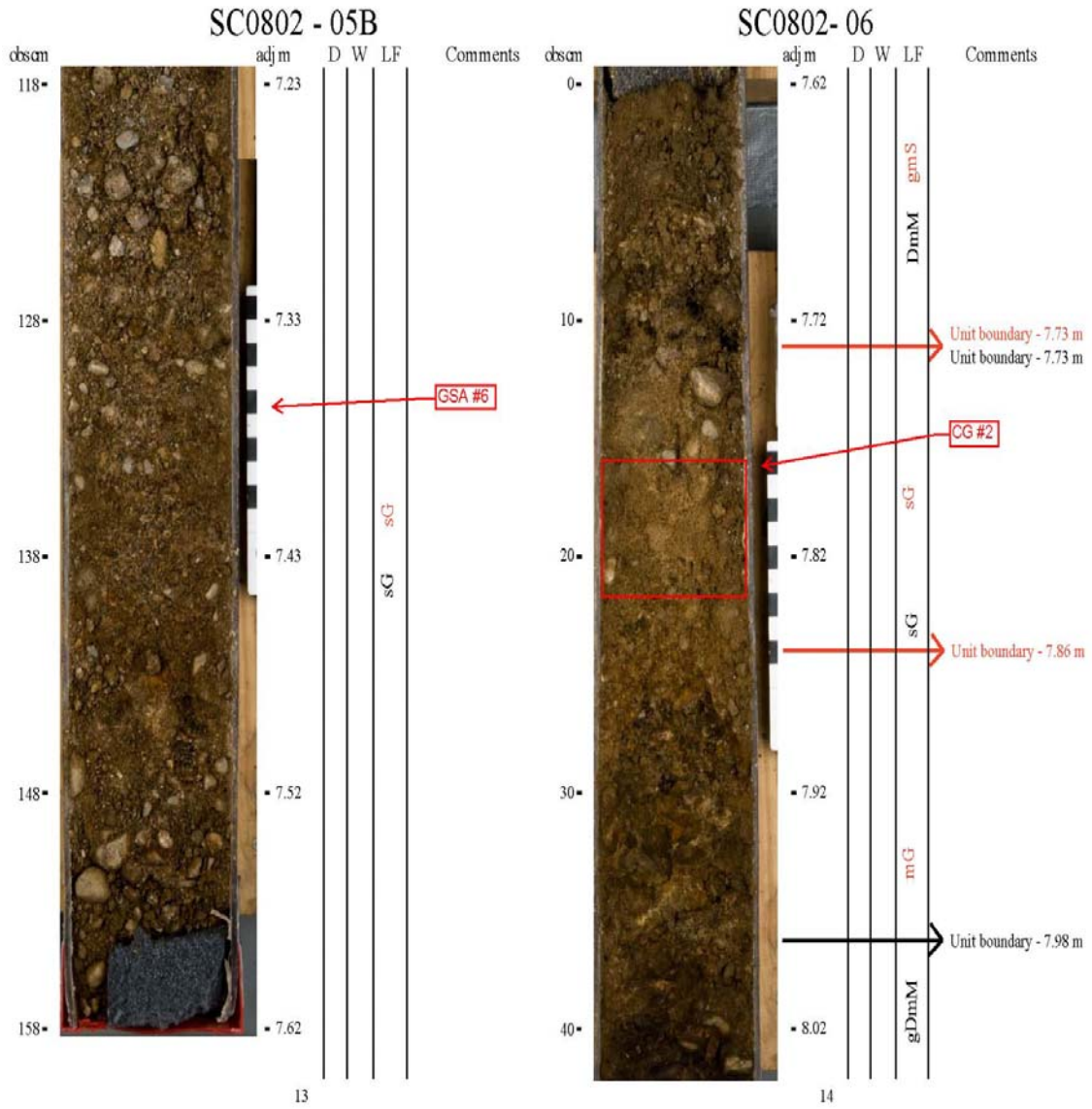




Appendix A cont: Photolog of SC0802



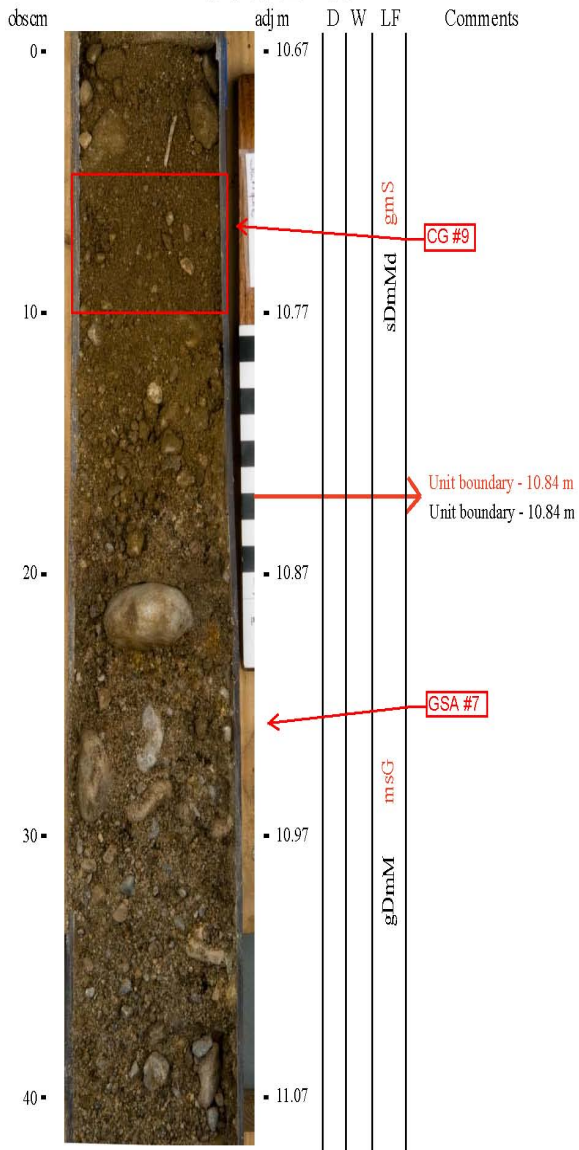
Appendix A cont: Photolog of SC0802





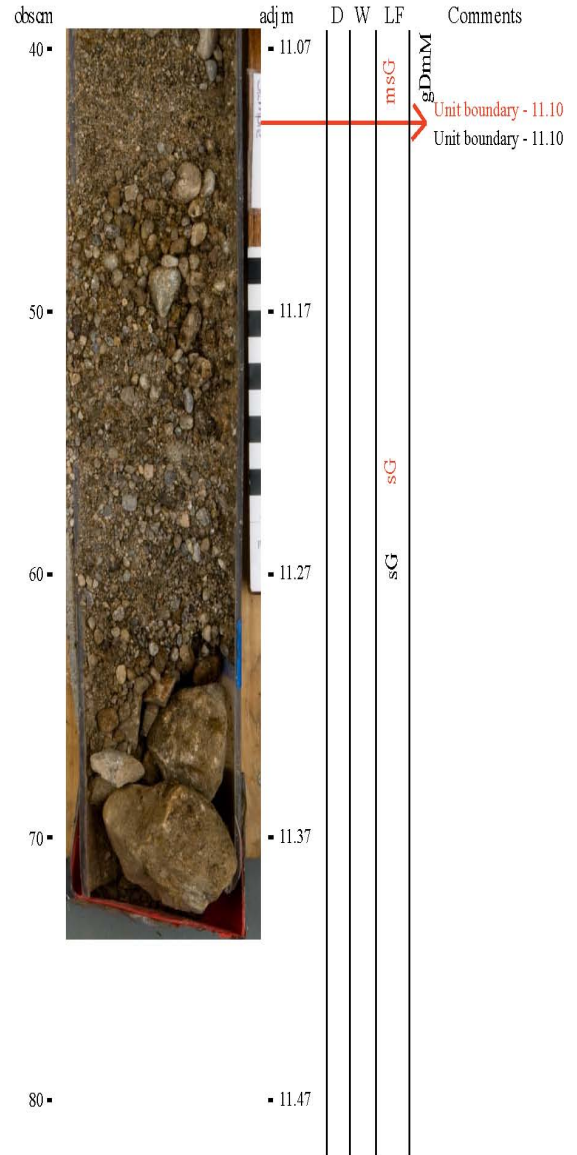
Appendix A cont: Photolog of SC0802

SC0802 - 08



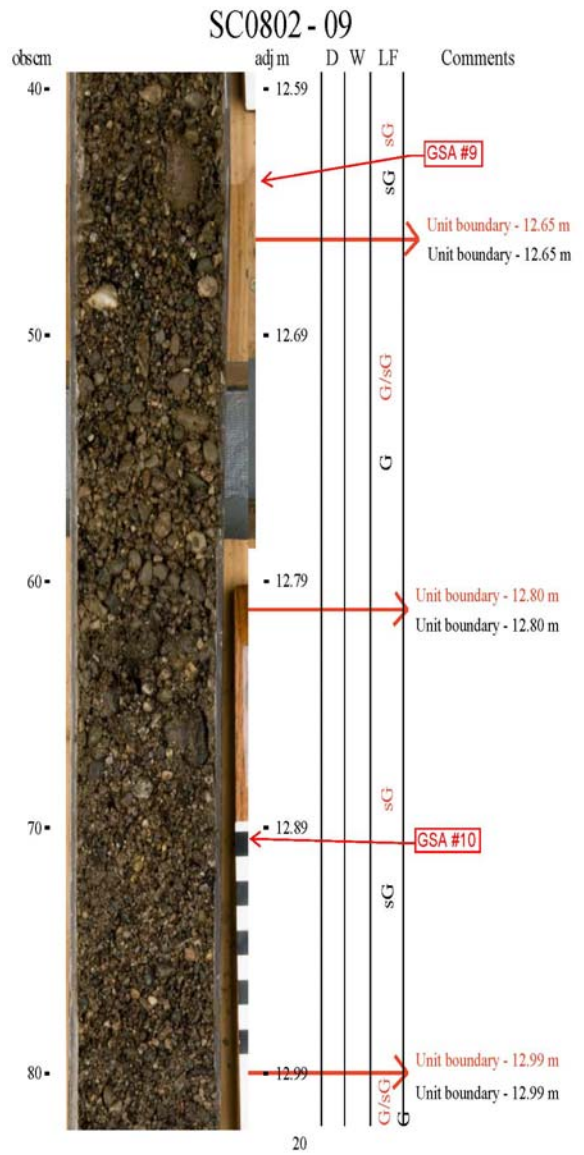
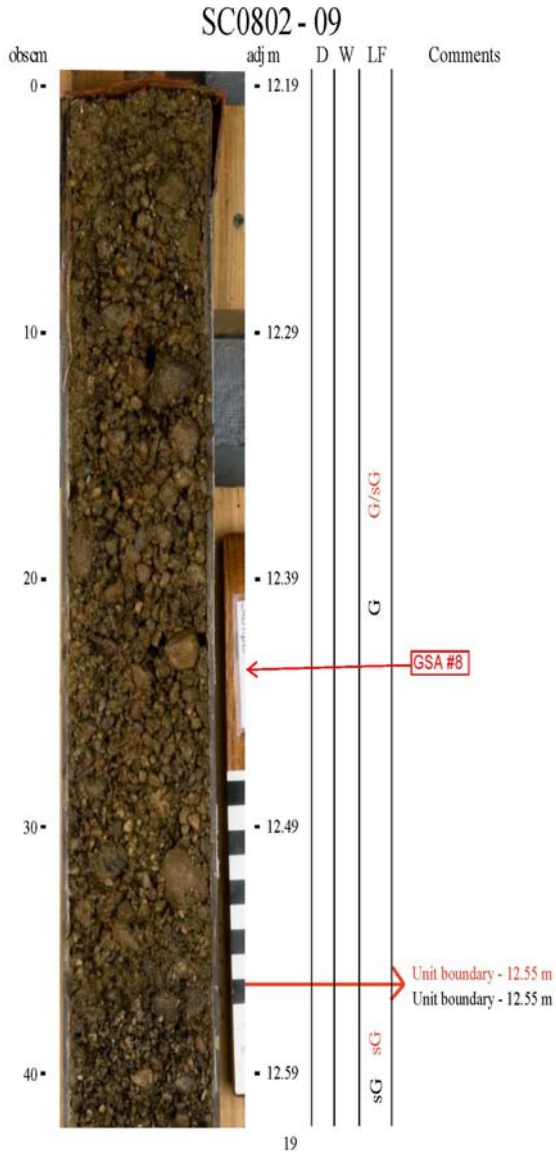
17

SC0802 - 08



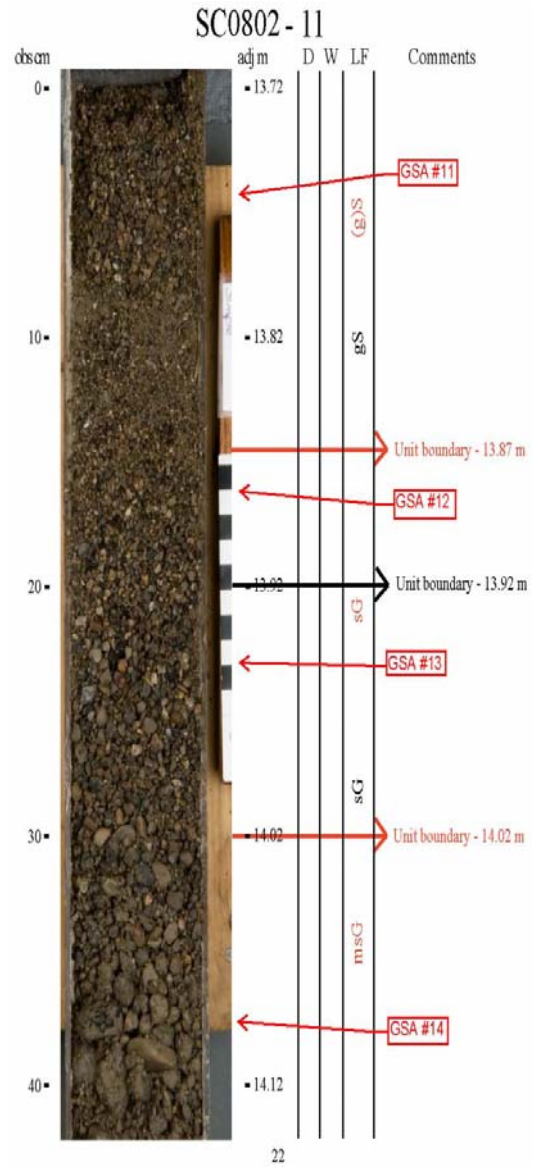
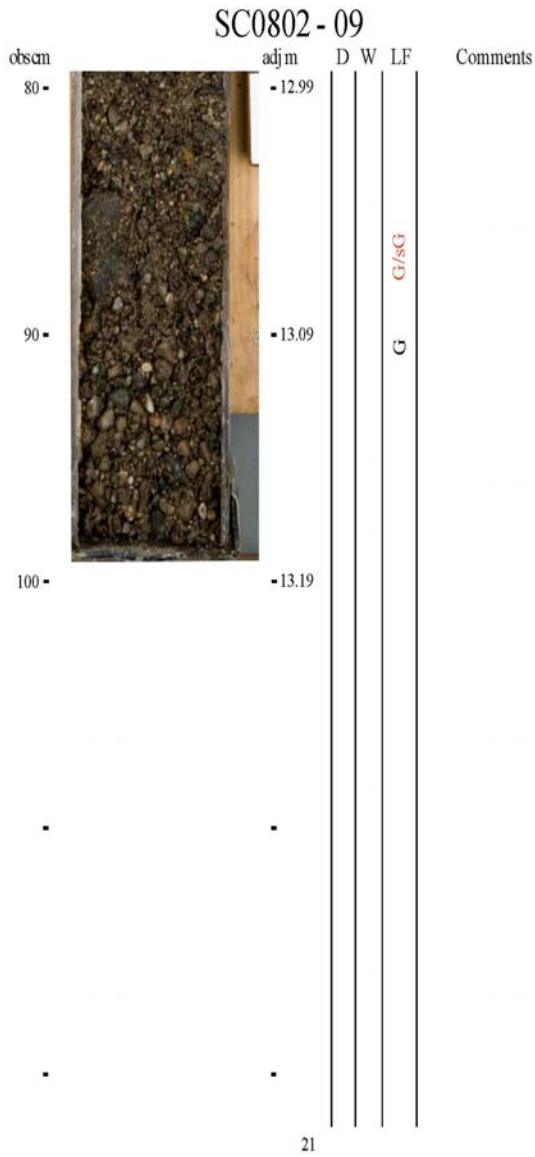
18

Appendix A cont: Photolog of SC0802

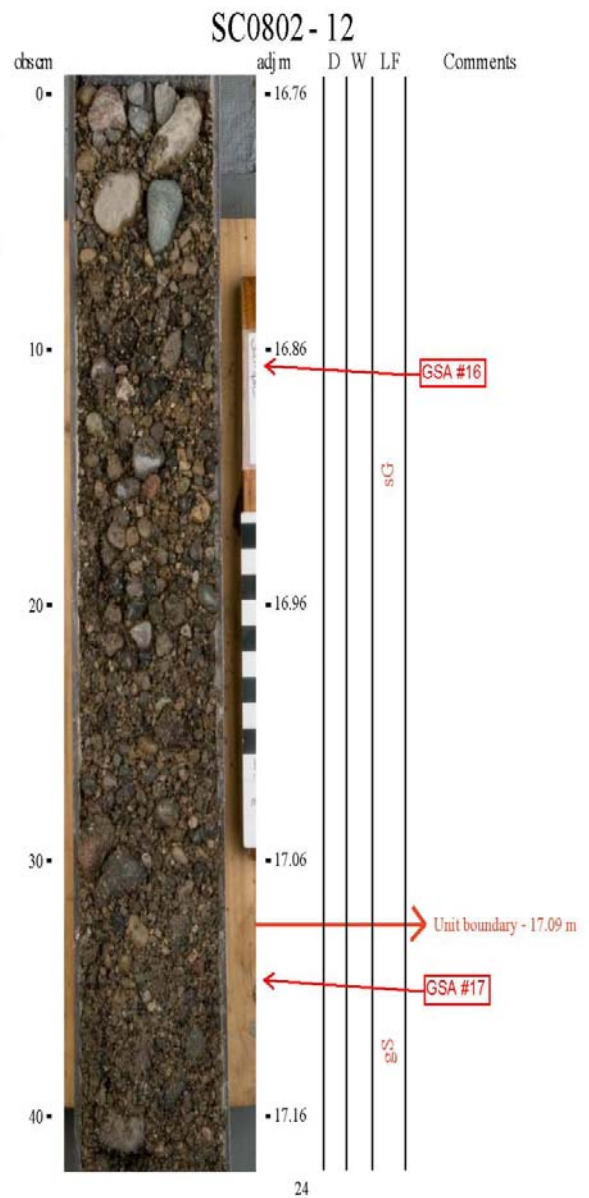
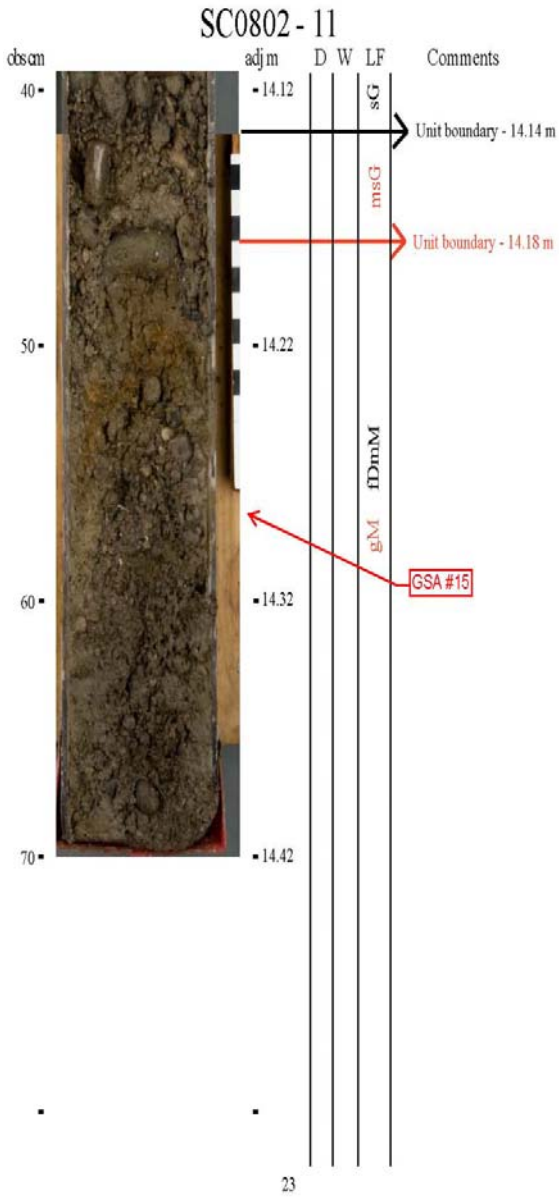




Appendix A cont: Photolog of SC0802

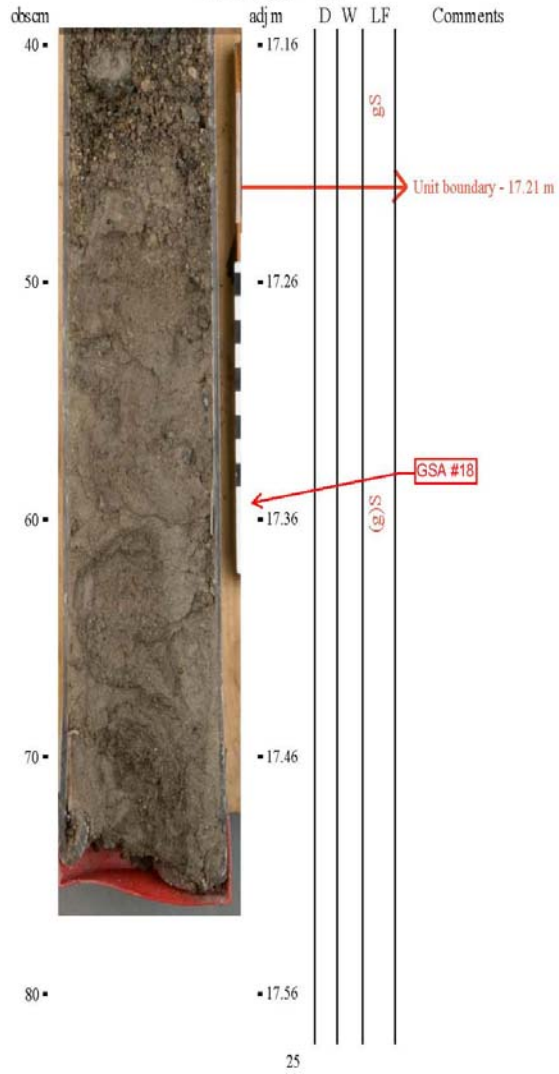


Appendix A cont: Photolog of SC0802

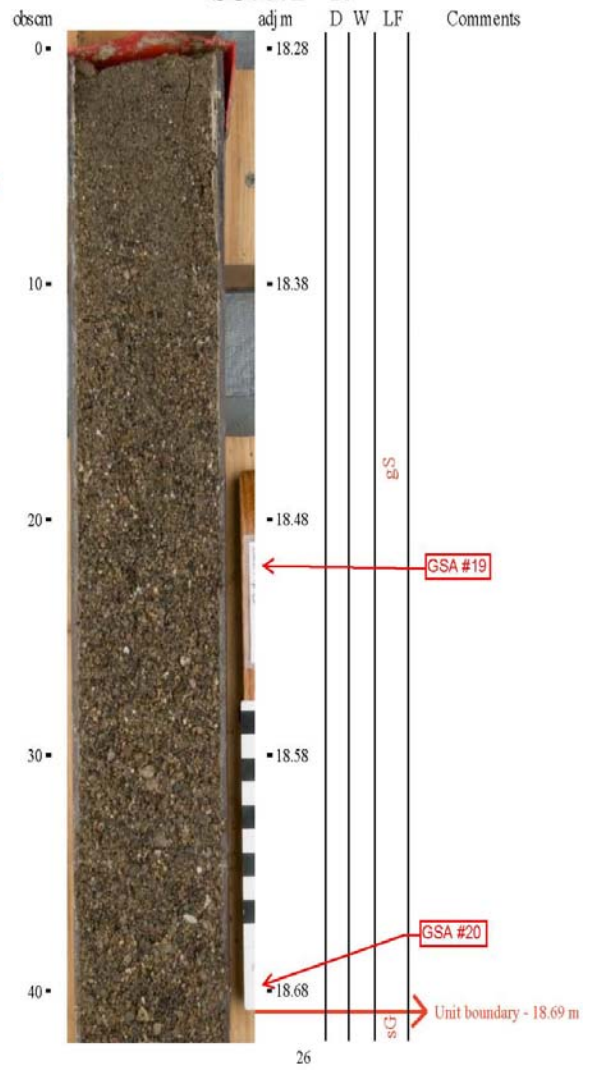


Appendix A cont: Photolog of SC0802

SC0802 - 12

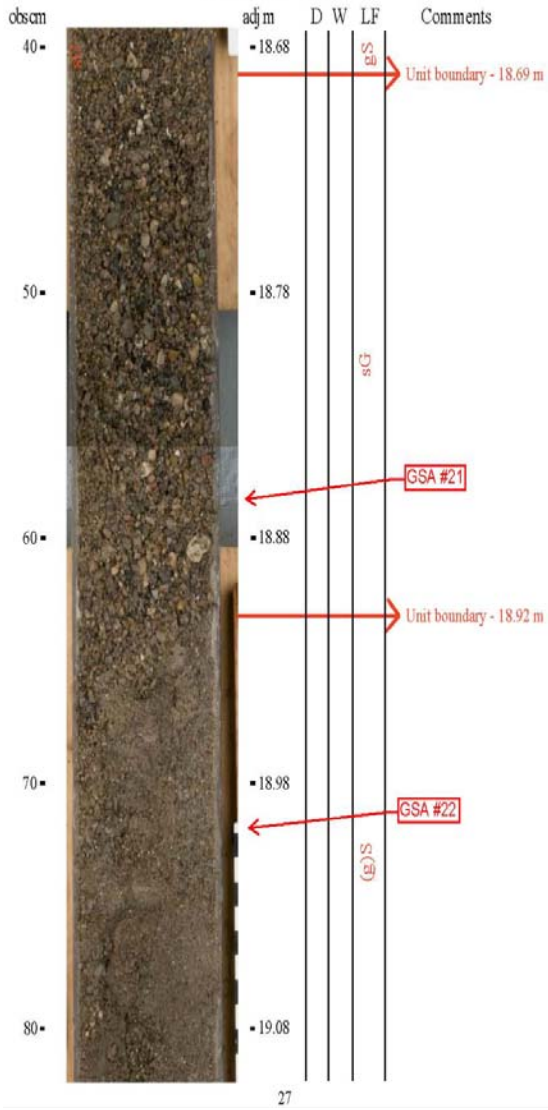


SC0802 - 13

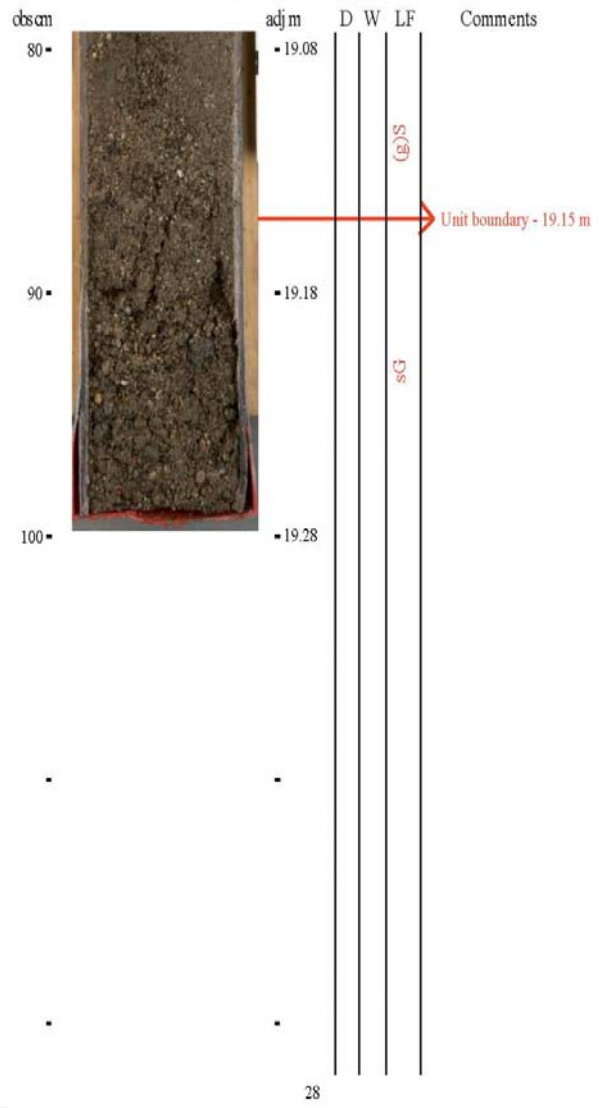


Appendix A cont: Photolog of SC0802

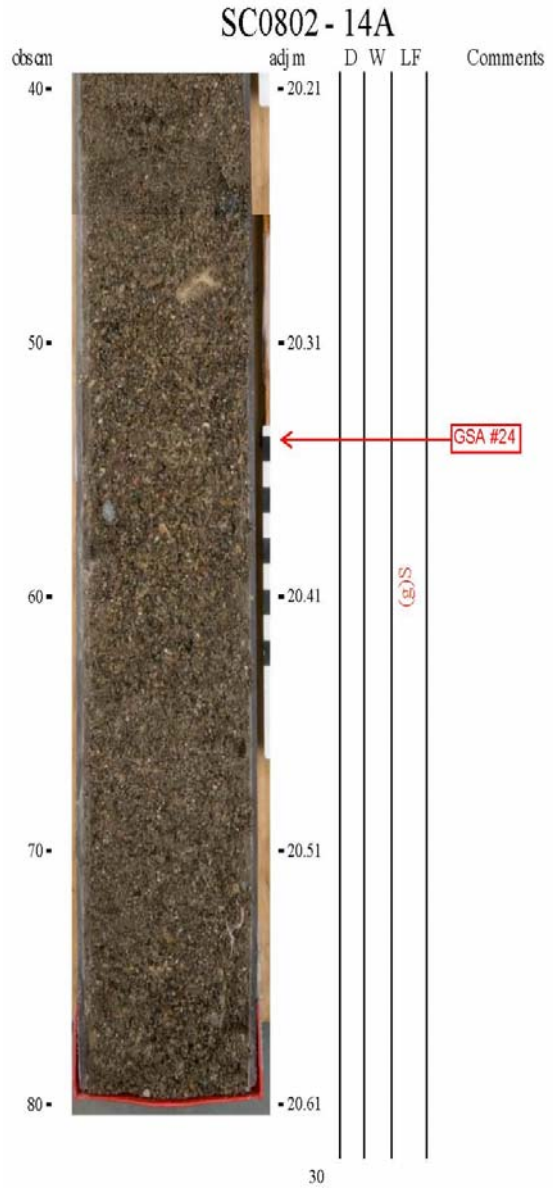
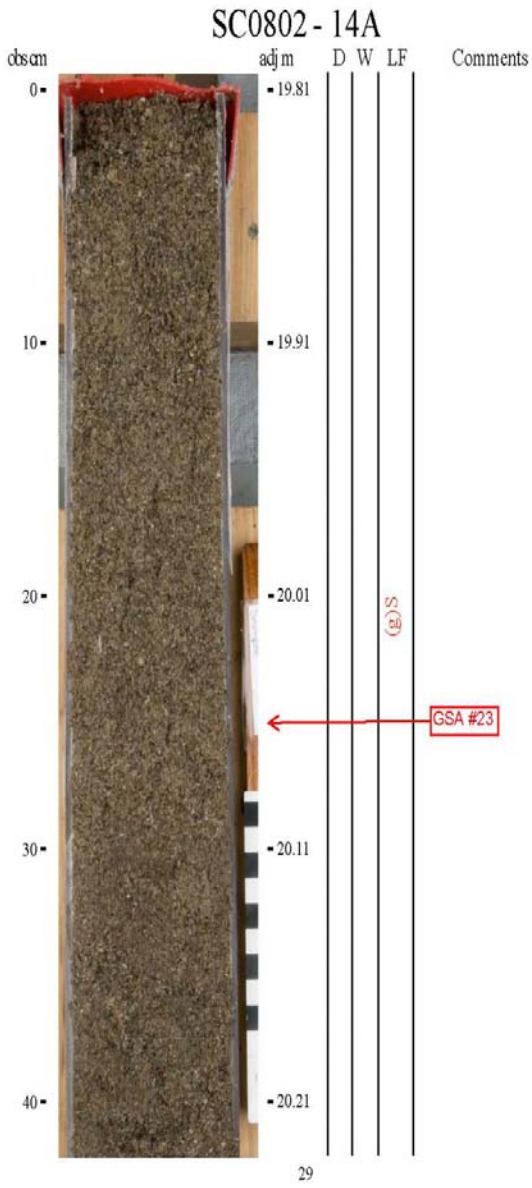
SC0802 - 13



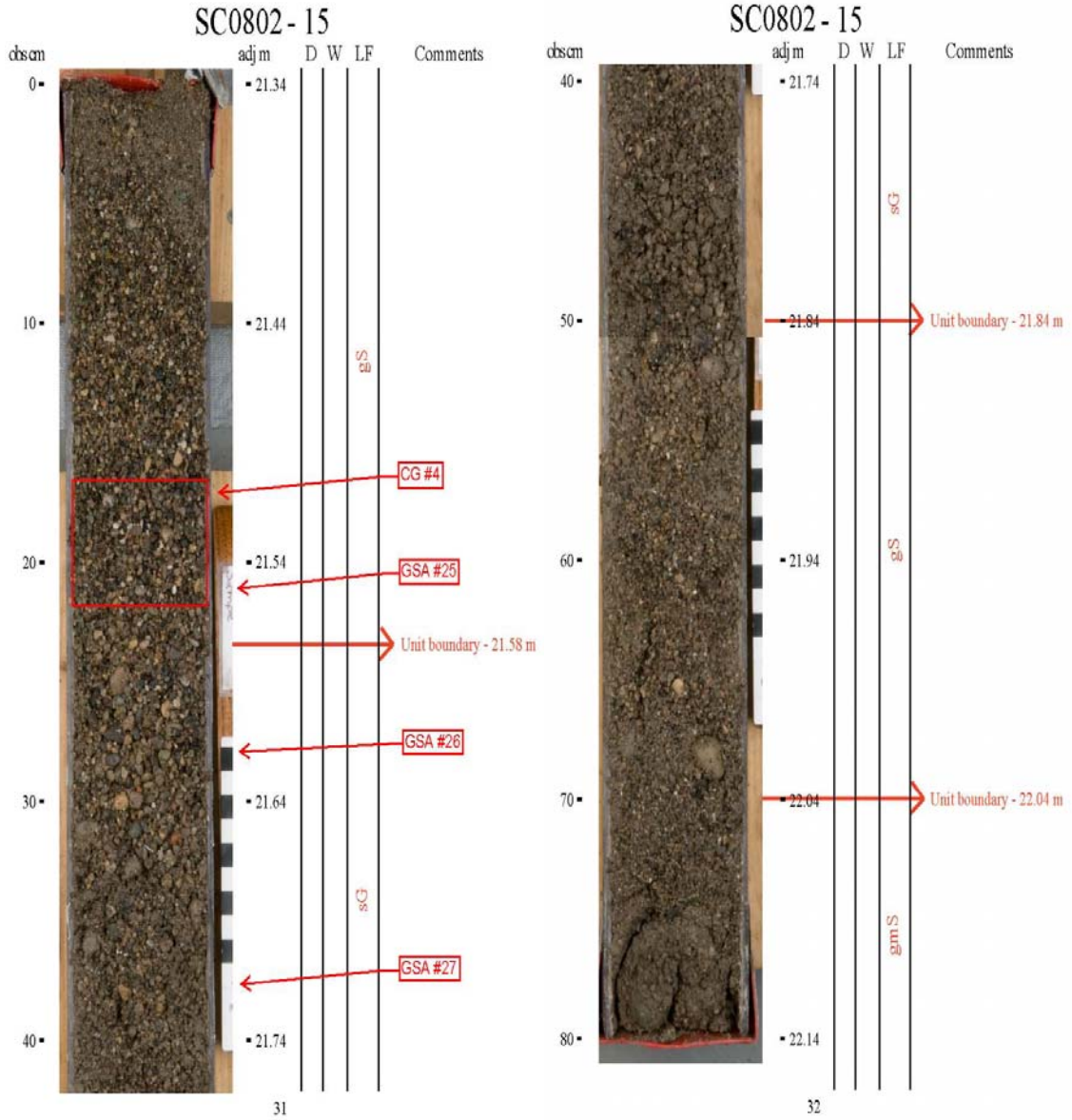
SC0802 - 13



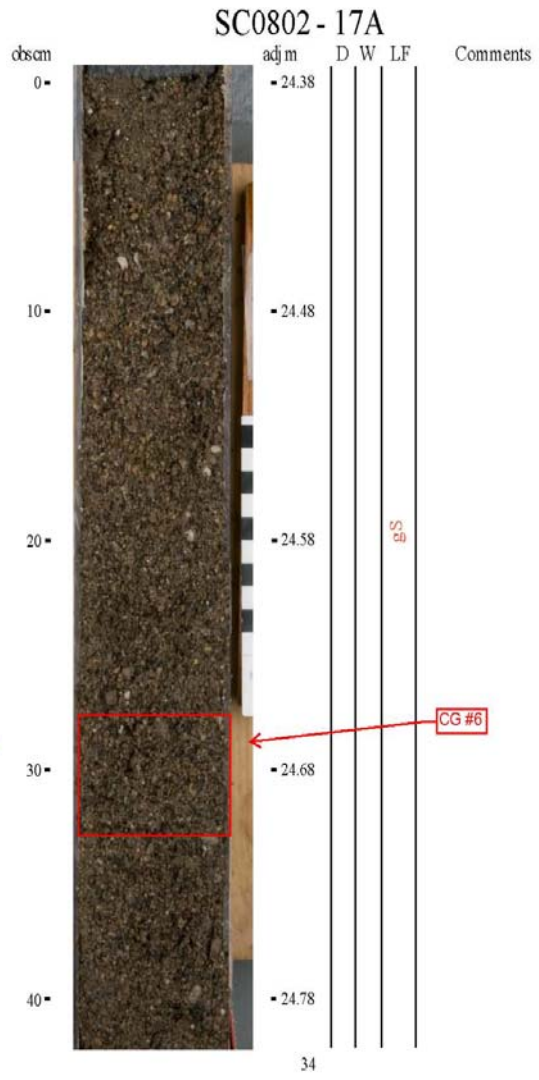
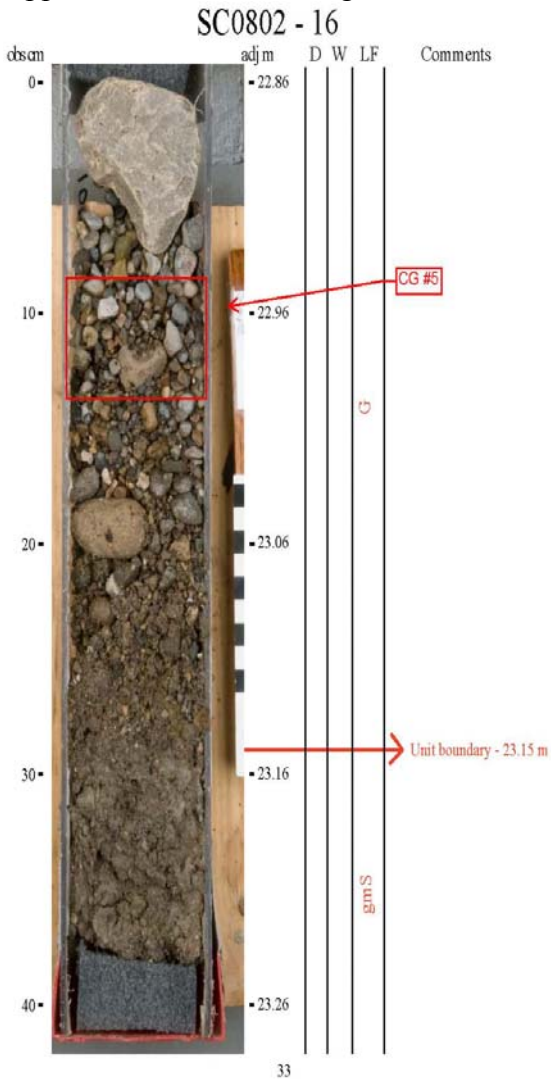
Appendix A cont: Photolog of SC0802



Appendix A cont: Photolog of SC0802



Appendix A cont: Photolog of SC0802



Appendix A cont: Photolog of SC0802

**SC0802 - 17A**

obs cm	adj m	D	W	LF	Comments
40-	- 24.78				
50-	- 24.88				
-	-				
-	-				
-	-				

35

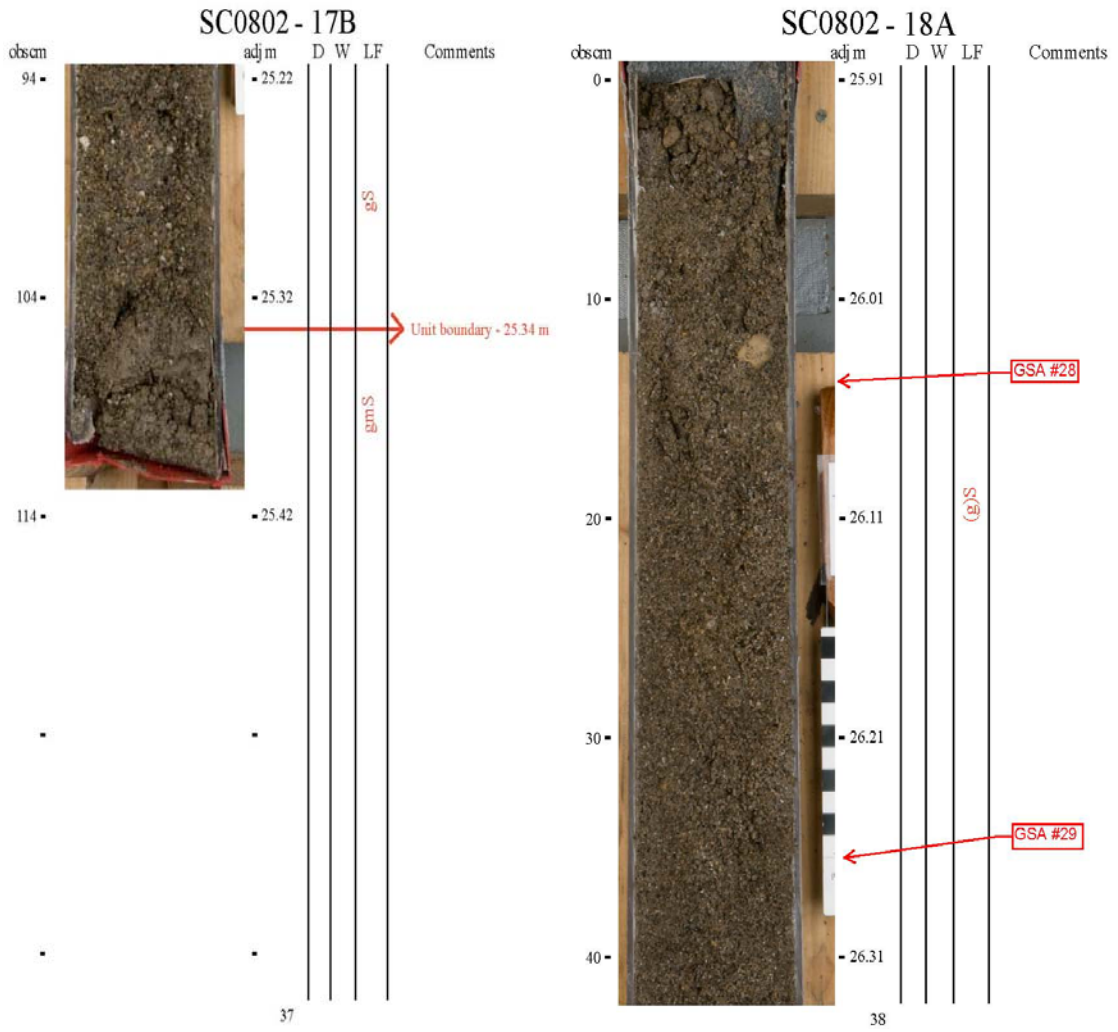
**SC0802 - 17B**

obs cm	adj m	D	W	LF	Comments
44-	- 24.82				
54-	- 24.92				
64-	- 25.02				
74-	- 25.12				
84-	- 25.22				

36

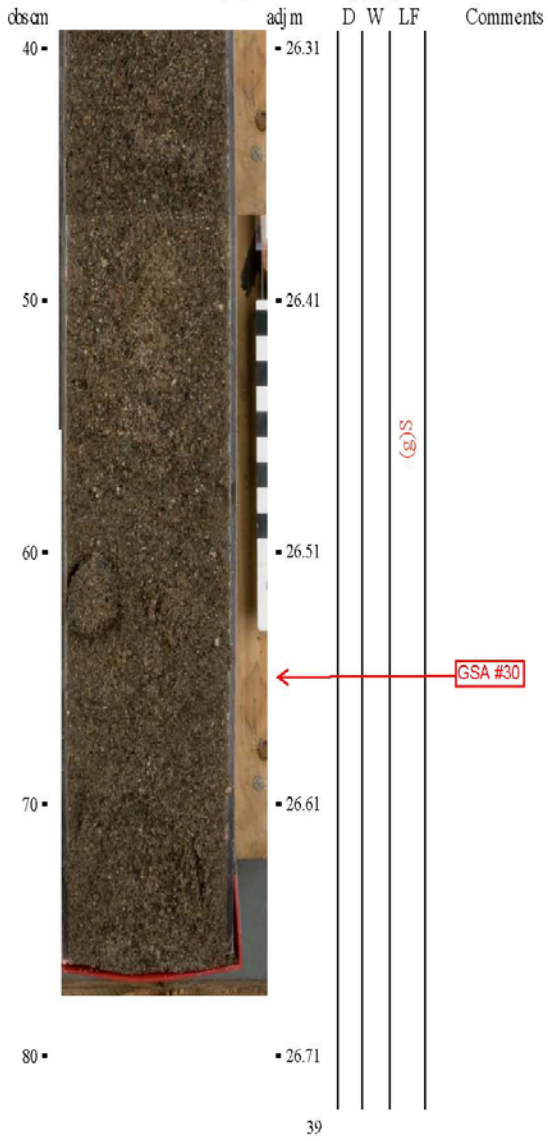


Appendix A cont: Photolog of SC0802

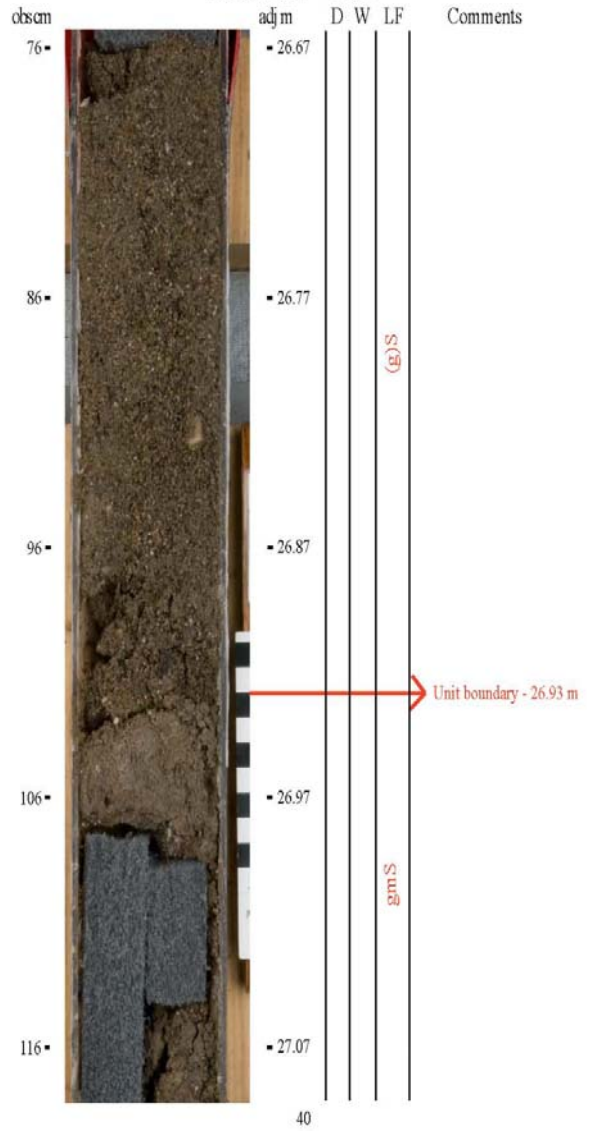


Appendix A cont: Photolog of SC0802

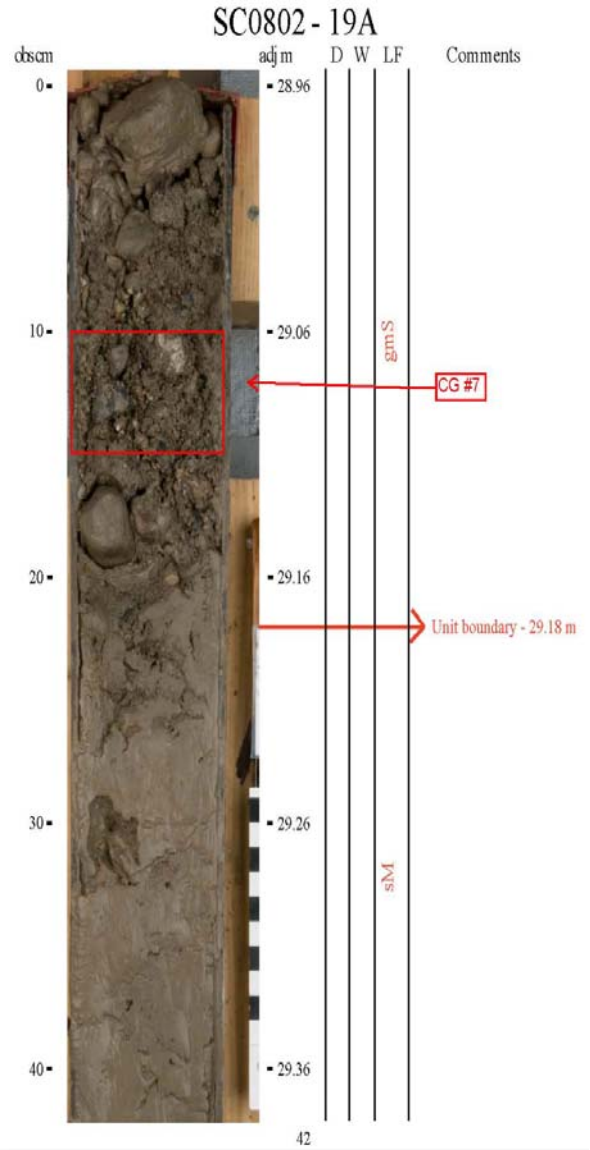
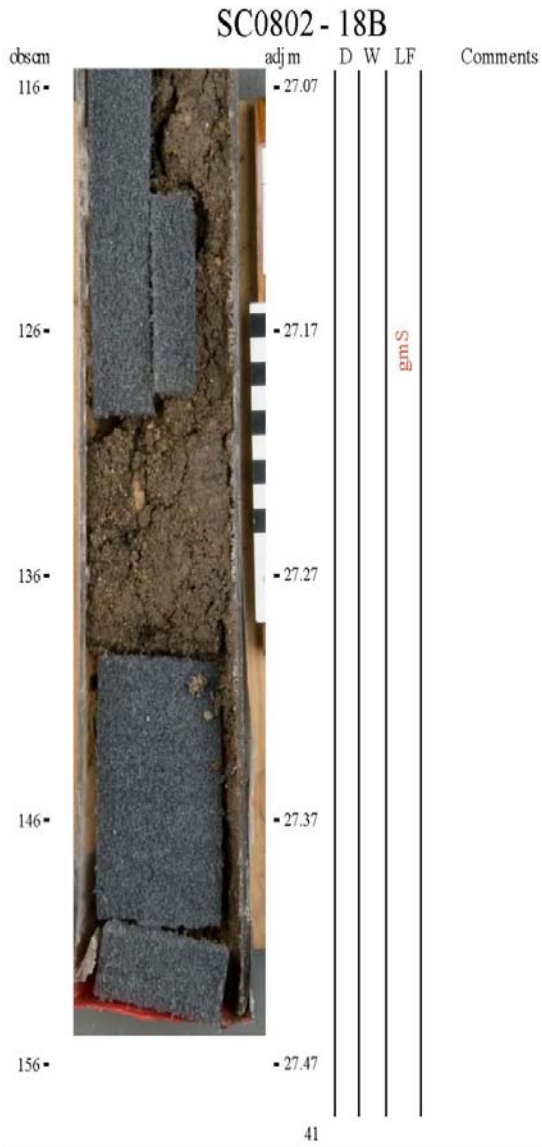
SC0802 - 18A



SC0802 - 18B



Appendix A cont: Photolog of SC0802



Appendix A cont: Photolog of SC0802

SC0802 - 19A

obs cm	adj m	D	W	LF	Comments
40	-29.36				
50	-29.46				
60	-29.56				sM
70	-29.66				
80	-29.76				

43

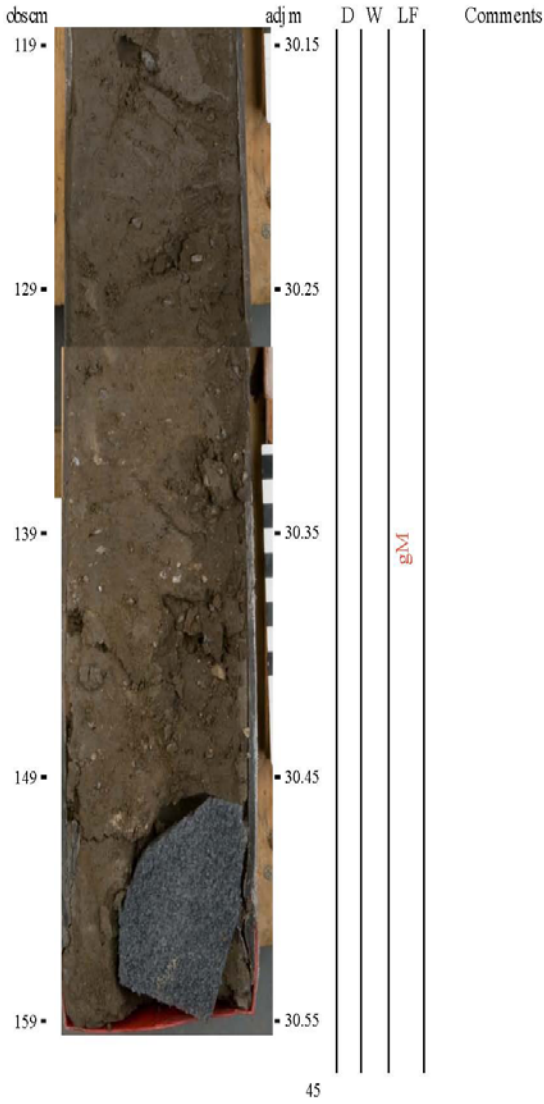
SC0802 - 19B

obs cm	adj m	D	W	LF	Comments
79	-29.75				
89	-29.85				sM
99	-29.95				Unit boundary - 29.93 m
109	-30.05				gM
119	-30.15				

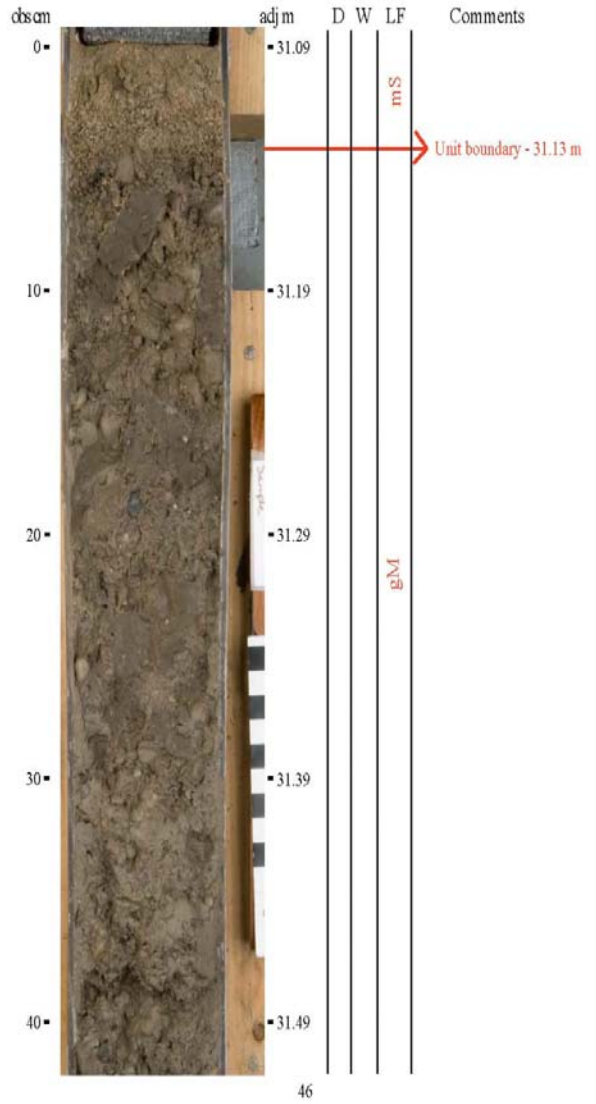
44

Appendix A cont: Photolog of SC0802

SC0802 - 19B



SC0802 - 20A



Appendix A cont: Photolog of SC0802

SC0802 - 20A

obs cm	adj m	D	W	LF	Comments
40 -	- 31.49				
50 -	- 31.59				
-	-				
-	-				
-	-				
gM					
47					

SC0802 - 20B

obs cm	adj m	D	W	LF	Comments
49 -	- 31.58				
59 -	- 31.68				
69 -	- 31.78				
79 -	- 31.88				
89 -	- 31.98				
gM					
48					

Appendix A cont: Photolog of SC0802  
 SC0802 - 20B

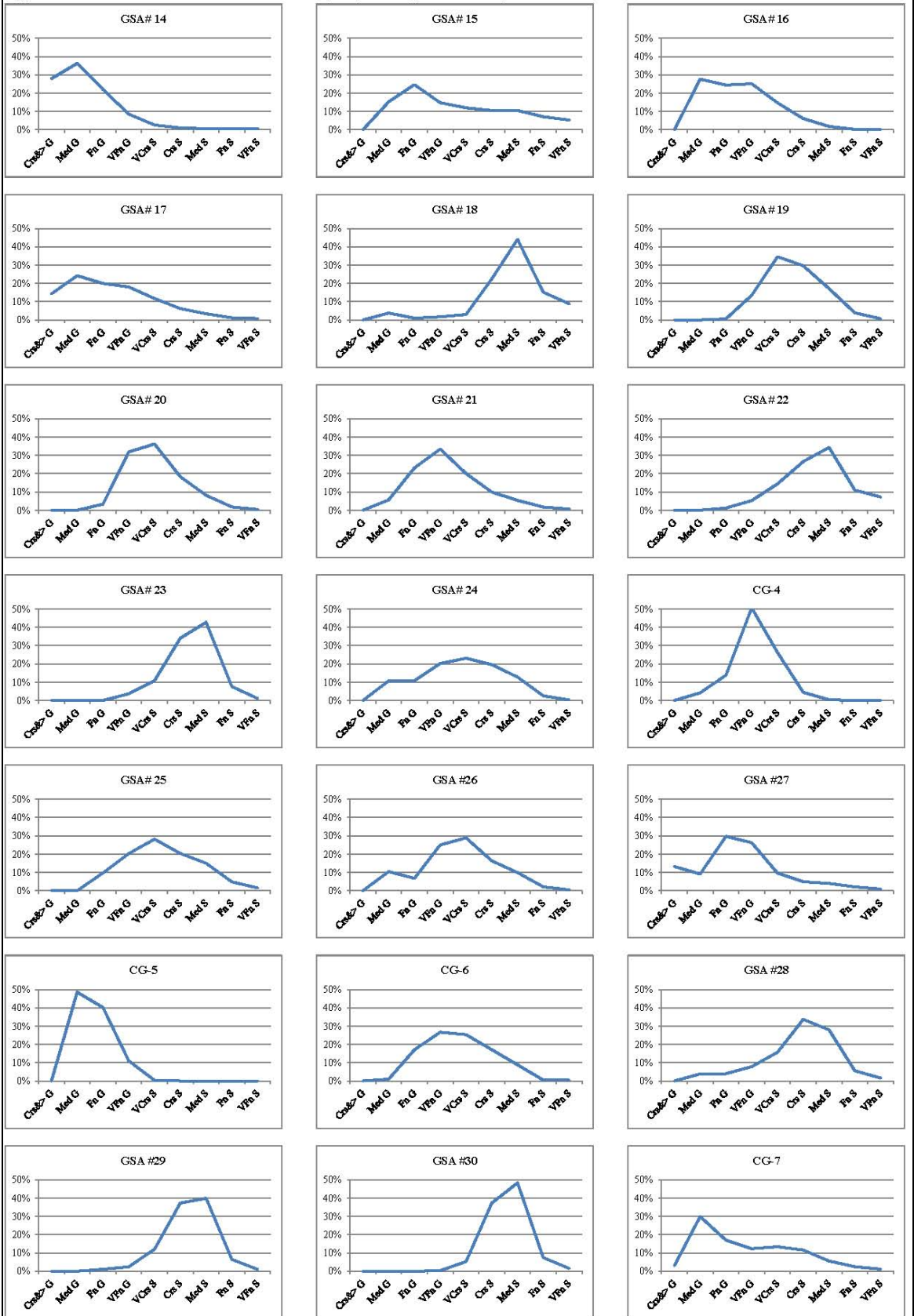
obs cm	adj m	D	W	LF	Comments
89 -	31.98				
99 -	32.08			gM	
109 -	32.18				
-	-				
-	-				

Appendix B: Grain size distribution of SC0802 samples (sand and gravel fractions)





Appendix B cont: Grain size distribution of SC0802 samples (sand and gravel fractions)



## REFERENCES CITED

- Anderson, R.C., 1957. Pebble and Sand Lithology of the Major Wisconsin Glacial Lobes of the Central Lowland. *Geological Society of America Bulletin*, v. 68, p. 1415-1450.
- Andrews, J.T., Kihl, R., Kristjansdottir, G.B., Smith, L.M., Helgadottir, G., Geirsdottir, A., and A.J. Jennings, 2002. Holocene sediment properties of the East Greenland and Iceland continental shelves bordering Denmark Strait (64-68 degrees N), North Atlantic. *Sedimentology*, v. 49, p. 5-24.
- Benn, D.I. and D.J.A. Evans, 2010. *Glaciers and Glaciation*, Second Edition. Hodder Education, London, 802 p.
- Bleuer, N.K., 1974. Buried Till Ridges in the Fort Wayne Area, Indiana, and Their Regional Significance. *Geological Society of America Bulletin*, v. 85, p. 917-920.
- Bleuer, N.K. and M.C. Moore, 1974. Buried pinchout of Saginaw Lobe Drift in Northeastern Indiana. *Indiana Academy of Sciences*, v. 84, p. 362-372. Department of Natural Resources Geological Survey Special Report 13. 72 p.
- Bleuer, N.K. and M.C. Moore, 1978. Environmental Geology of Allen County, Indiana. Department of Natural Resources Geological Survey Special Report 13. 72 p.
- Boggs, S., 2001. *Principles of Sedimentology and Stratigraphy*, Third Edition. Prentice Hall, Upper Saddle River, 726 p.
- Clark, P.U., 1987. Subglacial Sediment Dispersal and Till Composition. *Journal of Geology*, v. 95, p. 527-541.
- Davis, J.C., 2002. *Statistics and Data Analysis in Geology*. John Wiley and Sons, Hoboken, NJ, 638 p.
- Dearing, J.A. 1998. *Environmental Magnetic Susceptibility: using the Bartington MS2 System*, Chi Publishing, Kenilworth, 104 p.
- Ducey, P.W., 2013. Erie Lobe fine-grained till in northeastern Indiana: insights into Lagro stratigraphy and depositional mechanisms from cores in the Wabash moraine. Indiana University Masters Thesis. 169 p.
- Eberl, D.D., 2003. User guide to RockJock: A program for determining quantitative Mineralogy from X-ray diffraction data. United States Geological Survey Open File Report 03-78. 48 p. Revised November 30, 2009.
- Eberl, D.D., 2004. Quantitative mineralogy of the Yukon River system: Changes with reach and season, and determining sediment provenance. *American Mineralogist*, v. 89, p. 1784-1794.
- Eckberg, M.P., Lowell, T.V., and R. Stuckenrath, 1993. Late Wisconsin glacial advance and Retreat patterns in southwestern Ohio, USA. *Boreas*, v. 22, p. 189-204.
- Evans, D.J.A. and D.I. Benn, 2004. *A Practical Guide to the Study of Glacial Sediments*. Hodder Education, London, 266 p.
- Fenelon, J. M., K.E. Bobay and others, 1994. *Hydrogeologic Atlas of Aquifers in Indiana*. U.S. Geological Survey, Water Resources Investigations Report 92-4142, 197 p.
- Fisher, T.G., Taylor, L.D., and H.M. Jol, 2003. Boulder-gravel hummocks and wavy basal till Contacts: products of subglacial meltwater flow beneath the Saginaw Lobe, south-central Michigan, USA. *Boreas*, v. 32, p. 1-9.

- Fleming, A.H., 1994. The Hydrogeology of Allen County, Indiana: A Geological and Ground Water Atlas. Indiana Geological Survey Special Report 57, 111 p.
- Folk, R.L. and Ward W.C., 1957. Bravos River Bar: A study in the significance of grain Size parameters. *Journal of Sedimentary Petrology*, v. 27, p. 3-26.
- Fraser G.S. and N.K. Bleuer, 1988. Sedimentological consequences of two floods of extreme magnitude in the late Wisconsinan Wabash Valley. *Geological Society of America, Special Paper 229*, p. 111-125.
- Gibbard P. and T. Van Kolfshoten, 2005. Chapter 22: The Pleistocene and Holocene Epochs in Gradstein, F.M., Ogg, J.G. and A.G. Smith, *A Geologic Time Scale 2004*. Cambridge: Cambridge University Press, 589 p.
- Gielar, A., Helios-Rybicka, E., Moller, S. and J.W. Einax, 2012. Multivariate analysis of sediment data from the upper and middle Odra River (Poland). *Applied Geochemistry*, v. 26, p. 1540-1545.
- Glover, K.C., Lowell, T.V., Wiles, G.C., Pair, D., Applegate, P. and I. Hajdas, 2011. Deglaciation, basin formation and post-glacial climate change from a regional network of sediment core sites in Ohio and eastern Indiana. *Quaternary Research*, v. 76, p. 401-410.
- Hammer, Ø., Harper, D.A.T and Ryan, P.D., 2001. PAST: Paleontological statistics software package for education and data analysis. *Palaeontologia Electronica* 4(1): 9 pp. (Version 2.02, 2010).
- Harrison, W., 1960. Original Bedrock Composition of Wisconsin Till in Central Indiana. *Journal of Sedimentary Petrology*, v. 30, n. 3, p. 432-446.
- Indiana Department of Natural Resources (IDNR), 1996. Water Resource Availability in the Maumee River Basin, Indiana. IDNR Division of Water, Water Resource Assessment 93-5. 235 p.
- Indiana Spatial Data Portal (ISDP). 2015. LiDAR DEM data source.
- Integrated Spatial Educational Experiences (ISEE). <http://isee.purdue.edu>. Accessed in 2014.
- Kovacic, M., Peh, Z. and A. Grizelj, 2009. Discriminant function analysis of Upper Miocene and Pliocene sands from the southwestern part of the Pannonian Basin System, Croatia. *Geologica Croatica*, v. 62, n. 3, p. 189-200.
- Letsinger, S.L., 2012. Three-dimensional geologic framework model of the glacial interlobate region of northern Allen County, Indiana: Indiana Geological Survey Open-File Study 12-02, 45 p.
- Leverett, F. and F.B. Taylor, 1915. The Pleistocene of Indiana and Michigan and the History of the Great Lakes. U.S. Geological Survey Monograph 53, 529 p.
- Mahar, B.A., Watkins, S.J., Brunskill, G., Alexander, J. and C.R. Fieldings, 2009. Sediment provenance in a tropical fluvial and marine context by magnetic 'fingerprinting' of transportable sand fractions. *Sedimentology*, v. 56, p. 841-861.
- Michigan Department of Natural Resources (DNR), 1987. Bedrock Geology of Michigan. Land and Minerals Services Division. 1 p., scale 1:500,000.
- Mickelson, D.M. and P.M. Colgan, 2003. The southern Laurentide Ice Sheet in Gillespie, A.R., Porter, S.C. and B.F. Atwater, *Developments in Quaternary Sciences, Volume 1, the Quaternary Period in the United States*, 584 p.
- Monasterio, E.M., 2000. An evaluation of the qualitative and quantitative approaches

- used in determining the provenance of the sediment in the River Eden catchment, Scotland. *Geogaceta*. v. 27, p. 103-106.
- Ohio Division of Geologic Survey, 1990 (rev. 2000, 2004), Generalized column of bedrock units in Ohio: Ohio Department of Natural Resources, Division of Geologic Survey, 1 p.
- Ohio Division of Geologic Survey, 2006. Bedrock Geology Map of Ohio. Ohio Department of Natural Resources, Division of Geologic Survey Map BG-1, generalized page-size Version with text, 2 p., scale 1:2,000,000.
- Prentice, M.L., Ducey, P.W., and R.F. Rupp, 2012. Report on 2008 IGS Rotosonic Cores SC0801, SC0803, and SC0804 from Huntington and Allen Counties. Indiana Geological Survey, Report of Progress, November 2012. 54 p.
- Shane, L.C.K. and K.H. Anderson, 1993. Intensity, Gradients and Reversals in Late Glacial Environmental Change in East-central North America. *Quaternary Science Reviews*, v. 12, p. 307-320.
- Srivastava, A.K. and N. Khare, 2009. Granulometric Analysis of Glacial Sediments, Schirmacher Oasis, East Antarctica. *Journal of Geological Society of India*, v. 73, p. 609-620.
- Stephenson, D.A., Fleming, A.H., and D.M. Mickelson, 1988. Glacial deposits *in* Back, W., Rosenshein, J.S., and P.R. Seaber, eds., *Hydrogeology: Boulder, Colorado*, Geological Survey of America, *The Geology of North America*, v. O-2.
- Strobel, M.L. and G. Faure, 1987. Transport of Indicator Clasts by Ice Sheets and the Transport Half-distance: A Contribution to prospecting for ore deposits. *Journal of Geology*, v. 95, p. 687-697.
- Stuiver M. and P.J. Reimer, 1993. Extended  $^{14}\text{C}$  data base and revised CALIB 3.0 age calibration Program. *Radiocarbon*, v. 35, p. 215-230.
- Swan, D., Clague, J.J., and J.L. Luternauer, 1978. Grain-size Statistics I: Evaluation of the Folk and Ward Graphic Measures. *Journal of Sedimentary Petrology*, v. 48, p. 863-878.
- Swinehart, A.L. and G.R. Parker, 2002. The relationship between glacial geologic processes and Peatland distribution in Indiana. *Proceedings of the Indiana Academy of Science*, v. 1, p. 21-31.
- Swinehart, A.L. and R.L. Richards, 2001. Paleobiology of a northeast Indiana wetland Harboring Remains of the Pleistocene Giant Beaver (*Castoroides Ohioensis*). *Proceedings of the Indiana Academy of Science*, v. 110, p. 151-166.
- Thornbury, W.D., 1950. Glacial Sluiceways and Lacustrine Plains of Southern Indiana. Department of Conservation, Division of Geology, Bulletin No. 4, 21 p.
- United States Geological Survey (USGS) Mr. Data. <http://mrdata.usgs.gov>. Accessed in 2013.
- USGS, 2013. 2009 Minerals Yearbook, Indiana (Advanced Release). December. 10 p.
- Waythomas, C.F., 1991. Magnetic Susceptibility of Fluvial Sediment, Lower Fox River, Northeastern Illinois, and Implications for Determining Sediment Source Area. U.S. Geological Survey, Water Resources Investigations Report 91-4013, 24 p.
- Wetzel R.G., 1970. Recent and Postglacial Production Rates of a Marl Lake. *Limnology and Oceanography*, v. 15, n. 4, p. 491-503.
- Zumberge, J.H., 1960. Correlation of Wisconsin Drifts in Illinois, Indiana, Michigan, and Ohio. *Bulletin of the Geological Society of America*, v. 71, p. 1177-1188.

# **CIRRICULUM VITAE**

**Charles B. Goodwin**

## **Education**

M.S., Geology, 2015  
Indiana University, earned at IUPUI  
Indianapolis, Indiana

B.A., Geology, 2000  
Minor in Physical Geography  
Miami University  
Oxford, Ohio

## **Professional Experience**

2011 – Present	ENVIRON International Corp. Manager
2004-2011	KERAMIDA, Inc, Project Geologist and Senior Project Manager
2001-2004	Heritage Environmental Services, LLC Environmental Technician and Project Geologist

## **License**

Indiana Licensed Professional Geologist